AN ABSTRACT OF THE DISSERTATION OF

Bahar Özmen Monkul for the degree of Doctor of Philosophy in Materials Science presented on May 12, 2010.

Title: Graphite Intercalation with Fluoroanions by Chemical and Electrochemical Methods.

Abstract approved:

_____

Michael M. Lerner

New acceptor-type graphite intercalation compounds (GICs) containing perfluoroalkyl anions have been synthesized by using both chemical and electrochemical methods and characterized by elemental and thermogravimetric analyses. Investigation into these graphite intercalation compounds can provide novel materials and a detailed understanding of their properties.

GICs of composition $C_x[FB(C_2F_5)_3]\cdot\delta F$ are prepared for the first time by the intercalation of fluoro-tris(pentafluoroethyl)borate anion, $[FB(C_2F_5)_3]^-$, under ambient conditions in aqueous (48 %) hydrofluoric acid containing the oxidant $K_2[MnF_6]$. Powder-XRD data indicate that products are pure stage 2 and physical mixture of stage 2 and stage 3 after 1 h to 20 h reaction times. The calculated basal repeat distance, I_c, is

1.20 nm for stage 2 and 1.54-1.56 nm for stage 3 GICs, corresponding to gallery heights of d_i= 0.86-0.89 nm. In addition, stage 2 GIC of $C_x[FB(C_2F_5)_3]\cdot\delta CH_3NO_2$ having d_i= 0.84 nm is prepared by electrochemical oxidation of graphite in a nitromethane electrolyte.

The elemental analyses of these complex GICs required that a new sample digestion protocol be developed. After digestion, the fluoride amounts in these GIC samples were analyzed by using ion-selective fluoride combination electrode. The method developed is able to provide fluoride anion content in GICs without interference from the decomposition products of $[FB(C_2F_5)_3]^-$ anion. For the boron analyses the same digestion procedure above is used and the B contents were determined by ICP-AES. For $C_x[FB(C_2F_5)_3]\cdot\delta F$, both compositional parameters x and δ are obtained from the results of elemental B and F analyses. For the chemically prepared GICs at 1 h to 20 h, calculated x values were in the range of 51-56 and the calculated δ values increased with reaction time from approx. 0-2. Combining B analysis and TGA mass loss gives a composition of x= 44 and δ= 0.37 for the electrochemically prepared GIC of $C_x[FB(C_2F_5)_3]\cdot\delta CH_3NO_2$. Energy minimized structure for the isolated borate anion and powder XRD data show that the borate anions adopt a "lying-down" orientation where the long axes of $[FB(C_2F_5)_3]^-$ intercalate anions are parallel to the encasing graphene sheets.

The same electrochemical synthesis strategy is also used for the preparation of a new acceptor-type GIC containing the cyclo-hexafluoropropane-1,3-bis(sulfonyl)amide anion, $[CF_2(CF_2SO_2)_2N]^-$. The gallery heights of 0.85-0.86 nm are determined by powder X-ray diffraction for stage 2 and 3 products. These GICs are obtained by electrochemical oxidation of graphite in a nitromethane electrolyte. GICs containing the

linear anion, $[(CF_3SO_2)_2N]^-$ are also prepared in order to compare the gallery heights and the electron charge distributions that helps to understand the GIC stabilities within the graphene sheets. The compositions of GICs containing $[CF_2(CF_2SO_2)_2N]^-$ are determined by thermogravimetric, fluorine and nitrogen elemental analyses.

GICs of composition $C_x[(C_2F_5)_3PF_3]$ are prepared for the first time by the intercalation of tris(pentafluoroethyl)trifluorophosphate (FAP) anion, $[(C_2F_5)_3PF_3]^-$ by electrochemical oxidation of graphite. Powder-XRD data indicate that products are of stages 2-4 with gallery heights of 0.82-0.86 nm. These GICs are characterized by the same methods using TGA and F ion-selective probe analyses.

Graphite Intercalation with Fluoroanions by Chemical and Electrochemical Methods

by
Bahar Özmen-Monkul

A DISSERTATION

submitted to

Oregon State University

in partial fulfillment of
the requirements for the
degree of

Doctor of Philosophy

Presented May 12, 2010

Commencement June 2010

Doctor of Philosophy dissertation of Bahar Özmen-Monkul presented on May 12, 2010

APPROVED:

Major Professor, representing Materials Science

Director of the Materials Science Program

Dean of the Graduate School

I understand that my dissertation will become part of the permanent collection of Oregon State University libraries. My signature below authorizes release of my dissertation to any reader upon request.

Bahar Özmen-Monkul, Author

ACKNOWLEDGEMENTS

The first person I would like to thank is my advisor Prof. Michael M. Lerner. I am very grateful for his excellent encouragement that he provided throughout my studies at Oregon State University. He always has interesting and exciting ideas about chemistry which helped me through my studies. He is a good mentor and boss who opens ways of understanding and getting through the challenges that I had faced in my early career. I am thankful for his guidance, useful suggestions and patience with me.

I would like to thank Profs. William H. Warnes, John Simonsen, Staci L. Simonich, Yun-Shik Lee and Dr. Patricia L. Dysart for serving on my doctoral dissertation committee and for their helpful suggestions and comments.

I want to acknowledge Profs. Rika Hagiwara, Helge Willner and Dr. Gottfried Pawelke for their contribution in data collection and syntheses of the salts. I thank to Dr. Victor Koch who helped in measuring electrochemical parameters and also provided many helpful discussions, Dr. Alan Richardson for his help in structural modeling, Dr. Chris Pastorek and Ted Hinke for their help in elemental analyses and experimental design.

My current Thai group members, Tosapol Maluangnont and Weekit Sirisaksoontorn, thank you for sharing your ideas and suggestions with me. Amila Liyanage is our new group member. I wish all of you the very best for your careers and lives.

Finally I wish to thank my loving husband M. Murat Monkul for sharing every minute of life together with me. Finishing both of our PhDs at OSU was one of the greatest accomplishments and experiences that we lived together. My other family

members: my mom, Ismahan Özmen, dad, Mehmet Ali Özmen, mother in law, H. Suna Monkul and father in law, O. Rifat Monkul were always there for me providing their endless love and support throughout my PhD studies and stay in US. Without their support I could not accomplish my goals, dreams and reach my current status. Thank you for being a great family and friend to me.

CONTRIBUTION OF AUTHORS

Prof. Michael M. Lerner has contributed to the design and writing of each manuscript. Prof. Helge Willner and Dr. Gottfried Pawelke synthesized the salts used in chapter 2. Prof. Rika Hagiwara provided the salt and collected the elemental analysis data explained in chapter 3.

TABLE OF CONTENTS

TABLE OF CONTENTS (Continued)

TABLE OF CONTENTS (Continued)

LIST OF FIGURES

LIST OF FIGURES (Continued)

LIST OF FIGURES (Continued)

LIST OF TABLES

LIST OF TABLES (Continued)

…dedicated to my beloved parents; my mom, Ismahan Özmen and my dad, Mehmet Ali Özmen.

GRAPHITE INTERCALATION WITH FLUOROANIONS BY CHEMICAL AND ELECTROCHEMICAL METHODS

CHAPTER 1

INTRODUCTION

1.1 GENERAL INTRODUCTION

In chemistry, the introduction of guests (atoms, ions or molecules) into a host lattice is generally called "insertion". When the host lattice is two-dimensional (layered) then this class of reactions is called "intercalation", and has been known since the mid-19th century. Insertion chemistry involves an increase in one or more dimensions that occurs together with the retention of strong bonding within the host structure. For layered hosts, the expansion occurs as an increase in the separation of the layers to incorporate guests. However, if the host is three-dimensional (a framework structure), appropriate dimensions for vacant lattice sites are required to provide accommodation and facile transport of guest species into the structure. Insertion can be a reversible reaction which requires sufficient kinetic or thermodynamic stability of the host lattice. A wide range of hosts are known, their properties range from metallic to non-metallic and having ionic or covalent bonding. Also, host structures can have dimensions from zero up to three-dimensions (0D-3D) (Figure 1.1). Examples of three-dimensional framework structures are zeolites, WO_3, Ti_3S_6, Nb_3S_4, Mo_6S_8; two-dimensional layered structures include TiS_2,

TaS_2, MoO_3, FeOCl, and graphite; one-dimensional chain structures include NbS_3, $NbSe_3$, $KFeS_2$, and AMo_3X_3 (A= alkali metal, In, Tl, X= S, Se); and an example of a zero- dimensional host lattice is C_{60} [1].

Layered inorganic hosts have strongly bound sheets held together by relatively weak forces. In many cases, the guest ions or molecules intercalate between the layers without breaking the strong bonds, but the distance between the host sheets can increase significantly, and in some cases complete "delamination" occurs. There are numerous types of layered materials including transition metal dichalcogenides (MX_2, M= Mo, Nb, Ta, Ti, Zr and X= S, Se), metal phosphorus trichalcogenides (MPX_3, M= Mg, Mn, Fe, Co, Cd, Ni, V, Zn and X= S, Se), transition metal oxyhalides (MOX, M= Cr, Fe, Ti, V and X= Cl, Br, I), transition metal oxides (MoO_3, V_2O_5, $MOXO_4$ where M= Mo, Ta, Nb, V and X= As, P, S), metal phosphates, metal phosphonates and layered double hydroxides (LDHs) or anionic clays, smectite clays, elemental host lattices as graphite [2].

Clay minerals and clay-based materials like polymer nanocomposites have been widely studied due to their technological importance. They can be used as adsorbents, pigments, electrical materials and also have uses in automotive, packaging, coating, and biomedical fields. Their high abundance, low cost, high strength, stiffness and rich intercalation chemistry are properties that make them advantageous in the above applications.

Clays have relatively low layer charge densities which means there is a relatively weak force between adjacent layers, making the interlayer cations exchangeable. Therefore, the intercalation of inorganic and organic cations and molecules into the

interlayer space is facile [3]. Some of the most known clay examples are layered silicic acids as $H_2Si_2O_5$, $H_2Si_{14}O_{29}$, smectite clays of montmorillonite, $Ca_{0.35}[Mg_{0.7}Al_{3.3}](Si_8)O_{20}(OH_4)$ and kaolinite, $Al_4Si_4O_{10}(OH)_8$. Clay adsorption chemistry involves negatively charged aluminosilicate sheet hosts that incorporate exchangeable cations in between the layers, montmorillonite is an example. In most cases, the intercalation reactions of clays do not involve redox chemistry; there is an exchange of intercalate cations or intercalation of molecules that interact with the intercalate cations or clay surfaces. A wide range of guests can be accommodated between clay sheets. When suitable conditions such as appropriate type of intercalate, pH or ionic strength are provided, intercalated clay sheets can completely delaminate to produce colloidal dispersions of single-sheets [2].

LDHs are another class of hosts for intercalation which are anion-exchangers. They contain positively charged layers based on neutral brucite, $Mg(OH)_2$ with higher valence substitutions such as Al^{3+} for Mg^{2+}. LDHs have a general formula of $[M_{1-x}^{2+} M_x^{3+}(OH)_2]^{x+}[An^{n-}]_{x/n}(H_2O)_y$, where M^{2+}= Ca, Mg, Ni, Co, Cu, Zn and M^{3+}= Al, Cr, Fe. An represents a charge-compensating anion that resides between host layers together with water [2].

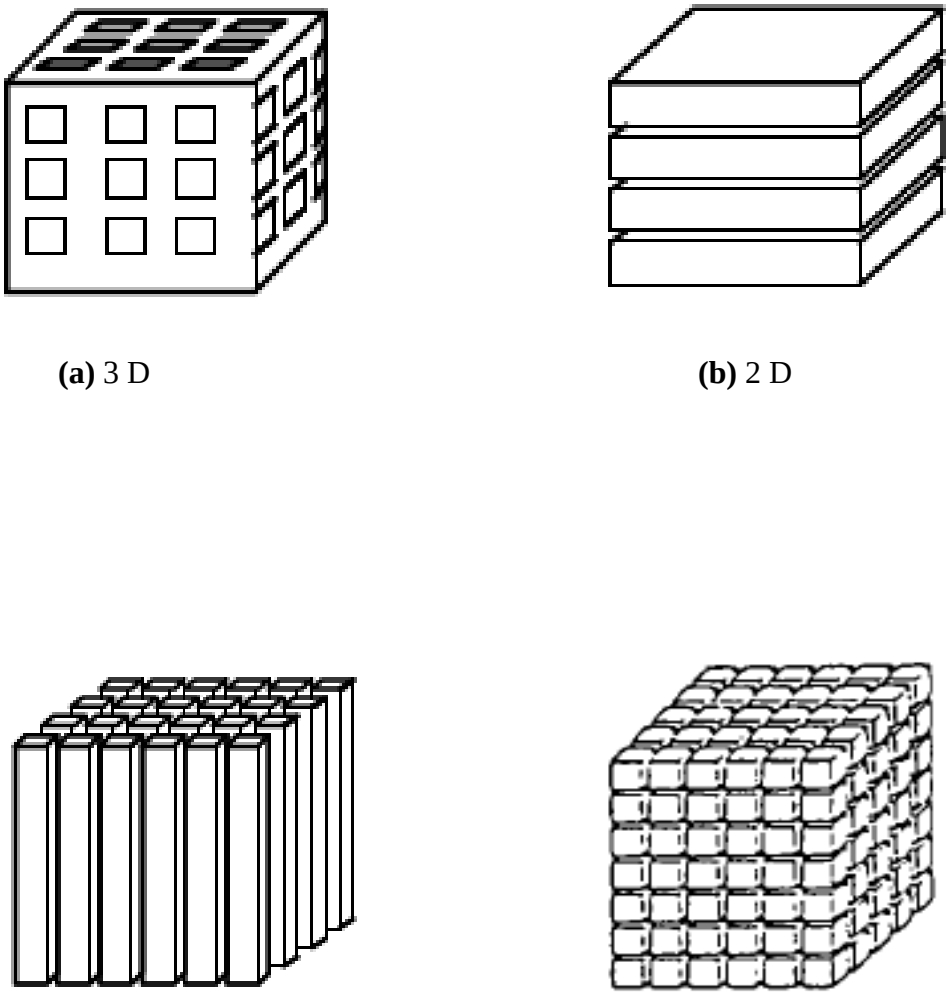

(a) 3 D

(b) 2 D

(c) 1 D

(d) 0 D

Figure 1.1 Insertion hosts shown with their structural dimensionalities [1]

1.2 GRAPHITE

Graphite is a layered host that is composed of hexagonal planar sheets of carbon atoms. Each planar single layer is called a graphene sheet. Within the graphene sheets the carbon atoms form σ bonds via sp^2 hybridization where the perpendicular non-hybridized 2p electrons are delocalized in a π bonding interaction. The intralayer C-C bond distance is 142 pm while the interlayer distance varies from 335 pm for HOPG (highly oriented pyrolytic graphite) and to about 345 pm for highly-disordered graphite. When these values are compared with the covalent and van der Waals radii of a carbon atom (r_{cov}= 77 pm, r_v= 185 pm) [4], it can be seen that while covalent bonding is present within the layers, only weak van der Waals interactions are present between adjacent layers. Due to the presence of weakly bound adjacent sheets, graphite is well-known for its intercalation of different atoms, ions and molecules within its gallery (interlayer space).

Graphite crystallizes in the space group $P6_3/mmc$ with lattice parameters of a=b= 0.246 nm, and c= 0.608 nm. There are two known stacking arrangements of the graphene sheets, the hexagonal (ABAB stacking order) (Figure 1.2) and the rhombohedral (ABCABC stacking order) phases [5]. The rhombohedral phase is metastable and transforms into hexagonal graphite if heated to high temperatures or by formation of an intercalation compound followed by its dissociation. Due to the low transformation energy of AB into ABC stacking (and vice versa), perfectly stacked graphite crystals are not readily available. The parameters of rhombohedral phase are a= 0.246 nm, c= 3*0.335 nm = 1.005 nm [6].

The electrical conductivity and many chemical properties of graphite are related to its delocalized π bonds. Graphite has an electrical conductivity of 5 Scm^{-1} (at 25 ^0C)

perpendicular to the planes which increases with the temperature (graphite is a semiconductor in that direction) and $3x10^4$ Scm^{-1} (at 25 ^0C) parallel to the planes which decreases as temperature is increased (metallic conduction) [7]. Graphite is also known for its ready cleavage parallel to the planes of atoms which makes the powder slippery so that it can be used as a lubricant [4].

There are many known polycrystalline graphites, examples include flaky graphite (average particle diameter ~250 μm), SP1 graphite (Union Carbide, average particle diameter ~100 μm), mesocarbon microbead (MCMB) type spherical graphite (average particle diameter ~1-10 μm), natural graphite (NG) (average particle diameter ~1-2 μm) from Madagascar or Ceylon and highly oriented pyrolytic graphite (HOPG). Detailed characterization of the structural and the physical properties of graphite compounds often requires the use of the most crystalline material (i.e. HOPG) [9]. In addition to these graphitic microstructures, other carbons include crystallites containing carbon layers having significant misfits and misorientation angles of the stacked segments to each other (turbostratic orientation or disorder). This disorder can be identified from an increased average planar spacing compared to graphite [8].

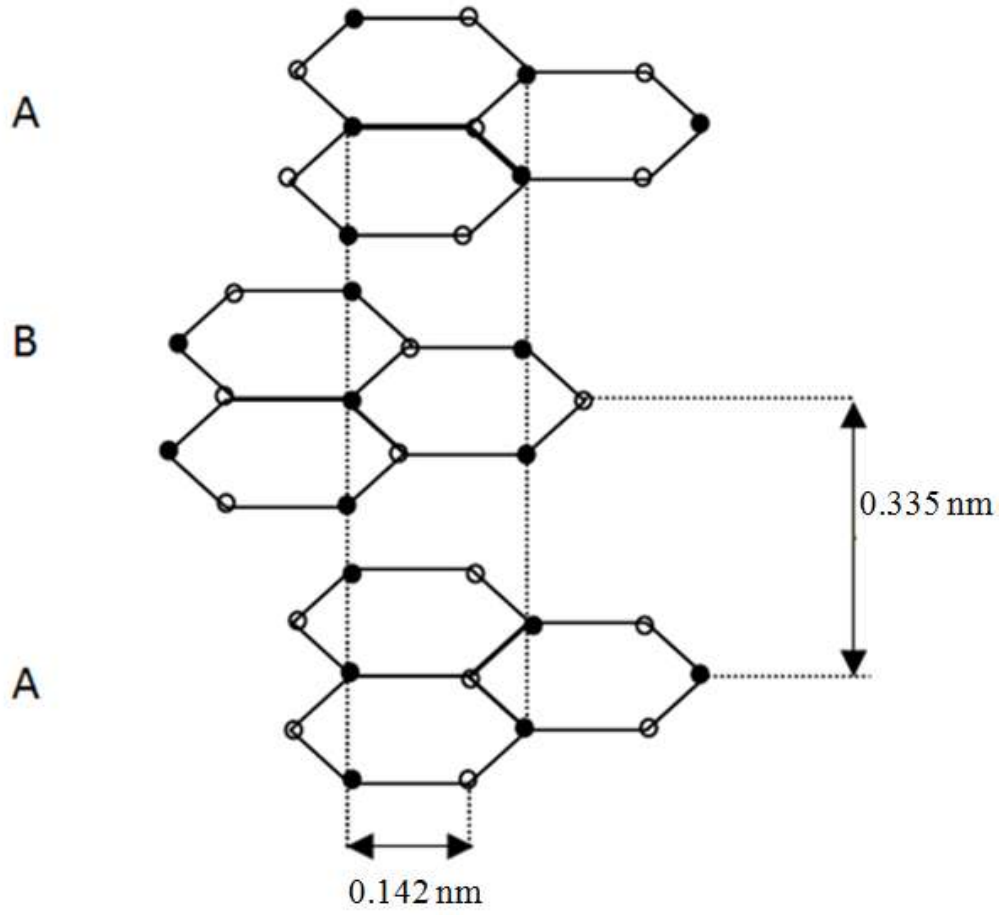

Figure 1.2 The ABAB hexagonal stacking of graphite structure

1.3 GRAPHITE INTERCALATION COMPOUNDS

Graphite can intercalate various guests in between its parallel sheets (Figure 1.3) to form graphite intercalation compounds, abbreviated as GICs [10]. The synthesis of a GIC using potassium was first reported by Schaffäutl (1841) [11]. However, the first systematic studies of these compounds began in the early 1930s with the introduction of X-ray diffraction techniques for stage index determinations [12]. Uniquely, graphite allows either anions or cations as intercalates, in the former case carbon sheets are oxidized and become positively charged (acceptor-type GICs) where in the latter, they are reduced and become negatively charged (donor-type GICs). Graphite intercalation is therefore a redox reaction and intercalation requires the use of either strong oxidizing or reducing agents or the application of a potential in an electrochemical cell.

The following two reactions are examples of acceptor-type and donor-type GICs, respectively. In Equation 1.1, the oxidizing agent is fluorine gas, and the intercalate anion is BF_4^- along with a neutral co-intercalate BF_3. In Equation 1.2, an electrolyte of KPF_6 in dimethylsulfoxide (DMSO) is used and graphite is electrochemically reduced to intercalate K^+ along with the solvent as co-intercalate [13].

$$x\mathrm{C\ (s)} + (1 + \delta)\ \mathrm{BF_3\ (g)} + \tfrac{1}{2}\ \mathrm{F_2\ (g)} \longrightarrow \mathrm{C_xBF_4 \cdot \delta BF_3\ (s)} \qquad (1.1)$$

$$x\mathrm{C\ (s)} + \mathrm{K^+\ (sol)} + \mathrm{e^-} \xrightarrow{\text{DMSO}} \mathrm{C_xK \cdot \delta DMSO\ (s)} \qquad (1.2)$$

1.3.1 Staging

An interesting and special feature of graphite intercalation is the process called "staging". Staging is defined as the ordering sequence of the occupied galleries and the neighboring graphene layers. In a GIC, not every adjacent graphene sheet is necessarily separated by an intercalate layer. For example, a stage 3 GIC has intercalate present between every third graphene sheet. For a stage 2 GIC, intercalates are present between alternating layers of graphene. Thus, the largest uptake of the intercalates occurs in stage 1 GICs where intercalate is present between all graphene sheets, as illustrated in Figure 1.3. The stage index (n) and the intercalate concentration are thus inversely proportional. This type of intercalate ordering is not common for other layered hosts; the high electronic conductivity and flexibility of the graphene sheets is thought to be responsible for staging, which minimizes electronic and mechanical strain energies [1].

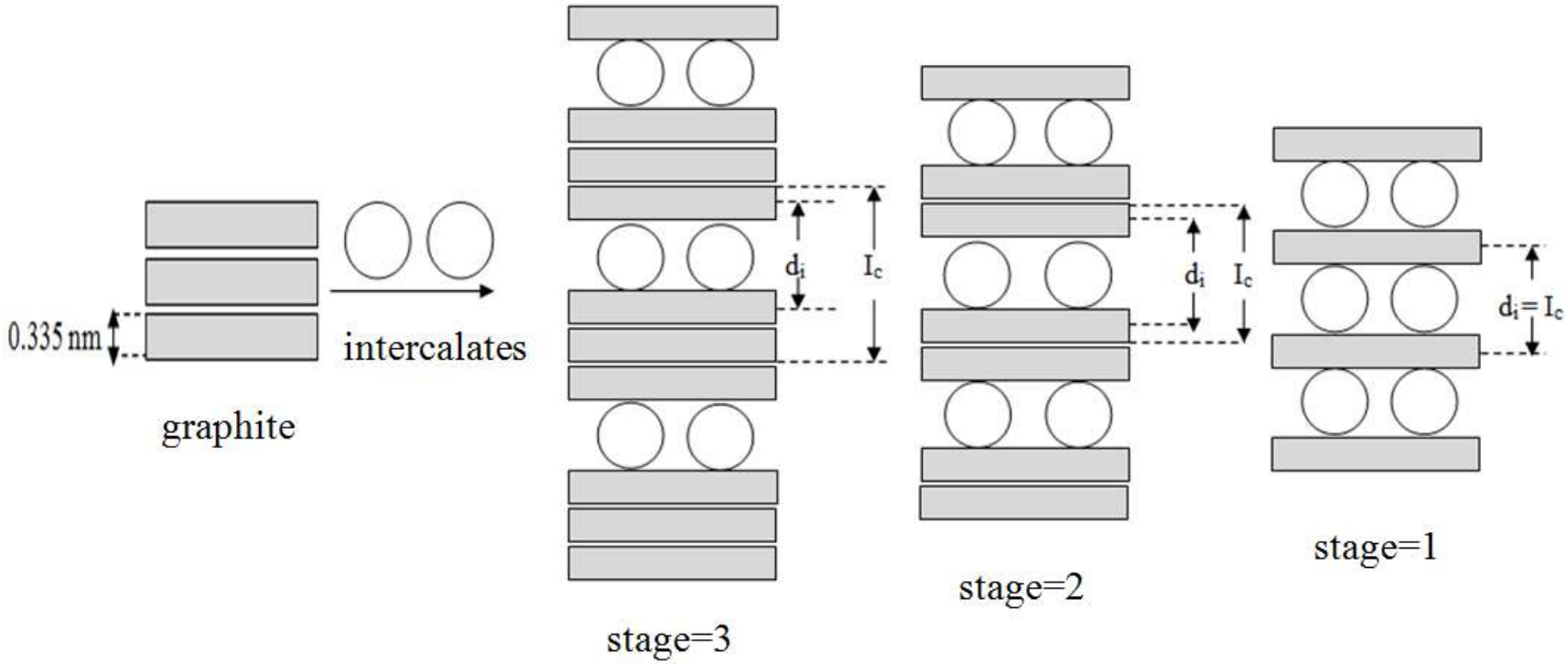

Figure 1.3 Graphite and the staging of GIC's along the stacking direction are shown schematically

The relationship between d_i, gallery height, I_c, periodic repeat distance along the stacking direction and n, stage is given by the following equation:

$$I_c = d_i + 0.335 * (n-1) = l * d_{obs} \quad (1.3)$$

where *l* is the index of *(00l)* planes that are oriented in the stacking direction, and d_{obs} is the observed value of the spacing between two neighboring planes. The value of *l* can be determined from d_{obs} of each diffraction peak.

The staging phenomenon which is shown in Figure 1.3 is known as the ideal Rüdorff staging model. This model does not explain the facile staging transformations between differently staged GICs. Later, a further refinement was adopted in order to explain the staging phenomenon and the stage transitions. This Daumas-Hérold domain model is illustrated in Figure 1.4 [14]. In this model, the average extension of an intercalate gallery was described by Daumas and Hérold, who showed that the intercalate volumes can be described as domains of intercalate islands, and stage transitions therefore requires only the motion of islands over the domain boundaries. The boundaries are formed by elastically deformed graphene layers. So, this explains the facile stage transitions that occur during intercalation [1]. There are two energetic terms associated with this type of staging, the first one is the coulombic repulsion of intercalated galleries due to oppositely charged graphene sheets, the second is the elastic strain energy required to mechanically surround the intercalated domains by graphene layers. The Daumas-Hérold model has been experimentally observed; the domains were directly imaged in $C_xFeCl_4.\delta FeCl_3$ using high resolution TEM [15].

In some GICs, there are neutral molecules present together with the intercalate ions in the galleries. These neutral molecules are called “co-intercalates”, and can originate from excess neutral reactants, from reaction by-products, or from solvents used in the intercalation reactions. The uptake of neutral co-intercalates is also observed with other layered hosts, such as transition metal chalcogenides. The neutral molecules might change the gallery heights of GICs depending on their dimensions, and also their uptake is often reversible and dependent on reaction conditions. Especially for GICs containing smaller intercalates, gallery heights can be related to the size of the solvent molecules or to the intercalates. The GICs will be represented in a formula of C_xAn.δN or C_xCat.δN in this thesis where An represents the anion, Cat represents the cation and N represents the neutral molecules. Donor-type examples include GICs synthesized by chemical method giving $C_{32}M(C_2H_6O)_y$ where M= Na, K, C_2H_6O= dimethylether (DME) and $C_xLi(C_4H_8O)_y$, where C_4H_8O= tetrahydrofuran (THF) [16]. The acceptor-type examples are the electrochemically synthesized GICs in electrolytes where PF_6^- and AsF_6^- anions dissolved in nitromethane which can produce GICs of $C_{48}PF_6(CH_3NO_2)_{2\text{-}4}$ (stage-2, d_i= 0.77 nm) and $C_{24}AsF_6(CH_3NO_2)_2$ (stage-1, d_i= 0.80 nm), respectively [17, 18]. A similar result was obtained with propylene carbonate solvent with anions of X= BF_4^-, PF_6^- and SbF_6^- yielding $C_{24}X(C_4H_6O_3)_x$ [19].

The neutral molecules can stabilize the lattice since they are positioned between intercalate ions and therefore reduce ionic repulsive interactions.

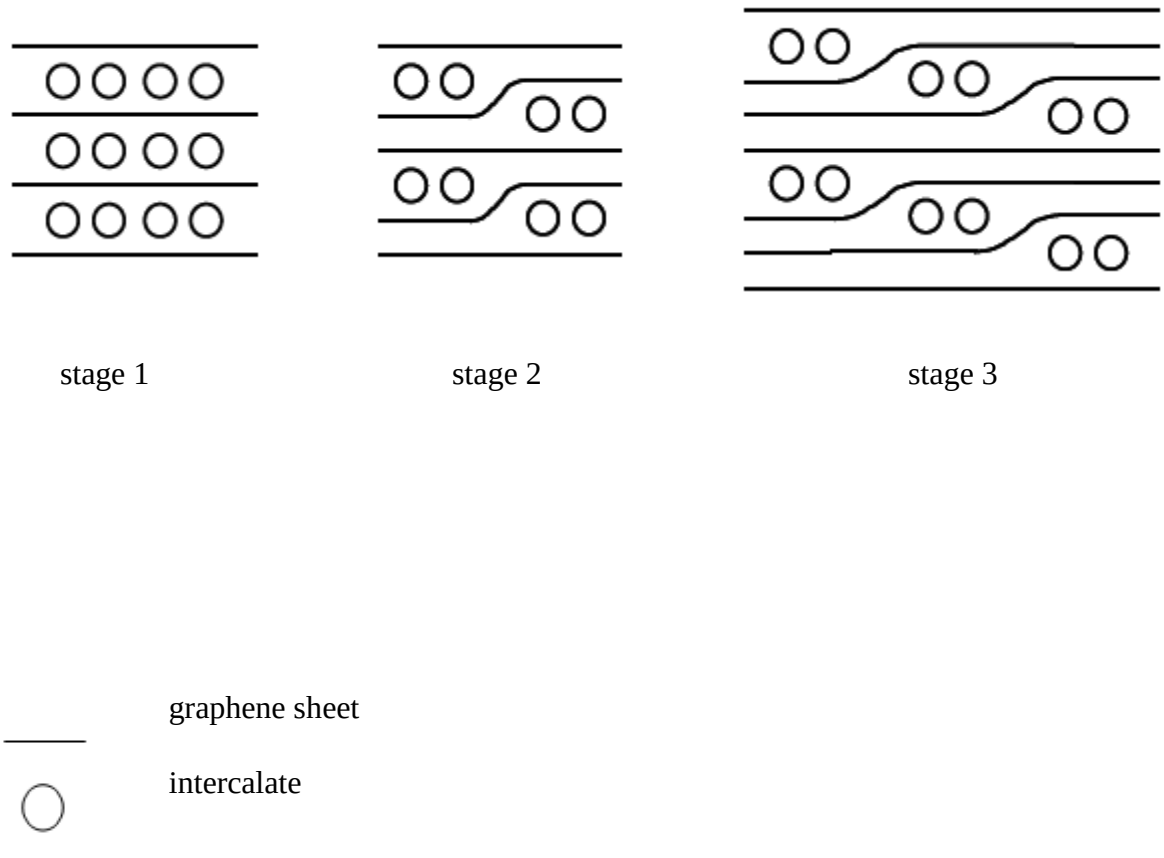

Figure 1.4 Daumas-Hérold domain model

1.3.2 Thermodynamics of intercalation reactions

A Born-Haber approach can be instructive in understanding the energetics of graphite intercalation. Here, the formation of acceptor-type GICs containing fluorometallate anions will be discussed as an example. The first application of a modified Born-Haber cycle to graphite acceptor compounds was made by Hennig [20]. Later, Bartlett and co-workers [21-23] noted that most of the fluoroanions have a similar effective diameter (~0.5 nm) in their intercalated form within the sheets of graphite. According to Hagiwara and Bartlett, [9] the explanation is that these anions all form, in effect, two layers of close-packed fluorine ligands with metal cations occupying either tetrahedral or octahedral sites in the double layer. In Figure 1.5, the packing arrangement of an octahedral MF_6^- anion is shown with the six fluorine atoms around the metal (3 on top, 3 at bottom). For a tetrahedral anion, the atom arrangement would be similar where the three fluorine atoms lie in the center of the 3 hexagons, and one fluorine atom sitting above.

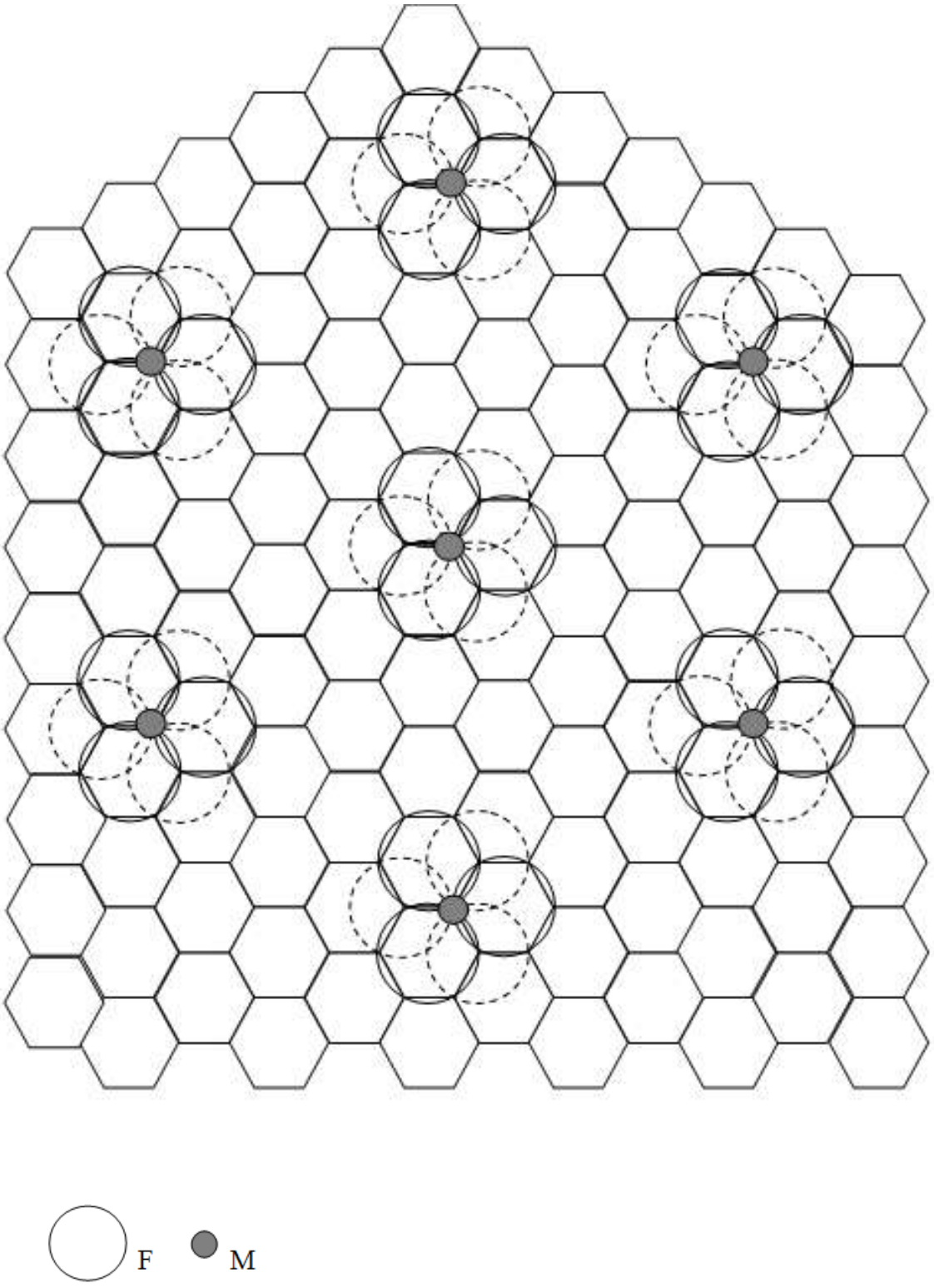

Figure 1.5 Packing arrangement of anions in $C_{24}MF_6$

The thermodynamic cycle of intercalation for MF_6^- type anions is shown schematically in Figure 1.6 where M= W, Re, Mo, Os, Tc, Ir, Pt. In this figure, there are four enthalpic steps associated with the intercalation reaction. These steps are the separation of graphite layers (step 1), ionization of graphite layers (step 2), electron affinity for formation of fluorometallate anion (step 3) and condensation of ions to form the GIC (step 4) [9]. If an intercalation reaction will occur, the enthalpy change of the net intercalation reaction must be sufficiently exothermic to balance the unfavorable entropy change. This cycle is similar to the Born-Haber cycle for simple ionic compounds. As a result of the model described above, the work of separating the graphene sheets and making them positively charged is similar for octahedral and tetrahedral fluorometallates (steps 1, 2 in Figure 1.6). Step 4 will also be similar when the ion packing densities within these galleries are similar. According to the investigations of various binary fluorides at RT, intercalation mainly depends on the electron affinity for the gaseous fluorometallate anions in step 3. The estimated threshold enthalpy for intercalation is an electron affinity of about -480 ± 40 kJ/mol. If the electron affinity is more favorable than -520 kJ/mol then first stage GICs are formed, no intercalation occurs if this enthalpy is less exothermic than -440 kJ/mol. In between those two enthalpies, higher stage GICs can be formed. This model also extends to other fluorometallate intercalates. The overall free energy change (ΔG^0) for the net interaction reaction can be used to evaluate whether a spontaneous intercalation occurs [9]. The formula below shows the free energy change for intercalation at T= 298 K where ΔH^0 is the enthalpy change and ΔS^0 is the entropy change.

$$\Delta G^0 = \Delta H^0 - T\Delta S^0 \qquad (1.4)$$

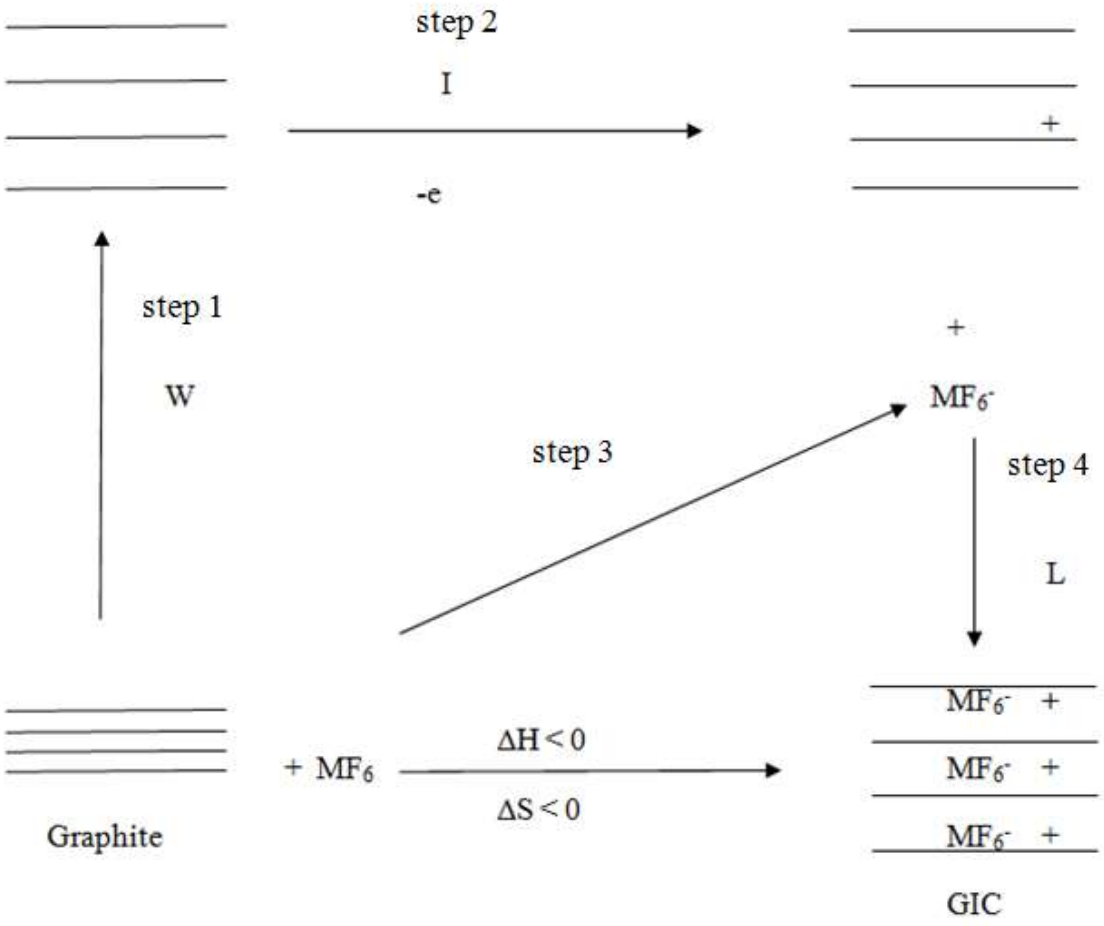

Figure 1.6 Thermodynamics of metal fluoride intercalation for MF_6^- type anions (M= transition metal) [9]

The entropy change for intercalation reactions should be negative. Although it is hard to precisely evaluate the entropy changes, they can be estimated in the following way. The entropy change for the net intercalation reaction can be approximated to be that for the transition of gaseous reactants to the solid state where the entropy changes of the graphite layers are taken as approximately zero [20]. Entropy data for the gaseous species at 298 K are available in literature [24] and the entropies of the solids are estimated by Latimer's method [25] using Equation 1.5.

$$S = 3/2*R*\ln A - 3.9\ JK^{-1}mol^{-1} \quad (1.5)$$

where A is a relative atomic weight.

For all reactions except those in which all reactants and products are solids (OsF_5, UF_5), the $T\Delta S$ entropy changes at 298 K are in the range 55 ± 33 kJ/mol. Thus, the entropic contribution to the overall energy changes are relatively small, and errors associated with this estimate are unlikely to change the overall sign of ΔG predicted [9]. Therefore, the enthalpy for the net intercalation reaction can be calculated from Hess's Law according to Equation 1.6 and the spontaneity of the intercalation reactions can be predicted.

$$\Delta H^0_{298}\,(\text{net intercalation reaction}) = \Delta H^0_{298}\,(\text{step 1} + \text{step 2} + \text{step 3} + \text{step 4}) \quad (1.6)$$

Another way of understanding the energetics of intercalation reactions is by evaluating the required electrochemical potentials for intercalation. For example, as

compared with the other layered hosts graphite requires a high oxidation potential, an onset of + 4.5 V vs Li/Li^+ is observed to form acceptor-type GICs, and a low reduction potential, an onset of + 0.4 V vs Li/Li^+ [1] to form donor-type GICs. These very high or very low potentials for intercalation of anions and cations respectively, place redox stability limits on the choice of intercalates and co-intercalates. For oxidative intercalation, fluorometallates, perfluoroalkyls, perfluorinated sulfonates and sulfonyl amides are some examples of stable intercalate candidates. There is also a relationship between the size (gallery height) and the oxidative potentials required for intercalation of these anions. In Figure 1.7, the intercalation chemical potential is shown to have an approximately linear relationship with the inverse gallery height ($1/d_i$). This is a simple extension of the Born-Haber model described above and has been proposed by our group. This model further indicates that, in order to intercalate larger size anions (d_i= 1.4 nm), a potential of about + 5.1 V vs Li/Li^+ will be required [26].

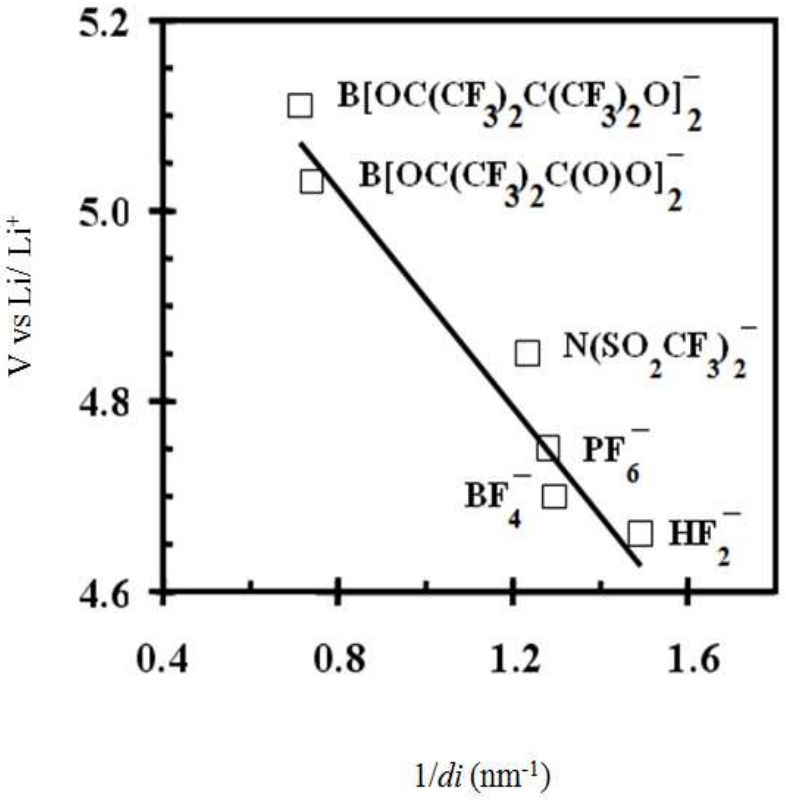

Figure 1.7 Relationship between oxidation potentials for stage 2 GICs and $1/d_i$ [26]

1.4 GRAPHITE OXIDE (GO)

Through the oxidation of graphite, covalent bond formation is possible where sp^2 to sp^3 hybridization transformation occurs for some or all of the carbon atoms. Covalent bonds can also be obtained in fluoride GICs of type $(CF)_n$. These covalent bonded compounds, are graphite oxide and graphite fluorides, will be described in more detail in the following sections.

GO is known from very early times, its first synthesis is reported by oxidizing graphite with $KClO_3$ / HNO_3 in the 1850's [27]. The two other common GO preparation methods are reported later by Staudenmeier [28] and Hummers [29]. All of these methods involve the oxidation of graphite but differ in the kind of mineral acids and oxidizing agents used, as well as in the time of preparation, and the type of washing and drying processes [30]. Some of the known oxidizing reagents are HNO_3 / $HClO_3$, H_2SO_4 / $NaNO_3$ / $KMnO_4$, H_2SO_4 / HNO_3 / KCl and H_2SO_4 / $(NH_4)_2S_2O_8$ / P_2O_5 [31].

GO is a layered structure as graphite, but has a brownish (Hummers) or slightly yellow (Brodie) appearance due to the loss of electronic conjugation upon oxidation. GO has a hydrophilic character which means water molecules can easily intercalate between graphene layers. This hydrophilic character is also responsible for the easy dispersion of GO in water, alkaline solutions or alcoholic media [32]. Generally, GO is consisted of oxidized graphene sheets which include mostly epoxide and hydroxyl groups in their basal planes, also carbonyl and carboxyl groups are located at the edges [33]. However, due to nearly amorphous nature of GO, there are ongoing debates on the structure of GO. The most recent models are proposed by Lerf and co-workers [34], Szabo and coworkers [35] and Gao and co-workers [36]. Lerf and co-workers envision GO as made of pseudo-

flat oxidized graphene layers. More precisely, the carbon grid would be formed by a random distribution of benzene and aliphatic rings. The oxygen functional groups would consist of 1,2-ethers and hydroxyl groups randomly distributed on the basal planes. In the model proposed by Szabo and co-workers, the carbon grid is not flat but puckered and is made of linked cyclohexane chairs connected to a benzene ring network. Besides, 1,3-ethers, hydroxyl groups and keto groups are present within the graphene layers. The most recent model proposed by Gao and co-workers is based on the model proposed by Lerf and co-workers except that five- and six membered- lactol rings are present along the edges of the layers.

GO itself can intercalate various types of guests including polar molecules as alkylamine [37] and ethylenediamine [38], polymers [39, 40] or ions [41, 42]. $Pd(NH_3)_4(NO_3)_2$ intercalated GO [43] and $NH_2C_3H_6SiCH_3(OC_2H_5)_2$ intercalated GO [44] are also known. These materials have micropores or mesopores between the carbon layers, and therefore may find use as adsorbents, catalyst supports and electrode materials for electric double layer capacitors, gas separation, etc [44].

GO is more recently of interest as an intermediate in the production of graphene. Several groups such as Stankovich et al., Gao et al. are searching ways to produce “cheap graphene” by chemical reduction of graphite oxide [33, 36] or graphite fluoride [45]. Until now, the formation of single-layer graphene with high conductivity, low functionality and high solubility has not yet been achieved on a large scale [36].

The target compound, graphene which is a single layer of carbon atoms bonded together in a hexagonal lattice, is of great interest due to its extraordinary electronic [46-48] and mechanical [49-51] properties. GO is thus used to produce primary cells having

high energy density which are required in the production of graphite nanoparticles and also used as an insulating material in nanodevices [52, 53]. The chemical reduction of GO used in the production of graphene can create highly functionalized carbon sheets (~3 % heteroatoms other than O) [54, 55] or materials with a surface polymer coating [56]. These functionalities can be -OH, C-O-C (epoxide) or –COOH groups [57]. In order to regain the advantageous electronic properties of graphene, defects caused by oxidation must be minimized [54]. For example, reacting graphene oxide with amines [58] produces octadecylamido graphite, G-CONH$(CH_2)_{17}CH_3$ (octadecylamine functionalized graphite), however the products not expected to exhibit the electronic attributes of graphene because of created residual (passivated) defects. According to TGA data in this study, the product retains about 7 wt % organic functional groups and 25 % acidic functional groups and residues. Some of these defects might arise from incomplete GO reduction or decreased particle dimensions during sonication [59].

There are other examples of defect generation in the production of graphene. Polymer-coated graphitic nanoplatelets can be obtained by using poly(sodium-4 styrene sulfonate) as a reducing agent to reduce exfoliated graphite oxide [60]. However, the presence of a polymeric dispersing agent in a graphene composite is undesirable for some applications. When ammonia is used as a reducing agent, this leads to graphene nanosheets with limited water solubility (< 0.5 mg/ mL) [55]. Si et al., developed a method to remove residual oxygen functionality [54]. They showed that by introducing sulfonic acid groups to partially reduced graphene oxide in a controlled manner, the majority of oxygen-containing functional groups can be removed. The charged -SO_3^- units prevent the graphitic sheets from aggregating in solution and yield isolated sheets of

graphene with improved water solubility. However, the product is a lightly sulfonated graphene. The electrical conductivity obtained from this graphene was comparable to graphite; however, in other cases the defects created during preparation are problematic for use in electronic devices [56].

1.5 POLY(CARBON) AND GRAPHITE FLUORIDES

Graphite is not intercalated spontaneously by elemental fluorine gas at room temperature and ordinary pressures; however, intercalation does occur in a temperature range of 400-600 ^{0}C to produce graphite fluorides consisting of poly(carbon monofluoride), $(CF)_n$ (first-stage) and poly(dicarbon monofluoride), $(C_2F)_n$ (second-stage) compounds. A second type of intercalation compound is called graphite fluoride, C_xF which is produced at lower temperatures [61, 62] by use of a carrier co-intercalate.

These two types of compounds differ in the nature of the carbon sheet structures, the type of C-F bonding, and their resulting properties. Poly(carbon fluorides), $(CF)_n$ and $(C_2F)_n$ can be found in white to almost black color and are prepared at temperatures as high as 300-600 ^{0}C. Their carbon skeleton is no longer planar, however, it includes trans-linked cyclohexane chairs with sp^3 bonding. In $(CF)_n$, the individual layer is formed with a 2D condensed cyclohexane network where the connected fluorine atoms protrude perpendicularly from the layer plane. The C-F bond length in C_xF is estimated at 0.140 nm, slightly longer than those in $(CF)_n$ and $(C_2F)_n$ (0.136 nm). The bond length of the C-C single bonds around the carbon atoms bound to fluorine atoms in C_xF are estimated by Sato et. al about 0.153 nm, slightly shorter than those in $(CF)_n$ and $(C_2F)_n$ (0.157-0.158

nm) [63]. The synthesis reaction of graphite fluorides can be shown as in Equation 1.7, where carbon reacts directly with fluorine gas. Both of the graphite fluoride materials can be used as active cathode materials in primary lithium batteries [64].

$$nC \text{ or } 2nC + (n/2)\ F_2 \longrightarrow (CF)_n \text{ or } (C_2F)_n \qquad (1.7)$$

Graphite fluorides, C_xF, are obtained by fluorination of graphite in the presence of a carrier Lewis acid such as HF. C_xF compounds retain planar (sp^2) graphene sheets with ionic or semi-ionic (semi-covalent) C-F bond formation. Fluorination can be done in the presence of Lewis acid or in anhydrous liquid HF (AHF) with elemental fluorine. Stage 1 C_2F compound can be synthesized under F_2 (g) / AHF environment [65] or in gaseous HF and IF_5 with elemental fluorine [66]. Compounds of stage 1-4 in a composition of $C_{4.2}F$-$C_{14.6}F$ can be produced by fluorination of graphite in the presence of AgF_3 or NiF_3 [67]. Fluorination of graphite in AHF with high-oxidation-state transition metal fluoride was employed to produce stage 1 C_xF with insoluble by-products [68]. While synthesizing C_xF under AHF, the fluorination reaction proceeds via co-intercalated C_xHF_2 formation according to Equation 1.8.

$$xC + \tfrac{1}{2}\ F_2 + (\delta+1)\ HF \longrightarrow C_xHF_2 \cdot \delta HF \longrightarrow C_xF \cdot \delta HF \qquad (1.8)$$

Bifluoride, HF_2^-, readily diffuses into graphite fluorides. Residual HF can be removed by evacuation. Stage 1 C_xF usually includes stage 2 and stage 3 phases as minority phases [69]. The intercalation of bifluoride, HF_2^- in K_2MnF_6 / aq HF

environment is also observed, a pure phase stage 2, C_xHF_2 can be produced within minutes at ambient temperature [70]. A bifluoride intercalated GIC is reported by Amine et al. with a composition of $C_{2-3}(HF_2)_{0.2-0.5}$ having a gallery height of 0.55-0.64 nm [71].

1.6 DONOR-TYPE GICs

In the preparation of the donor-type GICs, a low electrochemical potential (0.4 V vs Li/Li^+), or strong chemical reductant, is required to obtain stage 1 GICs. At these potentials many common electrolytes are themselves reduced, and even in successful reactions a passive surface formation on the graphite is seen for GICs synthesized electrochemically. Alkali metals, alkali earth metals, rare earth metals are the major examples of intercalate guests for donor-type GICs. Specifically, alkali metal stage-1 GICs are known for their gold color and their rapid decomposition under ambient atmosphere [7]. Among these, LiC_x is the most technologically important donor-type GIC because of its use as the anode in commercial Li-ion batteries [72].

Many methods have been employed to synthesize these GICs, including vapor-phase, solution-phase, high pressure and electrochemical reactions. For example, using the vapor-phase reaction, alkali metal GICs (K, Rb, Cs) can be easily synthesized at temperatures of 200-550 ^{0}C in a Pyrex tube, or using the electrochemical method, K-GICs can be produced in dimethylsulphoxide (DMSO) [73]. For Li-GIC synthesis, due to high reactivity of Li metal instead of pyrex, a stainless steel tube can be used or a solution-phase method can be accomplished by dissolving a lithium salt in solvents such as liquid ammonia or DMSO [7]. For some alkali metal GICs, only limited stages have

been reported, which has been explained by the relative sizes and ionization potentials of the intercalates. For example, only high stage Na-GICs are reported with composition $C_{8n}Na$ (n= 4-8) [74, 75]. Using a Born-Haber analysis, Hérold and coworkers [76] explained the relative instability of low-stage C_xNa. The ionization potential decreases from Li to Cs while the ionic radius increases. Lower ionization potentials indicate that electrons are more readily transferred to graphite. Nevertheless low-stage Li-GICs are very well known, this can be explained by the smaller radius of Li metal, leading to a greater lattice enthalpy for the GIC product, which offsets the higher ionization potential [7].

Alkaline earth metals such as calcium, strontium and barium can also form GICs despite their high ionization energies; however, slow kinetics are observed due to the low diffusivities of the divalent cations. These properties along with their low vapor pressures, require higher temperature (400-500 ^{0}C) syntheses and long reaction times to obtain low-stage GICs [77]. Ternary GICs of these alkaline earths together with Li and Na are also known [78]. GICs with small size donors as Li, alkali earth metal and rare earth metal have been reported in a composition of $C_{6n}M$ however stage-1 GICs of larger alkali metals like M= K, Rb, Cs have a composition of C_8M and higher stage GICs are formulated as $C_{12n}M$.

The gallery heights of the GICs containing alkali metals increases with increasing the ionic radius from Li to Cs. The d_i values for the stage 1 GICs are reported as 0.37 nm for $C_{6n}Li$, ($n \geq 1$) [79], 0.46 nm for $C_{6n}Na$, (n=4-8) [74], 0.54 nm for C_8K [79], 0.57 nm for C_8Rb [80], 0.46 nm for C_6Ca [77, 81], 0.49 nm for C_6Sr, 0.52 nm for C_6Ba [77]. Other stage 1 GICs of C_2Li [82], $C_{2-3}Na$, C_4K, C_4Cs [83], $C_{4.5}Rb$ [84] have been prepared

under high pressures. Ternary graphite-sodium-halogen compounds are reported by heating graphite in molten sodium in the presence of NaCl, NaBr and NaI salts in solid or liquid state [85]. GICs of $C_{3n}NaCl_{0.5}$ (where n is the stage) with stages 2-4 are produced by this method having about 0.756 nm gallery heights, also second and third stage ternary GICs with sodium and bromide are prepared with about 0.771 nm gallery heights and second stage GICs of $C_{3n}NaI_{0.166}$ or $C_{3n}NaI_{0.333}$ with 0.769-0.790 nm gallery heights [86]. This study reports the quaternary compounds of stage 2, $C_{7.5}NaI_{0.28}Cl_{0.15}$ and similar GICs with the intercalation of Na-I-F and Na-Cl-F.

GICs of low vapor pressure metals are difficult to synthesize except for stage 1 GICs of rare-earth metals, C_6Eu, C_6Sm and C_6Y [87]. The high stage compounds of rare earth metal are prepared by vapor transport technique in two steps. In the first step, co-intercalation of alkali metal and rare earth occurs and stage is mainly controlled by vapor pressure of alkali metal, in the second step preferential deintercalation of alkali metal produces high stage rare earth GICs together with residual alkali metal (ex: $C_yEu_xK_{1-x}$ where x= 0.75). These compounds are interesting due to their two-dimensional magnetism and their potential applications as magnetic storage materials [88]. The preparation of lanthanide-ammonia-GICs of $C_xLn(NH_3)_y$ (Ln represents many of the elements from this group) have been reported. Metallic solutions of these elements in liquid ammonia were obtained by anodic dissolution of the metals [89].

1.7 ACCEPTOR-TYPE GICs

There is a wide range of anions that can intercalate to form acceptor-type GICs, including tetrahedral, octahedral fluoro-, chloro-, bromo- or oxo-metallates, perfluorinated sulfonates and sulfonyl amides. The known fluorinated intercalation compounds have interlayer spacings from 0.67 nm for monolayer HF_2^- [90] up to 3.4 nm for $C_{10}F_{21}SO_3^-$ bilayers [91]. Acceptor-type GICs will be discussed below according to the intercalate type, sections will describe GIC's containing fluorometallates, chlorometallates, oxoanions, borates, and phosphates.

1.7.1 Fluorometallate Intercalates

The research interest in fluorometallate intercalated GICs was sparked by the study of Vogel et al. in 1977 who found that the electrical conductivity (at 300 K) of C_xAsF_y exceeded that of copper metal [92]. The intercalation reaction of AsF_5 is shown in Equation 1.9 below. According to this equation, the intercalate species is AsF_6^- where neutral AsF_5 is denoted with δ, to represent the co-intercalate (this is one of the many references that report the GIC formula as if only neutral intercalates are present, i.e. "C_xAsF_5", and will be re-formulated here as the $C_xAn\cdot\delta N$ model). A later report, however, found that the conductivity of $C_xAsF_6\cdot\delta AsF_5$ was only 1/3 or 2/3 of that of copper [93, 94]. Later, vapor-grown fibers intercalated by AsF_5 have also been claimed to have very high electrical conductivities ($\sigma_{300K}\sim10^6$ S/cm) [95, 96].

$$2xC\,(s) + (3+2\delta)AsF_5\,(g) \longrightarrow 2C_xAsF_6\cdot\delta AsF_5\,(s) + AsF_3\,(g) \qquad (1.9)$$

Hexafluorometallate intercalates are denoted as MF_6 where M= Mo, Os, Ir, Pt, U. The reaction of these fluorometallates with graphite may result in partial (UF_6 [97, 98]) or complete reduction of the produced species to oxidation number V for Mo, Os, Ir and to oxidation number IV for Pt to produce stage 1 compounds [99] or higher stage GICs [100]. Reaction of graphite with pentafluorometallates of AsF_5 and SbF_5, can produce GICs which range from stage 1 to stage 3. The intercalation of species like SbF_3Cl_2 produces stage 1 GICs of $C_{27}SbF_3Cl_2$ [101]. Some transition hexafluoro, pentafluoro, tetrafluoro and oxyfluoro metallates require the addition of a strong oxidant for intercalation to occur, examples include VOF_3 [102], CrO_2F_2 [103], VOF_3-CrO_2F_2 [104], WO_2F_2 [105] and $MoOF_4$, WOF_4 [106]. The examples of oxidative atmospheres include gases like F_2, Cl_2, a mixture of F_2 and HF, CrO_2F_2 [107, 108].

As mentioned in above section 1.3.2, generally there is a minimum electron affinity requirement of the fluorometallate anion for intercalation (-480 ± 40 kJ/mol) [99]. However, even when the transition metal hexafluoride (e.g. WF_6 [107]) does not have sufficient electron affinity to react directly with graphite, if a strong oxidant is added (such as F_2 gas) it is possible to form stage 1 GICs. For example for hexafluorometallates including Mo, W and Re metals, stage 2 and stage 1 GICs ($C_{10\text{-}20}MF_6$) can be obtained under F_2 and HF gas mixture [108, 109]. The intercalation reactions including the species listed in Table 1.1 occur under an oxidative atmosphere of $MF_y + F_2$.

There are many methods for the intercalation fluorometallates including gas-solid phase reactions (with F_2 gas or HF gas), solution-phase reactions, nonaqueous solvent reactions and solid state reactions [110]. For example, intercalation of

pentafluorometallates including Ru and Os metals require high temperatures, 120 ^{0}C (for RuF_5) and 90 ^{0}C (for OsF_5) to produce stage 1 GICs of compositions $C_{\sim 5}RuF_{4.5}$ and $C_{\sim 8}OsF_5$ [111]. Another example is $C_{8n}AsF_6 \cdot \delta AsF_5$, which can be produced using different AsF_5 partial pressures [93, 112]. The intercalation of SbF_5 is much slower compared to AsF_5, (about 20 days is required to form a stage 1 GIC at 20 °C) and requires higher temperatures, about 70 ^{0}C to obtain $C_{6.5}SbF_6$ [113].

Table 1.1 For the selected oxometallates and fluorometallates, the oxidants, GIC formulas and stages are given [9].

$M(O, F)_y$	**Oxidant**	**GIC (stage)**	**Reference**
MF_5 (M=Mo, W, Re)	F_2	$C_{10\text{-}20}MF_6$ (1,2)	[108,109,114]
VF_5	F_2	$C_{8\text{-}80}VF_6$ (1-8)	[109]
MF_5 (M=Nb, Ta)	F_2, Cl_2	$C_{8\text{-}10}MF_{\geq 5}$ (1)	[109,106,114,115]
PF_5	Cl_2	C_xPF_6 (2)	[116]
BF_3	F_2, Cl_2	C_xBF_4 (1), (4)	[116,117]
GeF_4	F_2, Cl_2	$C_{12}GeF_5$ (1), $C_{24}GeF_{5.1}$ (1)	[116,118]
SiF_4	F_2	C_xSiF_5 (2)	[119]
TiF_4	F_2, Cl_2	$C_{10\text{-}16}TiF_y$ (2), $C_{19\text{-}24}TiF_4$ (3)	[111,120,121]
IF_5	F_2	-	[9]
$TiF_4 + TiOF_2$	F_2	-	[9]
VOF_3	F_2, Cl_2	$C_{15}VOF_4$ (2), $C_{37}VOF_3(Cl_2)_{0.16}$ (3)	[122,123]
CrO_2F_2	-	$C_{22}CrO_2F_2$ (3)	[106]
MOF_4 (M=W, Mo)	F_2	$C_{\sim 12}MOF_4$ (1-5)	[61, 106]
F(HF)	F_2	$C_{2.8}F(HF)_{0.4}$-$C_{16}F(HF)_{4.3}$ (1)	[90]

In an oxidizing environment containing a mixture of F_2 and HF, graphite fluorine-rich GICs are produced where bifluoride intercalates and then is exchanged for a larger fluorometallate anion [124]. This type of exchange reaction is observed with the following oxidative reagents, IF_7, ClF_5, ClF_3, BrF_5 or BrF_3 at room temperature [124, 125].

Liquid AHF is common solvent for oxidation of fluorinated species. General reaction conditions are at RT or below RT with the use of a cryostat in transparent FEP Teflon tubes. Reaction time varies from a day to a week. The rate of intercalation can be raised by bubbling F_2 gas through AHF [70]. Some of the intercalates that produce stage 2 GICs by this method are SnF_4 and PbF_4 with an intermediate of graphite bifluoride, C_xHF_2 [126]. Stage 4 GIC of $C_{40}VOF_3$ is reported to form after being heated at 20-60 ^{0}C for several weeks [102].

Recently, several examples of noble metal fluoride GICs have been obtained, with M= Ru, Os, Rh, Ir, Au using either solid-gas (gaseous pentafluorides) or the solid-liquid (AHF) reactions where the gallery heights of the GICs range from 0.45-0.52 nm [127].

1.7.2 Chlorometallate Intercalates

Research for GICs containing chlorometallates speeded up, especially with transition metals, following the first report by Rüdorff et al. in 1963 [127]. These GICs attracted attention due to their high electrical conductivity, magnetic properties, catalytic activity, and relatively high air stability [128, 129]. GICs containing metal chlorides can

be obtained by a vapor-phase method [128, 130], molten-salt method [131, 132], Cl_2(g) saturation followed by light irradiation [133], electrochemical oxidation using organic solvents [129] or aqueous acid solutions [134] and in molten chlorides such as $AlCl_3$ [135], $BiCl_3$ [136]. In the vapor-phase method, the vaporized metal chloride reacts with graphite in the presence of Cl_2 gas or vaporized $AlCl_3$ at the temperature where metal chloride is in the gas phase according to the following reaction [10]:

$$x\text{C (s)} + MCl_n\text{ (g)} + (\delta/2)\ Cl_2\text{ (g)} \longrightarrow C_xMCl_{n+\delta}\text{ (s)} \qquad (1.10)$$

Metal chlorides of type $FeCl_3$, $CuCl_2$, $AuCl_3$ and $SbCl_5$ do not need an external Cl_2 gas source since their own dissociation reaction (Equation 1.11) produces Cl_2 gas [7].

$$AuCl_3\text{ (g)} \longleftrightarrow AuCl_2\text{ (s)} + (1/2)\ Cl_2\text{ (g)} \qquad (1.11)$$

The two-zone vapor-phase preparation method is applied to prepare GICs with $FeCl_3$ (stage 2, 3), $CuCl_2$ (stage 1, 2) at temperatures of 295-450 ^{0}C in 2 days and 430-510 ^{0}C in 7 days respectively [130]. $NiCl_2$, $BiCl_3$ are known as intercalates, too [137].

The intercalation of chlorometallates including rare earth (Ln) metals was shown with the addition of $AlCl_3$ [138]. The formation of ternary-GICs containing $FeCl_3$ and the solvent was studied in propylene carbonate via electrochemical method producing GICs with gallery heights of 0.95 nm ($FeCl_6$ octahedra), 1.18 nm (double layers of $FeCl_6$ octahedra) and 1.03 nm ($FeCl_4$ tetrahedra) depending on the electrolyte

concentration [139]. There are reports on ternary GICs of graphite-$FeCl_3$-CH_3COOH (stage 3, d_i= 0.95 nm) and graphite-$CuCl_2$-H_2SO_4 (stage 1.5, I_c= 2.15) [140].

1.7.3 Oxoanion intercalates

GICs containing the anions present in acids as HNO_3, H_2SO_4, etc. are common examples of acceptor-type GICs. They are extensively studied because they can be used to generate exfoliated graphite (EG), an important industrial material. EG will be discussed later in section 1.8. For the formation of these GICs it is necessary to use chemical oxidizing agents as HNO_3, CrO_3, $KMnO_4$, $HClO_4$ and H_2O_2 or perform an anodic oxidation of graphite in a solution of the appropriate acid. The feasibility and the degree of intercalation are largely determined by the acidic properties of the intercalate and by the conditions of oxidation. For example, in strong inorganic acids (HNO_3, H_2SO_4, $HClO_4$), highly saturated first stage GICs can be formed; however, in weaker acids (H_3PO_4, $H_4P_2O_7$) related oxoanions are intercalated into graphite only upon long term heating in the presence of an oxidant to give only second stage GICs [141]. It is noted that [142] the higher the degree of dissociation of the acid, the lower the threshold concentration for the intercalation its conjugate oxoanion into graphite, and the lower the redox potential for the formation of the GIC.

These GICs are formed by oxidation of graphite and the insertion of the oxoanion (A^-) species along with the acid co-intercalates (HA= HNO_3, H_2SO_4, $HClO_4$, H_3PO_4, $H_4P_2O_7$) in the presence of an oxidant (Ox) [143, 144].

$$C_x^+ + A^- + \delta HA \longrightarrow C_xA\cdot\delta HA \qquad (1.12)$$

The oxidant is required in the intercalation of most oxoanions due to their low redox potentials except in concentrated nitric and perchloric acids. Nitric and perchloric acids can function as both co-intercalates and oxidants, *i.e.*, their direct reaction with graphite produces GICs.

For the stage 1 GIC containing HSO_4^-, the intercalation occurs electrochemically in H_2SO_4 just below the potential for the decomposition of the acid [145]. The intercalated oxoanion species are summarized in Table 1.2. In addition, there are ternary GICs of graphite-HNO_3-R (R= CH_3COOH, H_3PO_4, H_2SO_4) [146, 147]. Recently, GICs prepared with carbon fibers containing conjugate oxoanions of formic acid (mixture of stage-2 and stage-3) [148] and nitric acid [149, 150] have been reported.

Table 1.2 Oxoanion intercalated GICs in their related acid environments shown together with their d_i and stages [7].

In acid	GIC	d_i (nm) (stage)	Reference
HNO_3	$C_{24}NO_3 \cdot 3HNO_3$	0.780-0.785 (1)	[151]
H_2SO_4	$C_{24}HSO_4 \cdot 2H_2SO_4$	0.798-0.801(1)	[152,153]
H_3PO_4	-	0.803 (2)	[152,154]
$H_4P_2O_7$	-	0.819 (2)	[152,155]
H_2SeO_4	$C_{24}HSeO_4 \cdot \delta H_2SeO_4$	0.825-0.826 (1)	[154]
$HClO_4$	$C_{24}ClO_4 \cdot 2HClO_3$	0.773-0.795 (1)	[156]
HSO_3F	C_5SO_3F	0.804 (1)	[157]
HSO_3Cl	$C_xSO_3Cl \cdot \delta HSO_3Cl$	0.80 (1)	[158]
CF_3COOH	$C_{26}CF_3COO \cdot \delta CF_3COOH$	0.82 (1)	[159]
HSO_3CF_3	$C_{26}CF_3SO_3 \cdot 1.63HSO_3CF_3$	0.80 (1)	[160]

1.7.4 Borate intercalates

Tetrahedral $[BF_4]^-$ anion is reported as an intercalate anion forming GICs of stages 1-7 with gallery heights of 0.78-0.79 nm in 1980s [17, 161-164]. Other oxidatively-stable borates are alkylborates, $[BR_4]^-$ and alkoxyborates, $[B(OR)_4]^-$ where R= alkyl or aromatic groups such as phenyl and pyrrolyl [165, 166]. Barthel et al. [167] studied a series of alkoxyborate chelates, $[B(ORR`O)_2]^-$, and determined that the oxidation potentials increase by 0.1 V for each fluorine added on the R groups. It was also reported that the electrolyte conductivity is increased with the degree of fluorination of R groups. These properties are important considerations in either chemical or electrochemical intercalation reactions.

In Table 1.3 the known GICs containing alkylborate and alkoxyborate anions are summarized. Chapter 2 of this thesis will report the first synthesis of $C_x[BF(C_2F_5)_3]$. Additionally, in this thesis and in other previous reports, the intercalation reactions with a number of borate anions were attempted, but did not succeed. These include from previous studies, $[B(C_6F_5)_4]^-$, $[BF_3C_3F_7]^-$, $[BF_3C_4F_9]^-$, $[BF_3C_6F_{13}]^-$ and from this study $[B(CN)_4]^-$, $[B_{12}F_{12}]^{2-}$,and a mixture of $[B(CF_3)_4]^-$ (85 %) and $[B(CF_3)_3F]^-$ (15 %). The non-reaction of these anions is strongly dependent on the type of the anion and the preparation conditions. For example, in electrochemical method, the important parameters that have to be considered are oxidation limits of the anions, electrolyte purity, electrolyte concentration and scanning rates [168].

There are also no reports on intercalation of perfluorinated phenyl groups up to date. An example is aromatic $C_6F_5SO_3^-$ anion that was reported to show no GIC

formation [169]. A plausible explanation lies in oxidative instability resulting in the decomposition of the anion prior to intercalation.

The electrochemical intercalation of $[B(CN)_4]^-$ anion was attempted in this work using a $KB(CN)_4$ / nitromethane electrolyte. Powder XRD data showed graphite peak along with unidentified crystalline phases (yellow and white precipitates coated on electrodes), there were no GIC diffraction peaks identified by this reaction.

The chemical intercalation of $[B_{12}F_{12}]^{2-}$ anion was attempted in this study using either K_2MnF_6 / aq HF or F_2 (g) / AHF, the anion decomposed in these environments. For electrochemical oxidation a $Li_2B_{12}F_{12}$ / acetonitrile electrolyte was used, however powder XRD data of the product showed only graphite peaks.

Similarly, a mixture of $K[B(CF_3)_4]$ (85 %) and $K[B(CF_3)_3F]$ (15 %) salts did not show any GIC formation using either chemical and electrochemical methods.

Table 1.3 GICs that are formed with alkylborates, $[BR_4]^-$ and alkoxyborates $[B(OR)_4]^-$ including d_i, corresponding stages and the method of preparation where Echem and Chem represent electrochemical and chemical methods respectively.

Anion	**Gallery height (d_i, nm)**	**Stage**	**Method**	**Reference**
$[BF_4]^-$	0.77-0.79	1-3	Chem	[161-164]
$[B(OC(CF_3)_2C(CF_3)_2O)_2]^-$	1.40-1.45	1-3	Echem	[170]
	1.45	1	Chem	[170]
$[B(OC(CF_3)_2C(O)O)_2]^-$	1.33-1.39	2-4	Echem	[171]
	1.44		Chem	[172]
$[B(OC(O)C(O)O)_2]^-$	1.42-1.43	1-3	Chem	[173]
$[BF(C_2F_5)_3]^-$	0. 87-0.89	2-3	Chem	[174]
	0.87	2	Echem	[174]

1.7.5 Phosphorus containing intercalates

There are previously reported acceptor-type GICs that include phosphorus, for example, graphite-phosphorus oxyfluoride intercalation compound with a composition of $C_{6,8}P_2O_3F_4$ (unit cell repeat distance, I_c= 0.827 nm) [175]. GICs containing phosphate were first reported in the 1930s. Second stage GICs with H_3PO_4 and $H_4P_2O_7$ were prepared under relatively high temperatures with strong oxidizers for long reaction times (80-100 ^{0}C, CrO_3, 150 h). The repeat distances (I_c) of the GICs containing H_3PO_4, $H_4P_2O_7$ are reported as 1.14, 1.15 nm for stage-2 compounds [154, 155]. Later GICs of $C_{12}PF_{5.5}$ (d_i= 0.77 nm) and $C_{23}PF_6 \cdot \delta CH_3NO_2$ (d_i= 0.77-0.79 nm for stage= 2-3) were reported [162, 164]. Third or higher stage graphite compounds (d_i= 0.76-0.80 nm) with PF_5 and Cl_2 (oxidizing agent) gases under high pressure, and second stage graphite compounds (d_i= 0.78 nm) with PF_5, Cl_2 and HF gases under low pressure, are known [23]. The ternary compounds of H_3PO_4 with sulfuric and nitric acids were described in section 1.7.3 above. New GICs containing the tris(pentafluoroethyl)trifluorophosphate, $[(C_2F_5)_3PF_3]^-$ anion will be described in Chapter 4. This GIC has gallery heights of 0.82 and 0.86 nm for stages 4 and 2, respectively [176].

There are reports of donor-type GICs containing phosphorus, for example, stage 1 ternary compounds of graphite-phosphorus-potassium were reported in a composition, $C_{3.2}KP_{0.3}$ [177] and the solutions of Li and Na metals in hexamethylphosphoramide solvent are reported to produce blue colored, ternary stage 1 GICs of $C_{32}LiX$ and $C_{27}NaX$ (X= $[(CH_3)_2N]_3PO$) with 0.762 nm gallery heights [178].

One of the phosphate containing intercalates is tris(oxalato)phosphate, $[P(C_2O_4)_3]^-$ which is attempted for intercalation in this study. However with the chemical methods its

lithium salt showed bifluoride formation in K_2MnF_6 / aq HF environment and reacted vigorously in AHF. The electrochemical method tried in nitromethane and acetonitrile solvents showed only graphite and crystalline impurity phases for this salt.

1.7.6 Perfluoroalkylacetate, Perfluoroalkylsulfonate and Perfluoroalkylamide intercalates

The gallery heights of GICs containing perfluoroacetate derivatives of type, $[CF_3COO]^-$, $[C_2F_5COO]^-$ are similar, about 0.82 nm [179] and C_3F_7COOH is 0.84 nm (stage 2 GIC) [169]. GICs with the anions of the general formula, $C_nF_{2n+1}COOH$ however have not been obtained for n= 4, 7, 8 and 12 [169].

The smallest member among perfluorosulfonate intercalates is $[CF_3SO_3]^-$, reported by Horn et. al in 1977 and has a gallery height of 0.80 nm [180]. The other members of $C_nF_{2n+1}SO_3H$ family for n= 4, 6, 8 were synthesized by electrochemical method in propylene carbonate giving bilayer anion arrangements [181-183]. The electrochemical formation of these GICs are also studied by our group and a simple bench-top synthesis was developed [184, 185]. Other fluoroalkylsulfonate group including GICs are synthesized by our group are $[C(SO_2CF_3)_3]^-$ [186, 187], $[C_{10}F_{21}SO_3]^-$, $[C_2F_5OC_2F_4SO_3]^-$ which is a fluoroether chain and $[C_2F_5(C_6F_{10})SO_3]^-$ which is a para-substituted cyclohexyl ring [26]. The application of longer chain perfluoroalkylsulfonates may be limited due to environmental concerns over transport and toxicity.

Some of the perfluoroalkylamide $[N(SO_2CF_3)_2]^-$, $[N(SO_2CF_2CF_3)_2]^-$, $[N(SO_2CF_3)(SO_2C_4F_9)]^-$ including GICs have been synthesized by our group [186, 187].

Table 1.4 summaries these GICs along with their syntheses methods, gallery heights (nm) and observed stages.

In this study, the anion dinitramide anion was evaluated as a potential intercalate. Lithium dinitramide (LiN_3O_4) was dissolved in nitromethane but the product following electrochemical oxidation showed only graphite diffraction peaks. Intercalation of this anion was not attempted by chemical methods since the salt is known to be unstable in an acidic environment.

Table 1.4 GICs containing perfluoroalkylsulfonates and perfluorosulfonylamides with d_i, stages (+ meaning mixed of stages) and synthetic methods.

Anion	Gallery height (d_i, nm)	Stage	Method	Reference
$N(SO_2CF_3)_2^-$	0.81	2	Chem	[186]
$NCF_2(CF_2\ SO_2)_2^-$	0.85-0.86	2-3	Echem	[188]
$N(SO_2CF_2CF_3)_2^-$	0.80-0.81	1-2	Echem	[189]
	0.82	2+3	Chem	[186]
$CF_3SO_3^-$	0.80-1.15	1-2	Chem, Echem	[180]
$N(SO_2CF_3)(SO_2C_4F_9)^-$	0.82	3	Chem	[186]
$C(SO_2CF_3)_3^-$	1.06	4	Chem	[186]
$C_{10}F_{21}SO_3^-$	3.45	2	Chem	[26]
$C_2F_5OC_2F_4SO_3^-$	2.29	2	Chem	[26]
$C_2F_5(C_6F_{10})SO_3^-$	2.44	2	Chem	[26]

1.8 GENERAL APPLICATIONS OF GICs

GICs have attracted attention of theoretical physicists, chemists and engineers starting from their discovery in the 19th century. The electrical, electronic and catalytic properties of these materials led to a variety of new applications in electrical, electrochemical and chemical industries over the decades. Some of these applications [190, 191] are summarized in Table 1.5. Nowadays, GICs are principally used as electrode materials in Li ion secondary batteries, as well as in the production of exfoliated graphite, and as catalysts. Other applications that are based on functional properties of GICs are still under investigation; one limitation is their air-sensitivity. GICs are unique materials from science and engineering standpoints, however, more research is needed to overcome the limitations due to physical properties and synthetic challenges [192].

The anodes of commercial lithium ion rechargeable lithium batteries are made of graphite or carbon-related material. Because, i) they exhibit higher specific charges and more negative redox potentials than most metal oxides, chalcogenides and polymers, and ii) they have dimensional stability, giving better cycling performance than materials such as Li alloys. The insertion of Li into graphite proceeds according to reaction 1.13. This reaction is reversible where electrolytic reduction (charge) of the graphite host occurs in the charging step [193].

$$C_nLi_x \underset{\text{charge}}{\overset{\text{discharge}}{\rightleftharpoons}} xLi^+ + xe^- + C_n \qquad (1.13)$$

GICs are used in composited form as fire retardants, [194] and as catalysts in hydrogenation of olefins [195] and initiation of polymerization [196]. Exfoliated graphite is a commercially used material which can be produced by either rapid heating of GICs, such as $C_xHSO_4 \cdot \delta H_2SO_4$ to 1000 ^{0}C where vaporized intercalates force graphene sheets apart to become a hundred times larger in volume [7] or by delaminating GICs in a hot liquid. The commercial exfoliated graphite is called GRAFOIL manufactured by GRAF TECH Co. which is made by exfoliated natural graphite and rolling them into thin sheets [192]. The sealing materials based on Grafoil used at fuel, power and mechanical engineering plants have properties of leak tightness, reduction of amount of hazardous emissions such as asbestos which is a carcinogenic material [141]. Exfoliated graphite is used in the production of very thin graphitic flakes [57], used for gaskets, packing materials, electromagnetic shields [192], it is a thermal insulator at high temperatures or in corrosive environments, used as a gas adsorbent for gases and heavy oils, used in electrodes, lubricant supports, as additives for some composites [197] and as thermal spreaders for electronics such as plasma displays [198]. Some promising areas of use are in double-layer electric capacitors due to high surface area [199, 200] and in fuel cells of vehicles where strength, robustness and conductivity are important parameters. A substrate made from EG shows relatively higher thermal conduction versus copper metal which is a widely used conductor for the industry [201].

Heavy alkali metals in composition of $C_{24}M$; M= K, Rb, Cs can absorb small molecules as H_2 [202], NH_3 [203], hydrocarbons [204] by physical or chemical sorption. For example potassium-GIC absorbs hydrogen and becomes $C_{24}K(H_2)_{1.84}$ at 77 K [205].

A recent study also describes hydrogen adsorption of acceptor-type GICs such as fluoride intercalated GIC [206].

The sorption properties of GICs might be applied in the fields of gas storage and preparation of molecular sieves [192]. The chemical reactions in the nano-space of $C_{24}M$ has certain properties for example $C_{24}Cs$ can absorb ethylene molecules to become air-stable GICs of $C_{24}Cs(C_2H_4)$ at room temperature [207]. Other reported unsaturated hydrocarbons as styrene, 1,3-butadien, isoprene can also be absorbed into nano-space of $C_{24}M$ and polymerize there to expand the galleries [208]. Some GICs such as alkali metal fluoride-GICs [209] and metal chloride-GICs [210] are also known as catalysts in organic reactions. For example, palladium nanoparticles produced by reduction of a $PdCl_2$-GIC's are used as catalysts in hydrogenation and isomerization reactions [211].

One potential application of GICs can be their use as highly conductive and lightweight materials, since they are lighter than metals and have higher in-plane electrical conductivities (RT) with respect to pristine graphite [212].

Some GICs also have higher Seebeck coefficients, and lower thermal conductivities (RT) than graphite. These GICs can be used in thermoelectric devices due to their light weight, high selectivity of shapes (plate, sheet, fiber, powder, etc.) and nontoxic nature. Examples of such GICs include Li, K, Cs for n-type and $FeCl_3$, $CuCl_2$, $MoCl_2$ for p-type intercalates [212].

There is an increased amount of research on novel nanomaterials based on graphite and carbon, especially nanotubes, fullerenes, and graphene which are promising for understanding the properties and exploring the future applications of graphite-related materials [192].

Table 1.5 Current and proposed applications of GICs with the intercalate types shown.

Applications		**Guest species**
Exfoliation of graphite		H_2SO_4, HNO_3, $FeCl_3$, K-THF, Na-THF
Electrode materials	Primary battery	$(CF)_n$, $(C_2F)_n$, graphite-oxide, $CoCl_2$, TiF_4
	Secondary battery	Li, H_2SO_4, $Ni(OH)_2$, $Mn(OH)_2$
	Thermocell	Br_2, HNO_3
Catalysts for organic syntheses		Li, K, K-Hg, K-$FeCl_3$, SbF_5, Br_2, H_2SO_4, HNO_3
Proposed Applications		
For gas storage and isotope of hydrogen		K, Cs, Rb
Highly conductive materials		AsF_5, SbF_5, HNO_3, $FeCl_3$
Thermal energy storage		$MnCl_2$-NH_3
Electrochromism		Li-DMSO (dimethyl sulfoxide)
Superconductivity		Li, Na, K, Cs, Rb, Ca, Yb, Tl, Hg (C_8K, C_2Li, C_8RbHg, $C_4KTl_{1.5}$, C_6Ca, C_6Yb, $C_6Li_3Ca_2$)

1.8.1 Proposed applications for GICs synthesized in this study

The motivation for the preparation of the GICs in this thesis is to obtain acceptor-type GICs containing new anions and to create larger and more chemically complex intercalate galleries. Larger galleries can be generated by selecting large guest molecules, and this opens the possibility of interesting new intragraphene chemistry such as selective sorption, catalysis, nanocomposite formation and new routes to exfoliated graphene sheets.

EG is currently obtained from acceptor-type GICs including oxometallates prepared in strong acids such as sulfuric and nitric acid and by their subsequent treatment involving hydrolysis and thermolysis. The GICs prepared in this study are potential new precursors for thermally exfoliated graphite, with industrial uses in sealing materials including gaskets, packings, sealing bands and box rings [213].

As mentioned previously**,** graphene has been the subject of many studies for the past few years. Its proposed applications are in devices including solar cells, transistors, LCDs, gas sensor membranes, filler in nanocomposites, components in ultracapacitors and nanoelectromechanical devices due to its high electrical and thermal conductivity, high surface area, stiffness and high strength [213]. If some of these applications are realized, there will be a concurrent demand for rational and scalable methods to produce graphene. Our approach is to select intercalates which are initially large and bulky anions, and then explore the subsequent separation of the individual graphene layers by exfoliation.

As explained in the previous sections, the current method of using GO for the preparation of the graphene sheets generates defects such as oxygen-containing moieties

that can be detrimental to the obtained properties [214]. Electrical and thermal conductivities as well as the mechanical properties of the graphene sheets can be highly sensitive to the presence of defects and lattice disorder [215]. For example, the undesired defects in these structures can inhibit the charge transport in their devices by serving as scattering centers [213, 216]. For instance, large-area and high-quality graphene films are necessary for applications such as graphene field effect transistors (FETs) [217], bilayer pseudospin field effect transistors (BiSFETs) [218] and transparent conductive electrodes [219].

Because of this, alternate synthetic approaches will be a critical factor in the future applications of graphene in areas such as high-speed electronics. Thermally and electrically insulating structures can be produced by the effect of carboxyl and hydroxyl groups, this has been shown by Teweldebrhan et al. recently [220]. A clean and highly ordered graphene should have unique properties of extremely high RT carrier mobility (~27,000 cm^2/Vsec) [221] and thermal conductivity (~4840-5300 W/mK) [222]. Novoselov et al. found that highest quality graphene can be produced by mechanically exfoliating highly oriented pyrolytic graphite (HOPG) [223], however this method is not scalable for commercial applications, so alternative chemically-driven approaches are necessary.

One of the recent approaches for the clean and highly ordered graphene production is the substrate-free gas phase method introduced by Dato et al [224]. This technique involves sending an aerosol including liquid ethanol and Ar gas into an atmospheric pressure microwave-generated argon plasma reactor. Although only

milligram quantities of graphene have been produced in short reaction times, this may ultimately provide another route to a scalable method.

1.9 INTERCALATION METHODS FOR ACCEPTOR-TYPE GICs

1.9.1 Chemical Methods

Chemical methods require selection of an appropriate oxidizing agent for graphite and an oxidatively stable solvent if necessary. There are two chemical methods applied in this thesis. In the first method, oxidation of graphite is performed in K_2MnF_6 / aqueous HF (48 %) medium and in the second method, F_2 gas in anhydrous HF (AHF) is used in a metal-vacuum line. For the former method, our group has found that the most appropriate and convenient oxidizer is K_2MnF_6 [184] which is very soluble and stable at room temperature, and can be easily prepared according to the literature method [225] as shown in Equation 1.14. Among the two chemical methods applied, only the first method was successful in producing GICs in thesis (Chapter 2 and Chapter 3).

$$2KMnO_4 + 2KF + 10HF + 3H_2O_2 \xrightarrow{48\ \%\ HF} 2K_2MnF_6 + 8H_2O + 3O_2 \qquad (1.14)$$

There are some limitations of this method, including the oxidative stability of aqueous HF where only stage-2 or higher GICs can be prepared [186], also careful handling is necessary when using hydrofluoric acid. Other oxidants that can be used for

the first method include $KMnO_4$ and $K_2Cr_2O_7$ in concentrated acids [141], PbO_2 and $NaBiO_3$ in aqueous HF, however these oxidizers are not very soluble and can produce unwanted solid products that are difficult to remove from the GIC product. In the second method, due to the powerful oxidizing nature of F_2 and oxidative stability of AHF, stage-1 GICs can be formed however; the handling of F_2 or AHF is relatively difficult, also the reactant amount cannot typically exceed 1 g. The intercalate anions have to be soluble in AHF and be stable enough to survive in strong oxidizing reagent F_2. Nevertheless, there are many GICs synthesized previously [172, 173] using F_2 (g) / AHF method.

There are many advantages of the first chemical method over the electrochemical method for example, in the chemical method bulk quantities (multi grams) of GICs can be produced, the reaction times are shorter (minutes to several hours), there are no requirements for selection of binders and additives to form electrodes. The only consideration for the chemical method usage can be the impurities in the GIC product that can arise from the selected oxidant.

1.9.2 Electrochemical Method

Electrochemistry is one of the methods used in the formation of GICs and has been known for many years [226]. The basic difference that electrochemistry has over the chemical methods is its controlled environment of rate and reaction conditions and no requirement for oxidants. However this method requires longer reaction times and it produces less amounts of product (< 1 g). The high driving potentials (4.0 V vs. Li/Li^+ for oxidation of graphite) for these types of reactions can be easily obtained, which are

quite important for obtaining low-stage GICs. The high oxidation potentials limit the selection of appropriate solvents, current collectors, and binders. Some examples of solvents used for anodic oxidation of graphite are carbonates, sulfonates, sulfites, esters, acetonitrile and nitromethane [226]. Among these solvents, nitromethane has been found to be the most oxidatively stable [171].

Electrochemistry provides additional information about GICs including its stage, charge density, current yield, composition and also by this method, the reversibility of the intercalation can be examined. An idealized galvanostatic charge curve of a stage 1 GIC is shown in Figure 1.8. There are plateau regions in the charge curve where the transition from a higher stage to a lower one occurs. At the end of each plateau a lower stage GIC has been formed. For subsequent stage transitions, both the charging potential and the charge required for the transition increase. After forming the GIC, if a current in the opposite direction is applied then the reverse process may occur, this is called de-intercalation.

In this thesis, both one-compartment and two-compartment cell with a glass-frit separator are used for the electrochemical GIC formation (see Figure 1.9). Working electrodes were prepared by painting cyclohexane slurries of SP-1 graphite powder (50-120 mg) and 8-10 wt % polymer binder (EPDM= ethylene propylene diene monomer) onto Ni or Pt mesh flags (nominal area~ 1 cm^2) welded to the wires made from the selected metal. The coated electrodes were air dried to remove excess solvent (cyclohexane) before the experiments. Counter electrodes were stainless steel (SS) mesh and reference electrodes were either Ni or Pt wires. Cells were subsequently assembled and operated in nitrogen atmosphere glove box at ambient temperature. The cells were

filled with electrolyte solutions prepared with nitromethane. Typical currents applied were in the range of 8-70 mA/g carbon. After the reactions, working electrodes were removed from the solvent and washed with 1-2 mL of nitromethane to remove residual liquid electrolyte remaining on the electrode then dried at 100 milliTorr pressure for characterization.

SP-1 grade powder (Union Carbide, average particle diameter ≅ 100 μm) is used in all of the experiments performed in this study.

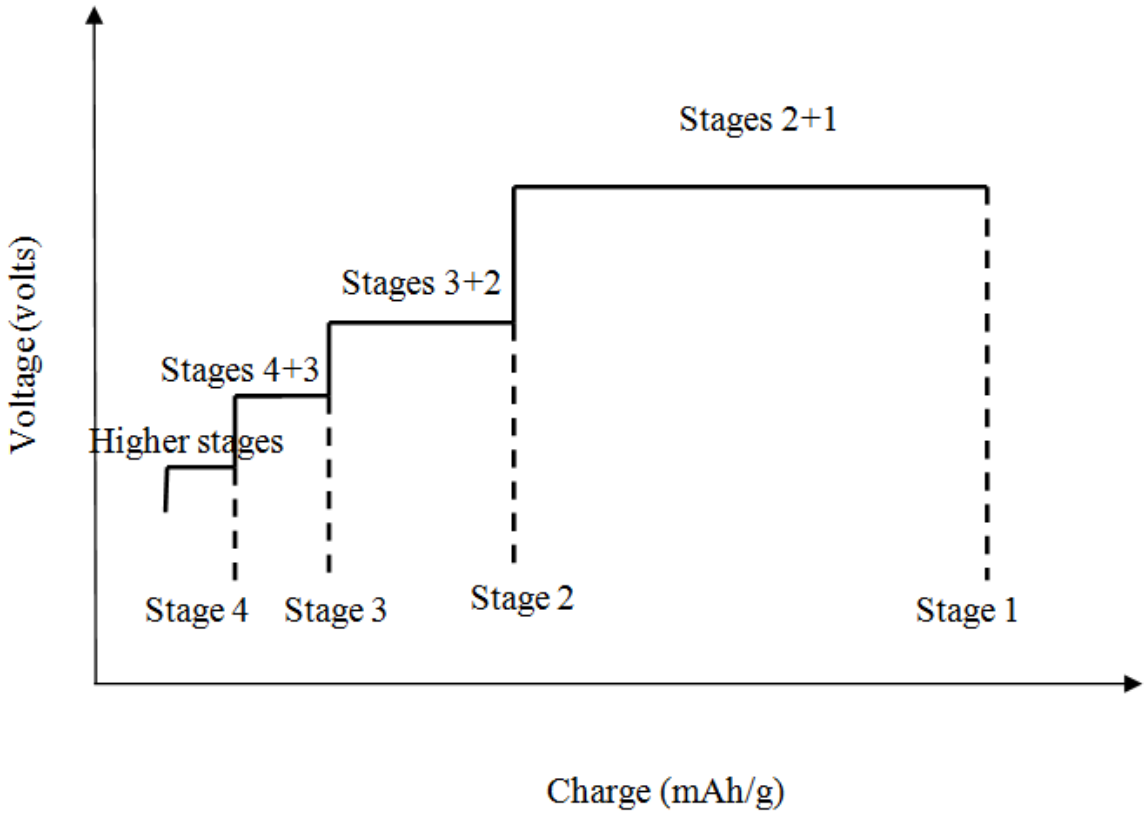

Figure 1.8 Ideal potential-charge curve for the preparation of an acceptor-type stage 1 GIC.

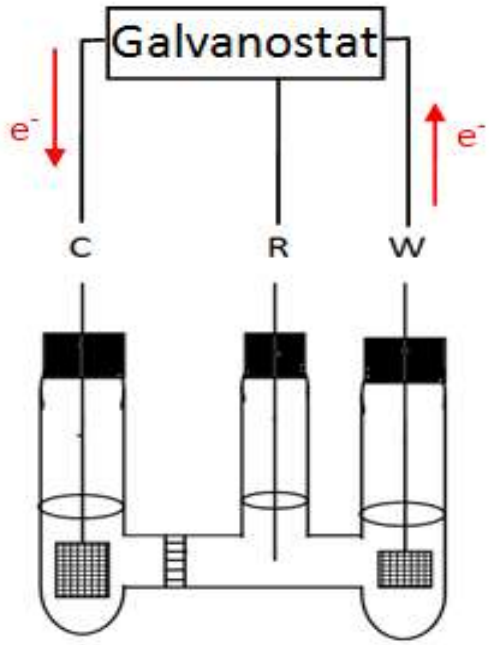

Figure 1.9 A two-compartment electrochemical cell with a glass frit including W= working electrode, R= reference electrode, C= counter electrode. The arrows indicate the electrons released during oxidation at anode and electrons added during reduction at cathode

1.10 ANALYSIS TECHNIQUES OF GICs

1.10.1 Powder X-ray diffraction (Powder-XRD)

Powder-XRD is a useful tool in understanding the structure of GICs, *(00l)* peaks in the preferred orientation (direction perpendicular to the graphene layers) are collected which are used in calculating the gallery heights and the unit cell repeat distances of GICs. Detailed explanation will be given in the following section.

Powder-XRD were collected on a Rigaku MiniFlex II diffractometer with Ni-filtered Cu K_α radiation using a detector slit width of 3 mm. Data were collected at a scan rate of 1^0 2θ / min, from 4^0 to 90^0 or from 4^0 to 65^0 at 0.02 min / step.

1.10.2 The calculation of gallery height and the repeat distance of a GIC

Generally $d_{(n+1)}$ and $d_{(n+2)}$ peaks are the two most intense peaks observed in powder-XRD of a stage n GIC. The ratios of $d_{(n+1)}$ / $d_{(n+2)}$ peaks and the most intense *(00l)* peaks are listed in Table 1.6 for stages 1-7. After finding the stage of a GIC then the calculations can be done from the observed *(00l)* peaks in order to find d_i and I_c. A representative example will be shown here. In Figure 1.10 powder-XRD of a stage 2 GIC of $C_x[(C_2F_5)_3PF_3]$ is given along with the observed d (d_{obs}) values listed in Table 1.7. According to the Equation 1.3 ($I_c = l * d_{obs}$), for each observed d_i, I_c can be calculated then an average I_c can be reported for that specific GIC. The d_i value then calculated (d_i, calc) according to the same equation ($I_c = d_i + 0.335 * (n-1)$) where n= 2 for the example given

here. The *(100)*, *(101)* and *(110)* indices that arise from the in-plane structure of the graphene sheets, so they are not used in the average I_c calculation.

Table 1.6 The strongest intensity *(00l)* indices and $d_{(n+2)}$ / $d_{(n+1)}$ ratios of a stage n GIC

stage (n)	$d_{(n+2)}$ / $d_{(n+1)}$	strongest *00l* peak
1	1.50	*002*
2	1.33	*003*
3	1.25	*004*
4	1.20	*005*
5	1.17	*006*
6	1.14	*007*
7	1.12	*008*

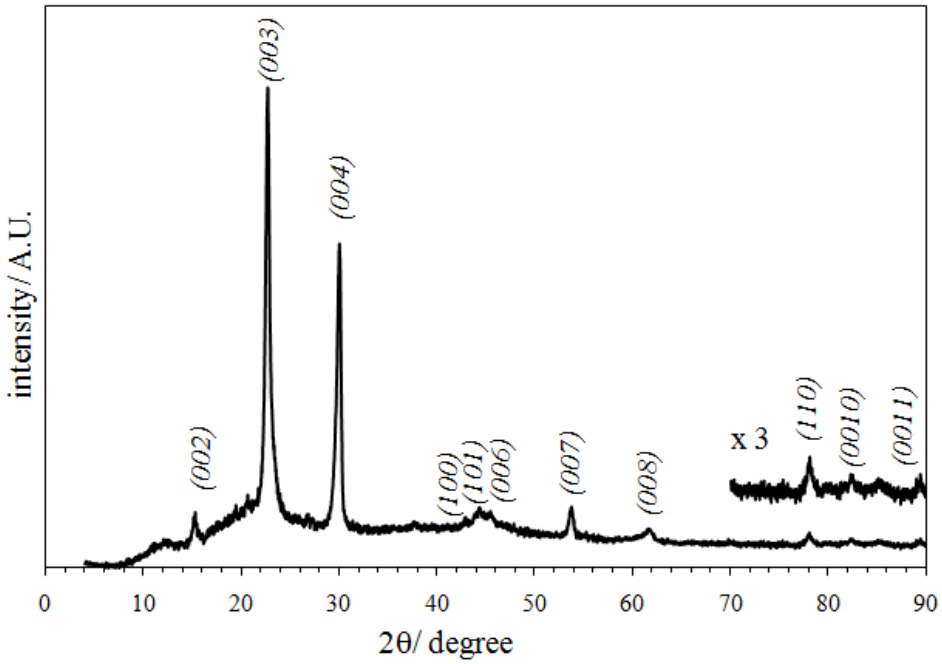

Figure 1.10 Powder-XRD peaks of a stage 2 GIC of $C_x[(C_2F_5)_3PF_3]$ along with the assigned *(00l)* indices.

Table 1.7 The assigned *(00l)* indices, observed d values and calculated Ic's and d_i are shown for stage 2 GIC of $C_x[(C_2F_5)_3PF_3]$.

(00l)	d, obs. (nm)	I_c, calc. (nm)
(002)	0.579	1.158
(003)	0.391	1.172
(004)	0.297	1.189
(006)	0.199	1.195
(007)	0.170	1.192
(008)	0.150	1.199
(0010)	0.117	1.168
(0011)	0.109	1.204
	I_c ave	1.184 ± 0.018
	d_i calc	0.850 ± 0.017

1.10.3 Thermal gravimetric analysis (TGA)

Thermal analyses were used to determine product compositions. The mass losses of the samples are observed with linearly increasing temperature. TGA data were obtained using a Shimadzu, Inc. TGA-50 thermogravimetric analyzer. Samples were loaded into a platinum pan; the sample chamber was flushed with Ar gas. Thermal scans from ambient to 800 ^{0}C-1000 ^{0}C were performed under flowing Ar at a rate of 5 ^{0}C/ min.

1.10.4 Elemental analyses

1.10.4.1 Fluoride analyses using an ion selective fluoride electrode

In this thesis, a new sample digestion procedure was developed in order to determine the free fluoride in GICs by using ion-selective fluoride electrode. A microwave digestion procedure of 22 min is adapted starting at 50 psi (~70 ^{0}C) for 15 min followed by 100 psi (~140 ^{0}C) for 7 min in a solvent of 1 ml 0.1 M NaOH (aq). Detailed explanation of this method can be found in the next chapters.

In order to create a calibration curve, stock and standard fluoride solutions are prepared using NaF as a standard fluoride reagent. The stock solution contains 100 ppm F^- (221.0 mg NaF in 1 L milli-Q water) and the standard solution prepared from the stock solution contains 24 ppm F^-. The subsequent standard solutions of 8.3 ppm, 2.9 ppm, 1.0 ppm and 0.5 ppm fluoride are prepared by dilutions from 24 ppm [F^-] standard solution. Equal volumes of (5 mL) of each standard solution or digested sample solution

and LLTISAB (low level total ionic strength adjustment buffer) solution are combined prior to analyses. Fluoride analyses were performed using an ion-selective fluoride combination electrode with a standard single-junction sleeve-type reference electrode and a mV scale voltmeter (VWR International, Inc.). The voltage measurements are repeated twice for 1 min periods, with a 5 min rest period between measurements, and an average voltage reading (mV) is calculated. During the rest period, the F^- probe is placed into a 5.8 ppm fluoride solution for 5 min with the voltmeter turned off. A calibration curve is obtained by plotting the obtained voltages versus logarithm concentrations (ppm [F^-]) of the standard solutions. A typical calibration curve is shown in Figure 1.11 (a). In some cases a linear relationship could not be obtained due to the aging of the probe, in such cases a second order polynomial calibration curve was used (Figure 1.11 (b)). The calibration curve is subsequently used to determine the concentrations of the GIC sample solutions by using the measured values of average potentials.

In order to check other interfering sources of fluoride the same procedure is repeated for samples including only millipore water, SP1 graphite and NaOH. The fluoride content observed in only SP1 solution was 0.02 mass percent and less than 0.5 ppm for millipore water and NaOH. Also, the validity of the procedure is checked by a control experiment prepared with a known concentration of NaF (aq) solution which is digested similarly and the results agree within < 1 %. The F^- content obtained by this method indicates the F^- content from the fluoroanion intercalates are < 0.1 %.

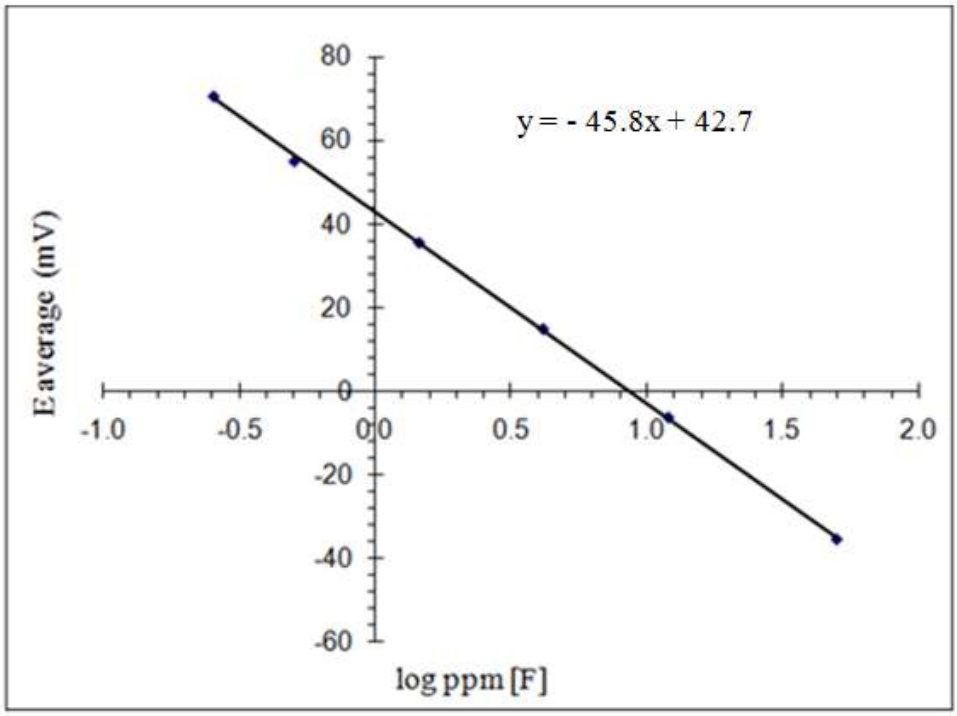

(a)

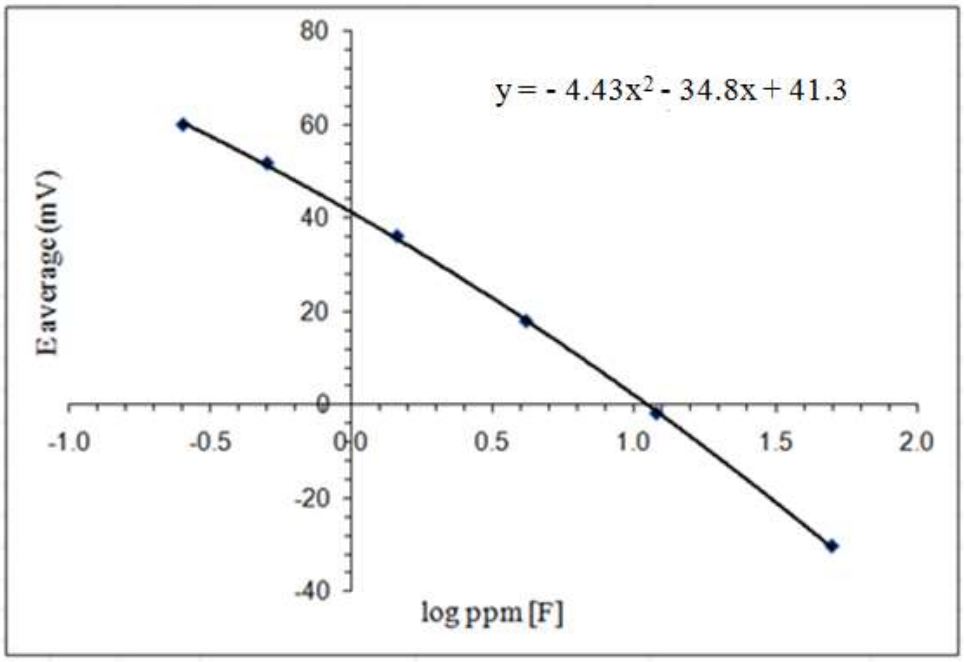

(b)

Figure 1.11 Typical calibration curves prepared with the measured average voltage and the log concentration (ppm) of the standard fluoride solutions

1.10.4.2 Inductively Coupled Plasma (ICP) for boron

For the characterization of synthesized GICs of $C_x[FB(C_2F_5)_3]$ (which is explained in detail in section 2.4 of this thesis), ICP-AES is used to determine the boron content of the GICs. The microwave digestion protocol described above is performed before the measurement. The selected B wavelength is 208.96 nm. A linear calibration curve (Figure 1.12) is obtained with four standard solutions of 2.5, 5, 10, 50 mg B/L by diluting a commercial boron standard (Spex Certiprep, 1000 mg B/L) (data are shown in Table 1.8). 2 % v/v HNO_3 acid solution is used as a blank for calibration. Using the calibration curve the concentrations (ppm) of the chemically prepared GICs at 1-20 h and the electrochemically prepared GIC (Echem) are determined in 2-8 % error as listed in Table 1.9. The calculated B mass % shown in this table is calculated using Equation 1.15 for each GIC after the x and δ parameters are calculated which will be explained in section 2.4. The measured ppm of B amounts with ICP are converted to mass % B amounts using Equation 1.16. As a control, the $K[FB(C_2F_5)_3]$ salt was digested and analyzed by the same method.

Table 1.8 The measured and calculated mg B/L the for standard solutions prepared and their measured intensities.

Std sol. #	mg B/L calc.	mg B/L meas.	Intensity
1	2.50	2.48	$2.15*10^4$
2	5.00	5.02	$4.41*10^4$
3	10.0	9.66	$8.54*10^4$
4	50.0	50.1	$4.45*10^5$

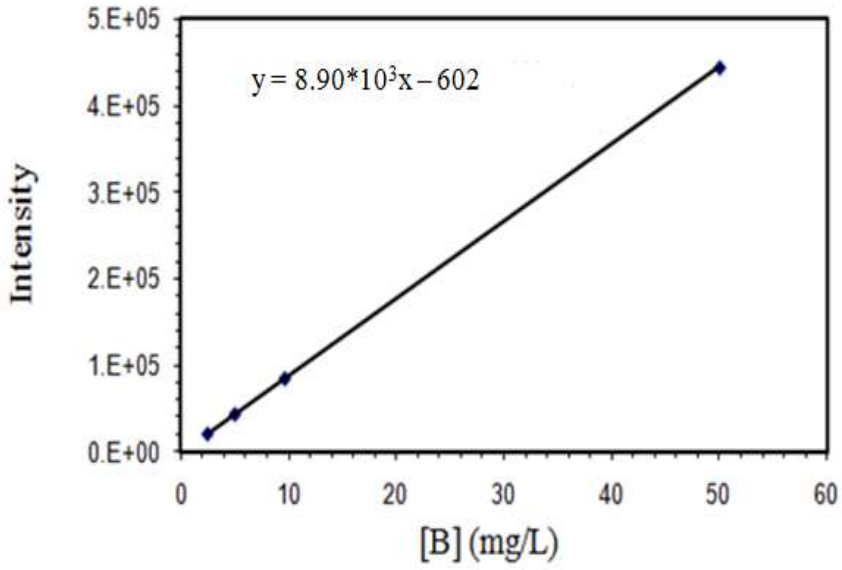

Figure 1.12 The calibration curve prepared for B analyses of the GICs

$$\text{mass \% B for GIC (calc.)} = \frac{10.8 * 100}{12x + MW_{anion} + 19\delta} \quad (1.15)$$

$$\text{mass \% B for GIC (meas. by ICP)} = \frac{\text{mg of B in digested solution} * 100}{\text{mg of GIC}} \quad (1.16)$$

Table 1.9 The measured (ICP) and calculated mass % B for GICs of $C_x[FB(C_2F_5)_3]$ at different reaction times along with the electrochemically prepared (Echem) GICs and the salt, $KB(C_2F_5)_3F$.

Sample	mass % B calc.	mass % B meas. (ICP)
1 h GIC	1.00	1.07
2 h GIC	1.02	1.07
5 h GIC	1.02	1.06
10 h GIC	0.95	0.99
20 h GIC	0.98	1.06
Echem GIC	1.13	1.16
$KB(C_2F_5)_3F$	2.54	2.59

1.11 STRUCTURAL MODEL CALCULATIONS FOR THE INTERCALATES

1.11.1 Energy minimization by using Gaussian software

All the molecular structures shown in this thesis are generated using Gaussian 03W software. The standard orientation geometry of the atoms is displayed in Cartesian coordinates. For the efficiency of the calculations, this orientation environment is chosen where center of nuclear charge of the molecule is placed to the origin. The energy-minimization of the isolated anions is calculated using the hybrid density functional method (B3LYP) with a 6-31G (d) basis set by GaussView 3.0 software.

1.11.2. Calculation of the GIC gallery height

One challenge is to determine the best fit for the energy minimized structure of the anion and the gallery heights (d_i) of the GICs that are calculated from powder-XRD data. The gallery heights along the stacking direction can be calculated by estimating the minimum height of the isolated anion according to the following formula;

$$d_i = h + 0.335 + 2r_F \quad (1.17)$$

where h is the vertical distance between two fluoride ion centers, 0.335 nm is the thickness of a graphene sheet and $2r_F$ is the van der Waals radii (0.133 nm) of two outer fluorine atoms with the highest and lowest heights along z direction. Figure 1.13 shows the gallery height, h and the van der Waals radius of a fluoride ion in a space filling

model of GIC schematically. The calculated gallery heights then compared with the ones calculated from powder-XRD data. Sometimes the overlaying or nestling of the fluorides onto the graphene sheets has to be considered which might predict slightly different d_i values compared to powder-XRD. For example, in the structure of a stage 2 GIC of C_2F this type of nestling is observed [227]. The double rows of intercalated fluorine have a close-packed structure where all the fluorine atoms are strongly nested into the hexagons of upper and lower carbon sheets. This nestling would decrease the repulsion force between two neighboring anions and stabilize the compound. The gallery height is calculated as 0.82 nm if the unnestled fluorine atoms are considered and 0.78 nm if nestled fluorine atoms are considered [9].

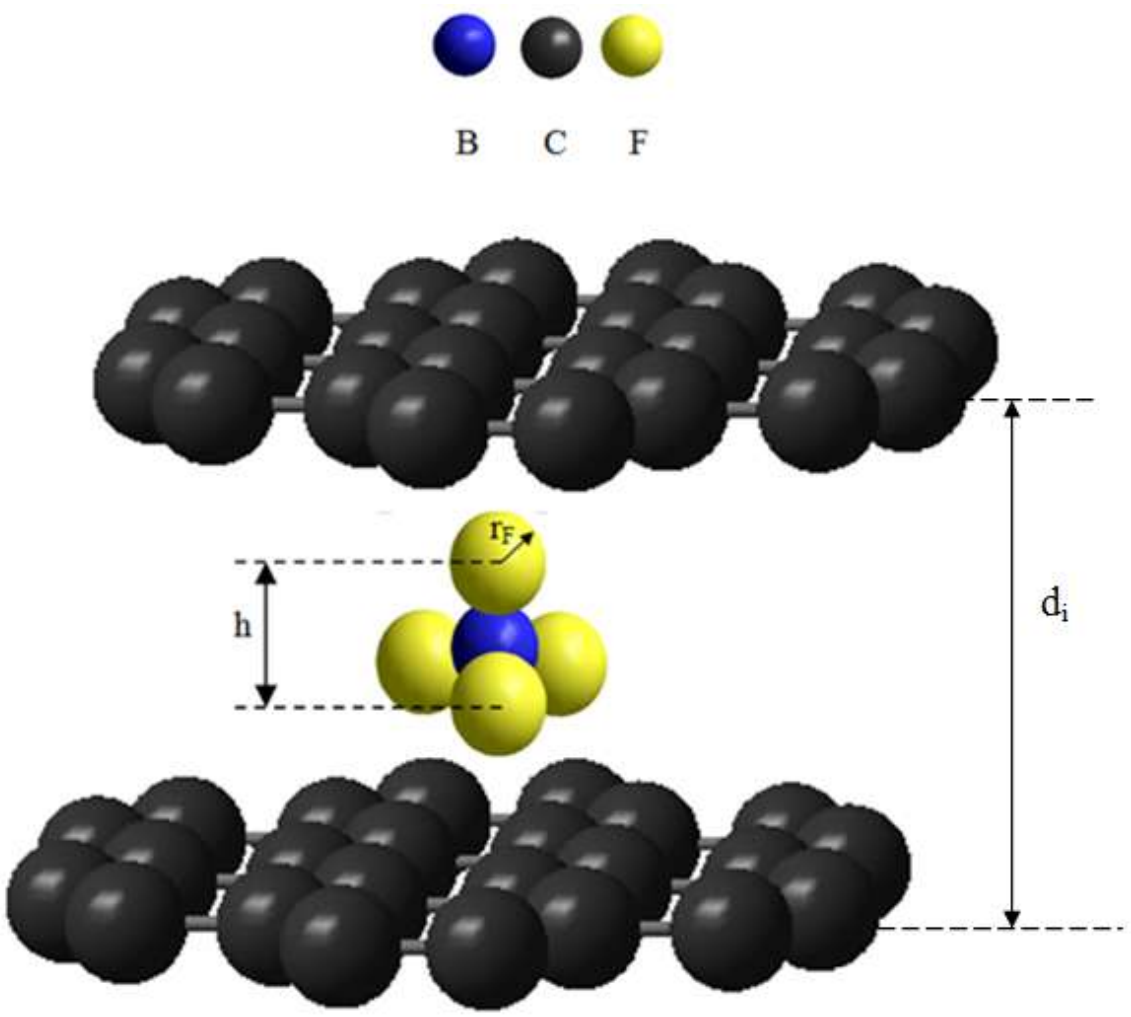

Figure 1.13 Schematic shown for the calculation of the gallery height of a GIC where d_i= gallery height, h= height of the anion, r_F= van der Waals radius of a fluorine atom.

1.12 THESIS OVERVIEW

In this thesis, acceptor-type graphite intercalation compounds (GICs) containing perfluoroalkyl anions are synthesized and characterized. The goal is to develop acceptor-type GICs containing new anions using both chemical and electrochemical methods. Investigation into these graphite intercalation compounds can provide new materials and better understanding of their properties.

Chapter 2 studies the synthesis of new GICs containing the fluoro-tris(pentafluoroethyl)borate anion, $[FB(C_2F_5)_3]^-$ by chemical and electrochemical methods. Powder XRD data indicate that the products are of mixed stage 2 and 3 with a gallery height of about 0.87 nm. A new digestion method is developed using an ion selective electrode and potentiometer that can quantitatively determine the fluoride co-intercalate content in the chemically prepared GICs. TGA data and the elemental B and F analyses are used to find the composition of the prepared GICs.

Chapter 3 describes the preparation of new GICs containing cyclo-hexafluoropropane-1,3-bis(sulfonyl)amide anion, $[CF_2(CF_2SO_2)_2N]^-$ by electrochemical method. The gallery heights of 0.85-0.86 nm are determined by powder-XRD data for stage 2 and 3 products. As a comparison of the GIC stabilities, linear bis trifluoromethane-sulfoylamide anion, $[CF_3SO_2)_2N]^-$ is also synthesized by the same method. TGA and elemental F and N analyses are used to characterize the electrochemically prepared GICs.

In chapter 4, the first GICs containing the tris(pentafluoroethyl)trifluorophosphate (FAP) anion, $[(C_2F_5)_3PF_3]^-$ have been prepared by electrochemical method. The chemical method was not sufficiently stable for the anion to form a GIC. The GICs of stages 2-4 are prepared in an ionic liquid/ nitromethane electrolyte with gallery heights of 0.82-0.86 nm.

1.13 REFERENCES

1. Schlögl, R. in *Progress in Intercalation Research; ed.* Müller-Warmuth, W.; Schöllhorn, R., Kluwer Academic: Dordrecht, the Netherlands, **1994**.

2. Oriakhi, C.O.; Lerner, M.M., Nanocomposites and Intercalation compounds, Encylopedia of Physical Science and Technology, Third Ed., Academic Press, **2002**, volume 10.

3. Zeng, Q.H.; Yu, A.B.; Lu, G.Q.; Paul, D.R., *J. of Nanoscience and Nanotechnology*, **2005**, 5, 1574.

4. Housecroft, C.E.; Sharpe, A.G., *Inorganic Chemistry*; Pearson Education Limited: England, **2001**.

5. Whittingham, M.S.; Jacobson, A.J., *Intercalation Chemistry*; Academic Press: New York, **1982**.

6. Levy, F., *Intercalated Layered Materials;* Reidel: Dordrecht, the Netherlands, **1979**.

7. Enoki, T.; Suzuki, M.; Endo, M., *Graphite Intercalation Compounds and Applications*, Oxford University Press, New York, **2003**.

8. Pierson, H.O., *Handbook of Carbon, Graphite, Diamond and Fullerenes*, Noyes, Park Ridge, NJ, **1993**, PV 93-24, p.1.

9. Nakajima, T.; Tressaud, A., *Fluorine-Carbon and Fluoride-Carbon Materials-Chemistry, Physics and Applications,* Marcel Dekker, NewYork, **1995**.

10. Dresselhaus, M.S; Dresselhaus, G., *Adv. Physics* **1981**, 30, 139.

11. Schaffäutl, P., *J. praft. Chem*., **1841**, 21, 155.

12. Hoffmann, U.; Frenzel, A., **1931**, *Z. Elektrochem*., 37, 613.

13. Besenhard, J.O., *Carbon*, **1976**, 14, 111.

14. Daumas, N.; Herold, A., *C.R. Acad. Sci*. *Paris*., **1969**, C286, 373.

15. Thomas, J.M.; Millward, G.R.; Schlögl, R.; Boehm, H.P., *Mater. Res. Bull*., **1980**, 15, 671.

16. Mizutani, Y.; Ihara, E.; Abe, T.; Asano, M.; Harada, T.; Ogumi, Z.; Inaba, M., *J. Phys. Chem. of Solids*, **1996**, 57(6-8), 799.

17. Billaud, D.; Pron, A.; Vogel, F.; Herold, A., *Mater. Res. Bull*., **1980**, 15, 1627.

18. Billaud, D.; Chenite, A.; Metrot, A., *Carbon*, **1982**, 20, 493.

19. Besenhard, J.O.; Fritz, H.P., *Naturforsc*h, **1972**, 27B, 1294.

20. Hennig, G.R., *Prog. Inorg. Chem*., **1959**, 1, 125.

21. Watanabe, N.; Touhara, H.; Nakajima, T.; Bartlett, N.; Mallouk, T.; Selig, H., *Fluorine intercalation compounds of graphite*, *in Inorganic Solid Fluorides* (P. Hagenmuller, ed.), Academic Press, New York, **1985**, p.331.

22. Bartlett, N; Okino, F.; Mallouk, T.E.; Hagiwara, R.; Lerner, M.; Rosenthal, G.L.; Kourtakis, K., *Oxidative intercalation of graphite by fluoroanionic species, Advances in Chemistry* Series No. 226, (Johnson, M.K.; King, R.B.; Kurtz, D.M.; Kutal, C.; Norton, M.L.; Scott, R.A., eds) ACS, Washington, D.C., **1990**, p391.

23. Lerner, M.; Hagiwara, R.; Bartlett, N., *J. Fluorine Chem*., **1992**, 57, 1.

24. Wagman, D.D.; Evans, W.H.; Parker, V.B.; Schumm, R.H.; Bailey, S.M.; Hallow, I.; Churney, K.L.; Nuttall, R.L., *in Handbook of Chemistry and Physics*, **1989-1990**, Vol. 70, 270(3)-270(8), CRC Press, Boca Raton, FL.

25. Johnson, D.A., *Some thermodynamic aspects of inorganic chemistry*, 2nd ed., Cambridge University Press, Cambridge, **1982**.

26. Yan, W.; Kabalnova, L.; Sukpirom, N.; Zhang, S.; Lerner, M., *J. Fluorine Chem*., **2004**, 125(11), 1703.

27. Brodie, B. *Ann. Chim. Phys.* **1855**, *45*, 351.

28. Staudenmaier, L., *Ber Dtsch Chem Ges*, **1898**, 31, 1481.

29. Hummers, W.S.; Offeman, R.E., *J. Am. Chem. Soc*., **1958**, 80, 1339.

30. Petit, C.; Seredych, M.; Bandosz, T.J., *J. Mater. Chem*., **2009**, 19, 9176.

31. Kovtyukhova, N.I.; Ollivier, P.J.; Martin B.R.; Mallouk T.E.; Chizhik, S.A.; Buzenava E.V.; Gorchinskiy, A.D., *Chem. Mater*., **1999**, 11, 771.

32. Szabo, T; Tombacz, E; Illes, E.; Dekany, I., *Carbon*, **2006**, 44, 537.

33. Stankovich S.; Dikin, D.A.; Piner, R.D., Kohlhaas, K.A., Kleinhammes, A.; Jia, Y.; Wu, Y., *Carbon*, **2007**, 45, 1558

34. Lerf, A.; He, H.; Forster, M.; Klinowski, J., *J. Phys. Chem. B*, **1998**, 102(23), 4477.

35. Szabo, T; Berkesi, O.; Forgo, P.; Josepovits, K.; Sanakis, Y.; Petridisand, D.; Dekany, I, *Chem. Mater*., **2006**, 18, 2740.
36. Gao, W.; Alemany, L.B.; Ci, L.; Ajayan, P.M., *Nat. Chem*., **2009**, 1(5), 403.

37. Matsuo, Y.; Miyabe, T.; Fukutsuka, T.; Sugie, Y., *Carbon*, **2007**, 45, 1005.

38. Valerga Jime´nez, P.; Arufe Martinez, M.I.; Martı´n Rodrı´ez, A., *Carbon*, **1985**, 23, 473.

39. Higashika, S.; Kimura, K.; Matsuo, Y.; Sugie, Y., *Carbon*, **1999**, 37(2), 351.

40. Liu, P.; Gong, K., *Carbon*, **1999**, 37, 701.

41. Matsuo, Y.; Niwa, T.; Sugie, Y., *Carbon*, **1999**, 37, 897.

42. Liu, Z.; Wang, Z.; Yang, X.; Ooi, K., *Langmuir*, **2002**, 18, 4926.

43. Mastalir, A.; Kiraly, Z.; Patzko, A.; De´ka´ny, I.; L'Argentiere, P., *Carbon*, **2008**, 46, 1631.

44. Matsuo, Y.; Sakai, Y.; Fukutsuka, T.; Sugie, Y., *Carbon*, **2009**, 47, 804.

45. Worsley, K.A.; Ramesh, P.; Mandal, S.K.; Niyogi, S.; Itkis, M.E.; Haddon, R.C., *Chem. Phys. Lett*., **2007**, 445, 51.

46. Boukhvalov, D.W.; Katsnelson, M.I., *J. Am. Chem. Soc.*, **2008**, 130, 10697.

47. Watcharotone, S.; Dikin, D.A.; Stankovich, S.; Piner, R.; Jung, I.; Dommett, G.H.B.; Evmenenko, G.; Wu, S.-E.; Chen, S.-F.; Liu, C.-P.; Nguyen, S.T.; Ruoff, R.S, *Nano Lett.*, **2007**, 7(7), 1888.

48. Stoller, M. D.; Park, S.; Zhu, Y.; An, J.; Ruoff, R.S., *Nano Lett.*, **2008**, 8, 3498.

49. Ramanathan, T.; Abdala A.A.; Stankovich, S.; Dikin, D.A.; Herrera-Alonso, M.; Piner, R.D.; Adamson, D.H.; Schniepp, H.C.; Chen, X.; Ruoff, R.S.; Nguyen, S.T.; Aksay, I.A.; Prud'Homme, R.K.; Brinson, L.C., *Nat. Nanotechnol.*, **2008**, 3, 327.

50. Paci, J.T.; Belytschko, T.; Schatz, G.C., *J. Chem. Phys.* **2007**, 111(49), 18099.

51. Kudin, K.N.; Ozbas, B.; Schniepp, H.C.; Prud'homme, R.K.; Aksay, I.A.; Car, R., *Nano Lett.*, **2008**, 8, 36.

52. Ruoff, R., *Nature Nanotechnol.*, **2008**, 3, 10.

53. Hirata, M.; Gotou, T.; Horiuchi, S.; Fujiwara, M.; Phba, M., *Carbon*, **2005**, 43, 503.

54. Si, Y.; Samulski, E.T., *Nano Lett.*, **2008**, 8(6), 1679.

55. Li, D.; Muller, M.B.; Gilje, S.; Kaner, R.B.; Wallace, G.G., *Nat. Nano.*, **2008**, 3, 101.

56. Li, X.; Zhang, G.; Bai, X.; Sun, X.; Wang, X.; Wang, E.; Dai, H., *Nature Nanotechnology, 2008,* **3,** 538.

57. Schniepp H.C.; Li, J.-L.; McAllister, M.J.; Sai, H.; Herrera-Alonso, M.; Adamson, D.H.; Prud'homme, R.K.; Car, R.; Saville, D.A.; Aksay, I. A., *J. Phys. Chem. B*, **2006**, 110, 8535.

58. Niyogi, S.; Bekyarova, E.; Itkis, M.E.; McWilliams, J.L.,; Hamon, M.A.; Haddon R.C., *J. Am. Chem. Soc*., **2006**, 128, 7720.

59. Badaire, S.; Poulin, P.; Maugey, M.; Zakri, C., *Langmuir*, **2004**, 20, 10367.

60. Stankovich, S.; Piner, R.D.; Chen, X.; Wu, N.; Nguyen, S.T.; Ruoff, R.S., *J. Mater. Chem.*, **2006**, 16, 155.

61. Nakajima, T.; Watanabe, N., *Graphite Fluorides and Carbon-Fluorine Compounds*, CRC Press, Boca Raton, Fla., **1990**.

62. Watanabe, N.; Nakajima, T.; Touhara, H., *Graphite Fluorides*, Elsevier, Amsterdam, **1988**.

63. Sato, Y.; Itoh, K.; Hagiwara, R.; Fukunaga, T.; Ito, Y., *Carbon*, **2004**, 42, 3243.

64. Amatucci, G.G.; Pereira, N., *J. Fluorine Chem*., **200**7, 128, 243.

65. Sato, Y.; Shiraishib, S.; Mazejc, Z.; Hagiwara, R.; Ito, Y., *Carbon*, **2003**, 41, 1971.

66. Yazami, R.; Hany, P.; Masset, P.; Hamwi, A., *Mol. Cryst. Liq. Cryst*., **1998**, 310, 397.

67. Nakajima, T.; Matsuo, Y.; Zemwa, B.; Jesih, A., *Carbon*, **1996**, 34, 1595.

68. Lemmon, J.P.; Lerner, M.M., *Carbon*, **1993**, 31, 437.

69. Nakajima, T.; Gupta, V.; Ohzawa, Y.; Groult, H.; Mazej, Z.; Zemwa, B., *J. Power Sources*, **2004**, 137, 80.

70. Touhara, H.; Kadono, K.; Imoto, H.; Watanabe, N.; Tressaud, A.; Grannec, J., *Synth. Metals*, **1987**, 18, 549.

71. Amine, K.; Tressaud, A.; Imoto, H.; Fargin, E.; Hagenmuller, P.; Touhara, H., *Mater. Res. Bull*., **1991**, 26, 337.

72. Li, H.; Wang, Z.; Chen, L.; Huang, X., *Adv. Mater*., **2009**, 21, 4593.

73. Okuyama, N.; Takahashi, T.; Kanayama, S.; Yasunaga, H., *Physica*, **1981**, 105B, 298.

74. Métrot, A.; Guérard, D.; Billaud D.; Hérold, A., *Synth. Metals*, **1979/1980**, 1, 363.

75. Sangster, J., *J. Phase Equilib. and Diffusion*, **2007**, 28(6), 571.

76. Hérold, C.; Goutfer-Wurmser, F.; Marêché J.-F.; Lagrange, P., *Mol. Cryst. Liq. Cryst*., **1998**, 310, 43.

77. Guérard, D.; Chaabouni, M.; Langrange, P.; El Makrini, S.; Hérold, A, *Carbon*, **1980**, 18, 257.

78. Pruvost, S.; Hérold, C., Hérold, A.; Lagrange, P., *Carbon*, **2004**, 42, 1825.

79. Parry, G.S.; Nixon, D.E.; Lester, K.M.; Levene, B.C., *J. Phys. C.* **1969**, *2*, 2156.

80. Underhill C.; Krapchev, T.; Dresselhaus, M. S., *Synth. Met.* **1980**, *2*, 47.

81. Emery, N.; Hérold, C.; Marêché1, J.F., Lagrange, P., *Sci. Technol. Adv. Mater.*, **2008**, 9**,** 044102.

82. Nalimova, V.A.; Guérard, D.; Lelaurain, M.; Fateev, O.V., *Carbon*, **1995**, 33, 177.

83. Avdeev, V.V.; Nalimova, V. A.; Semenenko, K.N., *Synth. Met.*, **1990**, *38*, 363.

84. Nalimova, V.A.; Chepurko, S.N.; Avdeev, V.V.; Semenenko, K. N., *Synth. Metals*, **1991**, 40, 267.

85. Hérold, A.; Lelaurain, M.; Maréche J.F.; Mc Rae E., *CR Acad Sci Paris*, **1995**, 321(2), 61 (Serie IIb).

86. Hérold, A.; Maréche J.F.; Lelaurain, M., *Carbo*n, **2000**, 38, 1955.

87. Makrini, M.E.; Guérard, D.; Lagrange, P.; Hérold, A., *Physica*, **1980**, B99, 481.

88. Takamoto, T.; Suematsu, H.; Murakami, Y., *Synth. Met*., **1990**, 34(1-3), 53.

89. Alheid, H.; Schwarz, M.; Stumpp, E., *Molecular Cryst. and Liq. Cryst. Science and Tech. Sec A.*, **1994**, 244, 191.

90. Takenaka, H.; Kawaguchi, M.; Lerner, M. M.; Bartlett, N., *J. Chem. Soc., Chem. Commun.* **1987**, 19, 1431.

91. Yan, W.; Lerner, M.M., *Carbon*, **2004**, 42, 2981.

92. Vogel, F.L.; Foley, G.M.T.; Zeller, C.; Falardeau, E.R.; Gan J., *Mater. Sci. Eng*., **1977**, 31, 261.

93. Interrante, L.V.; Markiewiz, R.S.; Mckee, D.W., *Synth. Metals*, **1979**, 1, 287.

94. Thompson T.E.; McCarron E.M.; Bartlett N., *Synth. Metals*, **1981**, 3, 255.

95. Shioya, J.; Matsubara, H.; Murakami, S., *Synth. Metals*, **1986**, 14, 113.

96. Shioya, J.; Mizoguchi, A.; Yamaguchi, Y.; Yasuda, N., *Synth. Metals*, **1989**, 34, 151.

97. Ebert, L.B.; Selig, H., *Mater. Sci. Eng*., **1977**, 31, 177.

98. Binenboym, J.; Selig, H.; Sarig, S., *J. Inorg. Nucl. Chem*., **1976**, 38, 2313.

99. Bartlett, N.; McCarron, E.M.; McQuillan, B.W.; Thompson, T.E., *Synth. Metals*, **1979/1980,** 1(3), 221.

100. Selig, H., *Graphite intercalation compounds with binary fluorides, in Inorganic Solid Fluorides*, P. Hagenmuller, ed., Academic Press, New York, **1985**, p354.

101. Boeck, A.; Rüdorff, W., *Z. Anorg. Allgem. Chem*., **1971**, 384, 169.

102. Vasse, R.; Furdin, G.; Melin J.; Herold, A., *Carbon*, **1981**, 19, 249.

103. Croft, R.C.; Thomas, R.G., *Nature*, **1951**, 168, 32.

104. Giraudet, J.; Claves, D.; Hamwi, A., *Synthetic Metals*, **2001**, 118, 57.

105. Nakajima, T.; Molinier, M., *Synth. Metals*, **1989**, 34, 103.

106. Hamwi, A.; Touzain, P., *Rev. Chim. Minér*., **1982**, 19, 432.

107. Hamwi, A.; Touzain, P., Bonnetain, L., *Mater. Sci. Eng*., **1977**, 31, 95.

108. Mouras, S.; Hamwi, A.; Djurado, D.; Cousseins, J.C, *Re. Chem. Miner*., **1987**, 24, 572.

109. Nakajima, T; Matsui, T.; Motoyama, M.; Mizutani, Y., *Carbon*, **1988**, 26, 831.

110. Grannec, J.; Lozano, L., *Preparation Methods, in inorganic Solid Fluorides*, P. Hagenmuller, ed., Academic Press, New York, **1985**, p18.

111. Flandrois, S.; Grannec, J.; Hauw, C.; Hun, B.; Lozano, L.; Tressaud, T., *J. Solid State Chem*., **1988**, 77, 264.

112. Falardeau, E.R.; Hanlon, L.R.; Thompson, T.R., *Inorg. Chem*., **1978**, 17, 301.

113. Pentenrieder, R.; Boehm, H.P., *Rev. Chim. Minér*., **1982**, 19, 371.

114. Hamwi, A.; Mouras, S.; Djurado, D.; Cousseins, J.C., Proceedings Carbon '86, Baden-Baden, Germany, **1986**, p454.

115. Ravaine, D.; Boyce, J.; Hamwi, A.; Touzain, P., *Synth. Metals*, **1980**, 2, 249.

116. Lerner, M.; Hagiwara, R.; Bartlett, N., *J. Fluorine Chem*., **1992**, 57, 1.

117. Cohen, A.D., Fr. Pat. **1975**, 2 291 151.

118. McCarron, E.M.; Grannec, Y.J.; Bartlett, N., *J. Che. Soc. Chem Commun*., **1980**, 890.

119. Rosenthal, G.L.; Mallouk, T.E.; Bartlett, N., *Synth. Met*., **1984**, 9, 433.

120. Nakajima, T.; Nakane, K.; Kawaguchi, M.; Watanabe, N., *Carbon*, **1987**, 25, 685.

121. Buscarlet, E.; Touzain, P., Bonnetain, L, *Carbon*, **1976**, 14, 75.

122. Nakajima, T.; Nagai, Y.; Motoyama, M., *Eur. J. Solid State Inorg. Chem*., **1992**, 29, 919.

123. Touzain, P.; Buscarlet, E.; Bonnetain, L, *Rev. Chim. Minér*., **1977**, 14, 482.

124. Hamwi, A.; Daoud, M.; Cousseins, J.C., *Synth. Metals*, **1988,** 26, 89.

125. Selig, H.; Sunder, W.A.; Vasile, M.J.; Stevie, F.A.; Gallagher, P.K.; Ebert, L.B., *J. Fluorine Chem*., **1978**, 12, 397.

126. Hattori, Y.; Kurihara, M.; Kawasaki, S.; Okino, F.; Touhara, H., *Synthetic Metals*, **1995**, 74, 89.

127. Tressaud, A.; Hagenmuller, P., *J. Fluorine Chem*., **2001**,111, 221.

128. Inagaki, M., *J. Mater. Res*., **1989**, 4, 1560.

129. Dunaev, A.V.; Sorokina, N.E.; Maksimova, N.V.; Avdeev, V.V., *Inorganic Materials*, **2005**, 41(2), 127.

130. Shioyama, H., *Tanso*, **1998**, 184, 202.

131. Inagaki, M, Wang, Z.D.; Okamoto, Y.; Ohira, M., *Synth. Met*., **1987**, 20, 9.

132. Hui, R.; Kang, F.Y.; Jiao, Q.J.; *New Carbon Materials*, **2009,** 24(1), 18.

133. Schloegl, R.; Boehm, H.P., *Synth. Met*., **1988**, 23, 407.

134. Shioyama, H.; Crespin, M.; Setton, R; Bonnin, D.; Beguin, F., *Carbon*, **1993**, 31, 223.

135. Fouletier, M.; Armond, M., *Carbon*, **1979**, 17, 427.

136. Stumpp, E.; Wloka, K., *Synth. Metals*, **1981**, 3, 209.

137. Ebert, L.B., Annu. Rev. *Mater. Sci*., **1976**, 6, 181.

138. Stumpp, E.; Nietfeld, G., *Z. Anorg. Allg. Chem*., **1969**, 456, 261.

139. Zhang, H.Y.; Shen, W.C.; Wang, Z.D.; Zhang, F., *Carbon*, **1997**, 35(2), 285.

140. Shornikova, O.N.; Dunaev, A.V.; Maksimova, N.V.; Avdeev V.V., *J. Phys. and Chem. of Solids*, **2006**, 67, 1193.

141. Sorokina, N.E.; Nikol´skaya, I.V.; Ionov, S.G.; Avdeev, V.V., *Russ. Chem. Bull., Int. Ed.*, **2005**, 54(8), 1749.

142. Herold, A.; Furdin, G.; Guerard, D.; Hachim, L.; Nadi, N.; Vangelisti, R., *Ann. Phys*., **1986**, 11, 3.

143. Herold, A., *NATO ASY, Ser. B*, **1987**, 172, 3.

144. Rudorff, U., *Adv. Inorg. Chem. Radiochem*., **1959**, 1, 223.

145. Métrot, A.; Fischer, J.E., *Synth. Metals*, **1981**, 3, 201.

146. Sorokina, N.E.; Maksimova, N.V.; Nikitin, A.V.; Shornikova O.N.; Avdeev, V.V., *Inorg. Mater*., **2001**, 37(6), 584.

147. Avdeev, V.V.; Sorokina, N.E.; Maksimova, N.V.; Martynov, I.Yu.; Sezemin, A.V., *Inorg. Mater*., **2001**, 37(4), 366.

148. Toyoda, M; Sedlacik, J.; Inagaki, M., *Synth. Met.*,**2002**, 130, 39.

149. Toyoda, M;. Katoh, H.; Inagaki, M., *Carbon*, **2001**, 39, 2231.

150. Toyoda, M; Shimizu, A.; Inagaki, M., *Carbon*, **2001**, 39, 1697.

151. Nixon, D.E.; Parry, G.S.; Ubbelohde, A.R., *Proc. Roy. Soc.*, London, **1966**, 291A, 32.

152. Lope-Gonzales, J.D.; Rodriguez, A.M.; Vega, F.D., *Carbon*, **1969**, 7, 583.

153. Chernysh, I.G.; Buraya, I.D., *Khim. Tverd. Topliva* (*Solid Fuel Chemistry*), **1990**, 1, 123.

154. Rüdorff, W.; Hoffmann, U., *Z. Anorg. Allg. Chem*., **1938**, 238, 1.

155. Rudorff, W., *Z. Phys. Chem*., **1939**, 45, 42

156. Nixon, D.E.; Parry, G.S.; Ubbelohde, A.R., *Proc. Roy. Soc*. London, **1964**, A291, 324.

157. Touzain, P., *Carbon*, **1978**, 16, 403.

158. Bartlett, N.; Biagioni, R.N.; McQuillan, B.W.; Robertson, A.S.; Thompson, A.C., *J. Chem. Soc. Chem. Commun.*, **1978**, 5, 200.

159. Rüdorff, W.; Siecke, W.-F., *Chem. Ber*., **1958**, 91, 1348.

160. Horn, D.; Boehm, H.P., *Mater. Sci. Eng*., **1972**, 31, 87.

161. Nikonorov, Y.I., *Kinet. Kutal.*, **1979**, 20, 1598.

162. Billaud, D.; Pron, A.; Vogel, F., *Synth. Met*., **1980**, 2, 177.

163. Ebert, L.B.; Selig, H., *Synth. Met*., **1981**, 3, 53.

164. Chenite, A.; Billaud, D., *Carbon*, **1982**, 20(2), 120.

165. Horowitz, H.H.; Haberman, J.I.; Klemann, L.P.; Newman, C.H.; Stogryn, E.L.; Whitney, T.A., *Proceedings-Electrochem. Soc*., **1981**, 81-4, 131.

166. Kita, F.; Kawakami, A.; Sonoda, T.; Kobayashi, H., *Proceedings-Electrochem. Soc*., **1993**, 93-23, 321.

167. Barthel, J.; Schmidt, M.; Gores, H.J., *J. Electrochem. Soc*., **2000**, 147(1), 21.

168. Ue, M.; Ida, K.; Mori, S., *J. Electrochem. Soc*., **1994**, 141, 2989.

169. Yan, W., Synthesis, Characterization, and Structural modeling of Graphite intercalation Compounds with Fluoroanions, Thesis, Oregon State University, 2004.

170. Yan, W.; Lerner, M.M., *J. Electrochem. Soc.*, **2003**, 150(9), D169.

171. Yan, W.; Lerner, M.M., *J. Electrochem. Soc*., **2004**, 151(2), J15.

172. Katinonkul, W.; Lerner, M.M., *Carbon*, **2007**, 45, 2672.

173. Katinonkul, W.; Lerner, M.M., *J. Phys. Chem. Sol.* **2007**, 68, 394.

174. Özmen-Monkul, B.; Lerner, M.M.; Pawelke, G.; Willner, H., *Carbon*, **2009**, 47, 1592.

175. Iskander, B.; Vast, P., *Carbon*, **1980**, 18(4), 299.

176. Özmen-Monkul, B.; Lerner, M.M., Carbon, accepted.

177. Hérold, C.; Goutfer-Wurmser, F.; Marêché J.-F.; Lagrange, P., *Mol. Cryst. Liq. Cryst*., **1998**, 310, 57.

178. Ginderov, D.; Setton, R., *Carbon*, **1968**, 6, 81.

179. Scharff, P., *Z. Naturforsch., Teil B*, **1989**, 44, 772.

180. Horn, D.; Boehm, H.P., *Mater. Sci. Eng*., **1977**, 31, 87.

181. Ruisinger, B.; Boehm, H.P., *Angew. Chem. Int. Ed. Engl*., **1987**, 26, 253.

182. Boehm, H.P.; Helle, W.; Ruisinger, B., *Synth. Met*., **1988**, 23, 395.

183. Ruisinger, B.; Boehm, H.P., *Carbon*, **1993**, 31, 1131.

184. Zhang, X.; Lerner, M.M., *Chem. Mater*., **1999**, 11, 1100.

185. Zhang, Z., Lerner, M.M., *Chem. Mater*., **1996**, 8, 257.

186. Zhang, X.; Sukpirom, N.; Lerner, M.M., *Mater. Res. Bull*., **1999**, 34, 363.

187. Zhang X.; Sukpirom, N.; Lerner, M.M., *Mol. Cryst. Liq. Cryst.*, **2000**, 340, 37.

188. Özmen-Monkul, B.; Lerner, M.M.; Hagiwara, R., *J. Fluorine Chem*., **2009**, 130, 581.

189. Yan, W.; Lerner, M.M., *J. Electrochem. Soc*., **2001**, 148(6), D83.

190. Inagaki, M., *J. Jpn. Inst. Energy*, **1998**, 77, 849.

191. Fujimoto, K.; Sugiura, T.; Iijima, T.; Sato, M., *Hyomen*, **1992**, 30, 310.

192. Matsumoto, R.; Akuzawa, N., *Recent Research Activities of Micro- and Nano-Scale Carbon Related Materials*, Ed. Miyagawa, H., **2008**, 145.

193. Winter, M.; Besenhard, J.O.; Spahr, M.E., Novak, P., *Adv. Mater*., **1998**, 10(10), 725.

194. Pollock, M.; Wetula, J.; Ford, B., U.S. Pat. 5443894, August 22, **1995**.

195. Tsuchiya, S.; Fukui, A.; Hara, M.; Imamura, H., *Proc. Int. Congr. Catal*. **1985**, 4, 635.

196. Rashkov, I., *Mat. Sci. For*. **1992**, 91/3, 829.

197. Inagaki, M.; Kang, F.; Toyoda, M., *Chemistry and Physics of Carbon*, **2004**, 29, 1.

198. Norley, J. Graphite-based heat sink. U.S. Pat. 6503626, January 7, **2003**.

199. Soneda, Y.; Toyoda, M.; Tani, Y.; Yamashita, J.; Kodama, M.; Hatori, H.; Inagaki, M. *J. Phys. Chem. Sol.,* **2004**, 65, 219.

200. Niyori, Y.; Katsukawa, H.; Yoshida, H.; Takeuchi, M.; Okamura, M., U.S. Pat. 6487086, **2002**.

201. Allied Business Intelligence, Fuel Cell Supply Chain: A Global Market Analysis, Potential and Forecasts March, **2003**.

202. Akuzawa, N.; Sakamoto, T.; Fujimoto, H.; Kasuu, T; Tkahashi, Y., *Synth. Met*., **1995**, 73(1), 41.

203. York, B.R.; Solin, S.A., *Phys. Rev. B*., **1985,** 31, 8206.

204. Beguin, F.; Pilliere, H, *Carbon*, **1998**, 36, 1759.

205. Akuzawa, N; Kamoshita, T; Tsuchiya, K; Matsumoto, R, *Tanso*, **2006**, 222, 107.

206. Cheng, H; Sha, X; Chen, L; Cooper, A.C; Foo, M-L; Lau, G.C.; Bailey III, W.H.; Pez, G.P., *J. Am. Chem. Soc*., **2009**, 131(49), 17732.

207. Takahashi, Y; Oi, K; Terai, T; Otosaka, T; Akuzawa, N, *Materials Science Forum*, **1992**, 91-93, 133.

208. Shioyama, H., *Mol. Cryst. and Liq. Cryst*., **2000**, 340, 101

209. Aksenov, V.V.; Vlasov, V.M.; Danilkin, V.I.; Rodionov, P.P.; Shnitko, G.N., *J. Fluorine Chem.*, **1990**, 46(1), 57.

210. Walter, J.; Heiermann, J.; Dyker, G.; Hara, S.; Shioyama, H., *Journal of Catalysis*, **2000**, 189, 449.

211. Mastalir, A.; Kiraly, Z.; Dekany, I.; Bartok, M., *Colloids Surf. A*, **1998**, 141, 397.

212. Matsumoto, R; Hoshina, Y; Akuzawa, N, *Materials Transactions*, **2009**, 50(7), 1607.

213. Allen M.J.; Tung, V.C.; Kaner, R.B., *Chem. Rev*., **2010**, 110, 132.

214. Dato, A.; Lee, Z.; Jeon, K-J.; Erni, R.; Radmilovic, V.; Richardson, T. J.; Frenklach, M., *Chem. Commun*., **2009**, 6095.

215. Meyer, J.C.; Kisielowski, C.; Erni, R.; Rossell, M.D.; Crommie, M.F.; Zettl, A., *Nano Lett*., **2008**, 8(11), 3582.

216. Berger, C.; Song, Z.; Li, X.; Wu, X.; Brown, N.; Naud, C.; Mayou, D.; Li, T.; Hass, J.; Marchenkov, A.N.; Conrad, E.H.; First, P.N.; de Heer, W.A., *Science*, **2006**, 312, 1191.

217. Kim, S.; Nah, J.; Jo, I.; Shahrjerdi, D.; Colombo, L.; Yao, Z.; Tutuc, E.; Banerjee, S.K., *Appl. Phys. Lett.*, **2009**, 94, 062107.

218. Banerjee, S.K.; Register, L.F.; Tutuc, E.; Reddy, D.; MacDonald, A.H., *IEEE Electron Device Lett*, **2009**, 30 (2), 158.

219. Kim, K.S.; Zhao, Y.; Jang, H.; Lee, S.Y.; Kim, J.M.; Kim, K.S.; Ahn, J.-H.; Kim, P.; Choi, J.-Y.; Hong, B.H., *Nature*, **2009**, 457, 706.

220. Teweldebrhan, D.; Balandin, A.A., *Appl. Phys. Lett*., **2009**, 94, 013101.

221. Geim, A.K.; Novoselov, K.S., *Nature Mater*., **2007**, 6, 183.

222. Balandin, A.A.; Ghosh, S.; Bao, W.; Calizo, I.; Teweldebrhan, D.; Miao, F.; Lau, C.N., *Nano Lett*., **2008**, 8, 902.

223. Novoselov, K.S.; Geim, A.K.; Morozov, S.V.; Jiang, D.; Zhang, Y.; Dubonos, S.V.; Grigorieva, I.V.; Firsov, A.A., *Science*, **2004**, 306, 666.

224. Dato, A.; Radmilovic, V.; Lee, Z.; Phillips, J.; Frenklach, M., *Nano. Lett*., **2008**, 8, 2012.

225. Bode, H.; Jenssen, H.; Bandte, F., *Angew. Chem*., **1953**, 65, 304.

226. Besenhard, J.; Wudy, E.; Moehwald, H.; Nickl, J.; Biberacher, W.; Foag, W., *Synth. Met*., **1983**, 7, 185.

227. Amine, K.; Nakajima, T., *Carbon*, **1993**, 31, 553.

CHAPTER 2

CHEMICAL AND ELECTROCHEMICAL SYNTHESES OF A GRAPHITE FLUORO-TRIS(PENTAFLUOROETHYL)BORATE INTERCALATION COMPOUND

Bahar Özmen-Monkul[a], Michael M. Lerner[a*],

Gottfried Pawelke[b], Helge Willner[b]

[a] Department of Chemistry,

Oregon State University

Corvallis, OR 97331-4003,

USA

[b] University of Wuppertal,

FBC Inorg. Chem. Gaußstr. 20,

D-42119 Wuppertal,

Germany

Carbon, **2009**, 47, 1592-1597

2.1 ABSTRACT

Graphite intercalation compounds (GICs) of composition $C_x[FB(C_2F_5)_3]\cdot\delta F$ are prepared for the first time by the intercalation of fluoro-tris(pentafluoroethyl)borate anion, $[FB(C_2F_5)_3]^-$, under ambient conditions in 48 % hydrofluoric acid containing the oxidant $K_2[MnF_6]$. Powder XRD data indicate that products are of mixed stage 2 and 3 after reactions for 1 to 20 h, with a gallery height of 0.87 nm. The intercalate orientation is modeled using an energy minimized anion structure. Microwave digestion followed by B and F elemental analyses, along with thermogravimetric analyses (TGA) provide compositional *x* and δ parameters for the GICs obtained. In addition, $C_x[FB(C_2F_5)_3]\cdot\delta CH_3NO_2$ with stage 2 is prepared by electrochemical oxidation of graphite in a nitromethane solution and characterized as above.

2.2 INTRODUCTION

Graphite intercalation compounds (GICs) are produced by the insertion of guest intercalate species between graphene layers. Intercalation reactions of this type are common for layered hosts where interplanar binding forces are relatively low or can be offset by redox reactions or solvation chemistry. Some examples of intercalation hosts include graphite, clays and a number of transition metal dichalcogenides. Graphite is unique in the extent of intercalate ordering known as staging [1]. For example, a stage 2 GIC has intercalate present between alternate sheets only, and a stage 3 GIC has intercalate between every third pair of graphene sheets. Graphite is also unusual in that it can be either oxidized or reduced to form GICs; these are often termed acceptor-type or donor-type compounds, respectively [2].

Graphite, composite materials based on graphite, and GICs have many current and potential technological applications [3,4]. GICs are a precursor of thermally expanded graphite, which is a porous, chemically inert, and heat resistant material used as low-density carbon and for manufacture of binder-free gaskets, seals, and liners [5]. An alternate means of generating exfoliated graphite involves generation and dispersion of graphite oxide [6]. Graphene-based nanocomposites have been proposed for use as electrode materials in electrochemical capacitors [7], or in high efficiency adsorption gas storage applications, also show improved properties in areas of transportation, mechanics and electronics [8,9].

Acceptor–type GICs have been long been known for a range of oxidatively-stable anions, including fluoride, bromide, and chloro-, fluoro- or oxometallates. Intercalation of larger fluoroalkylanions has been reported more recently, these include

perfluoroalkylsulfonates $C_yF_{2y+1}SO_3^-$ (y = 1, 4, 6, 8, or 10) [10-12], trifluoroacetate, CF_3COO^- [13], perfluoroalkyl-substituted sulfonyl imides and methide anions such as $N(SO_2CF_3)_2^-$, $N(SO_2CF_2CF_3)_2^-$, $N(SO_2CF_3)(SO_2C_4F_9)^-$ and $C(SO_2CF_3)_3^-$ [14,15]. For perfluoroalkylsulfonate anions, the gallery height, d_i, which corresponds to the separation of graphene sheet centers in an intercalated gallery, can be up to 3.4 nm [16]. GICs with large perfluorinated anion intercalates are also often much more air stable than those containing smaller anions. In addition, the formation of GICs with larger intercalate galleries opens the possibility of graphene analogs to micro- or mesoporous structures and the corresponding host-guest chemistry known for other layered hosts.

The tetrahedral $[BF_4]^-$ anion is well known to form GICs with $d_i \approx 0.78$-0.79 nm. Equations 2.1 and 2.2 show a representative chemical and electrochemical oxidation reaction [17,18]:

$$C_x + NO_2[BF_4] \xrightarrow{\text{solvent}} C_x[BF_4].\delta\text{solvent} + NO_2 \qquad (2.1)$$

$$C_{24n} + [BF_4]^- \xrightarrow{CH_3NO_2} C_{24n}[BF_4].\delta CH_3NO_2 + e^- \qquad (2.2)$$

where n is the GIC stage produced.

Oxidative stability is a key consideration in selecting intercalate anion candidates for GICs, since the threshold voltage for graphite intercalation is approximately + 4.5 V vs. Li/Li^+. For example, no anion containing a C-H bond has been shown to form a stable GIC. Barthel et al [19] studied a series of alkoxyborate chelates, $[B(ORR'O)_2]^-$, and determined that the oxidation potentials increase by ≈ 0.1 V for each fluorine substituent on the R groups. GICs containing the borate chelate anions $[B(OC(CF_3)_2C(CF_3)_2O)_2]^-$

[20], $[B(OC(CF_3)_2C(O)O)_2]^-$ [21], and $[B(OC(O)C(O)O)_2]^-$ [22] were prepared by our group recently. The borate chelate anion $[B(OC(O)C(O)O)_2]^-$ has also attracted attention as a potential electrolyte anion for lithium-ion batteries. GICs with stages 1-4 were obtained by both chemical and electrochemical methods with d_i= 1.40-1.45 nm. Intercalate galleries contain a monolayer anion arrangement with anions oriented with long axes perpendicular to the graphene sheets. This unusual orientation was explained by considering the gallery packing densities of different anion orientations [21].

Similarly, perfluorinated organoborate anions, $[B(R_f)_4]^-$ where R_f is a perfluorinated alkyl or aryl group show greater oxidative resistance than their non-fluorinated analogs. The perfluoroalkyltrifluoroborate salts ($K[C_nF_{2n+1}BF_3]$ n= 3,6 [23] and $K[RCF=CFBF_3]$ [24] and the anions of $[C_nF_{2n+1}BF_3]^-$ n= 1-4 [25]) have been synthesized with a proposed application in Li-ion battery electrolytes. However, no intercalation chemistry has been reported to date. In this paper, the first preparation and characterization of GICs containing fluoro-tris(pentafluoroethyl) borate is described.

2. 3 EXPERIMENTAL

SP-1 grade graphite (Union Carbide, 100 μm average particle diameter), hydrofluoric acid (Mallinckrodt AR, 48 % w/o), hexane (Fischer Chem, certified grade), cyclohexane (Fisher Scientific, HPLC grade), glacial acetic acid (EM Science, 99.7 %), NaCl (Mallinckrodt, AR grade), NaOH (Mallinckrodt, ACS grade) and NaF (J.T. Baker, ACS grade) were used as received. $KB(C_2F_5)_3F$ [26] and K_2MnF_6 [27] were synthesized according to literature methods. Ultrapure water (resistivity= 18 MΩ·cm at 25 °C) from a Milli-Q Labo system (Millipore, Milford, MA), was used throughout the experiments.

In the chemical reactions, $K[FB(C_2F_5)_3]$ (71 mg, 0.17 mmol) and $K_2[MnF_6]$ (206 mg, 0.83 mmol) were first dissolved into hydrofluoric acid (10 mL), and then graphite (20.4 mg, 1.7 mmol) was added to obtain mole ratios of 10:5:1 for graphene C: Mn (IV): borate anion. The solutions were stirred under ambient conditions for the specified reaction time, and then filtered through a hydrophilic polypropylene membrane (47 mm diameter, 0.2 μm pore diameter). The filtrate was rinsed with 5 mL hexane briefly and dried overnight under vacuum. Products were subsequently stored under an inert atmosphere.

For the electrochemical experiments, $K[FB(C_2F_5)_3]$ was dried *in vacuo* at 100 ^{0}C for 48 h and nitromethane (Sigma-Aldrich, > 99 %) was stirred over 4 Å molecular sieve for 48 h. Reagents were subsequently handled and the cells assembled and operated under inert atmosphere at ambient temperature. Two-compartment cells with a glass-frit separator were filled with a 0.15 M $K[FB(C_2F_5)_3]$ / CH_3NO_2 electrolyte. Working electrodes were prepared by painting a cyclohexane slurry of SP-1 graphite powder (100-120 mg) and 10 wt pct polymer binder (EPDM) onto a Ni mesh flag (area ≈1 cm^2) welded to a Ni wire. Counter electrodes were stainless steel mesh, and reference electrodes were Ni wire. Current was applied at 8.6 mA/g carbon for 8.3 h. Following the electrochemical oxidation, the working electrode was removed and washed with 3-4 mL of nitromethane under inert atmosphere and then dried *in vacuo* for 0.25 h.

Powder X-ray diffraction data (PXRD) were collected on a Rigaku MiniFlex II diffractometer with Ni-filtered CuKα radiation using a detector slit width of 3 mm. Data were collected at 0.02° 2Θ steps, between 4° and 65° for 1 h for the chemically-prepared

GICs and between 4° and 90° at a scan rate of 1^0 / min for the electrochemically-prepared GIC.

TGA data were obtained using a Shimadzu, Inc. TGA-50 thermogravimetric analyzer. Samples were loaded into a platinum pan; the sample chamber was flushed with Ar gas. Thermal scans from ambient to 1000 °C were performed under flowing Ar at 5 °C/min.

A new sample digestion protocol was developed for the GIC products. Samples (20-30 mg) were digested with 0.1 M NaOH (1 mL) using a microwave digester (CEM Corporation, MDS 2000) at 50 and then 100 psi for 0.12 h and 0.25 h, respectively. The resulting solutions were diluted to 10.0 mL and stored in Nalgene® plastic bottles. Low Level Total Ionic Strength Adjustment Buffer (LLTISAB) was prepared by addition of glacial acetic acid (57 mL) and NaCl (58 g) to 500 mL water, followed by the slow addition of 5 M NaOH until the pH was between 5.0-5.5, and then dilution to 1.00 L total volume [28]. Digested sample solutions were added to equal volumes of LLTISAB prior to analysis.

Fluoride analyses were performed using an ion-selective fluoride combination electrode with a standard single-junction sleeve-type reference electrode and a mV scale voltmeter (VWR International, Inc.). A calibration curve was obtained using fluoride standards prepared by diluting a standard solution (10 μg F/1.00 mL). All dilutions were performed using standard silica glassware at ambient temperature. Below pH 5, the formation of HF or HF_2^-, which are not detected by the fluoride electrode, can result in inaccurate F^- analyses [28]. In addition, the total ionic strength of the sample solutions must be maintained with the specification range of the electrode. The procedures adopted

above provided the required ranges of both pH and ionic strength. As a control, the $K(C_2F_5)_3BF$ salt was digested and analyzed according to the above procedure. The F content obtained indicated that < 0.1% of the F content from these fluoroanions is detected. The method developed is therefore able to provide fluoride anion content in GICs without interference from the larger $[FB(C_2F_5)_3]^-$ anion.

For the boron analyses the digestion procedure described above is used. Digested sample solutions were diluted using 2 % v/v HNO_3 and the B content determined by ICP-AES (S.A. Inc., JY2000U analyzer). A linear calibration curve from 2.5-50 mg B/L was obtained by diluting a commercial boron standard (Spex Certiprep, 1000 mg B/L). A 2 % v/v HNO_3 acid solution was also used as a control blank for calibration. As a control, the $K[FB(C_2F_5)_3]$ salt was digested and analyzed according to the above procedure. The B content obtained (mass pct: obs 2.59, calc 2.54) was in good agreement with the theoretical value.

The energy-minimized structure of the $[FB(C_2F_5)_3]^-$ anion was calculated using the hybrid density functional method (B3LYP) with a 6-31G (d) basis set and GaussView 3.0 software.

2.4 RESULTS AND DISCUSSION

After the addition of graphite to a solution of $K_2[MnF_6]$ and $K[FB(C_2F_5)_3]$ in hydrofluoric acid, GICs containing the $B(C_2F_5)_3F^-$ anion with stages 2, 3 or mixtures of these stages are obtained at different reaction times. Due to the limited chemical oxidation potential in 48 % hydrofluoric acid, stages 1 GICs are not observed, and have

never been obtained by chemical oxidation in this solvent [11]. Longer reaction times lead to a higher-stage GIC. The powder XRD and compositional data for the products obtained are provided in Figure 2.1 and Table 2.1. Diffraction samples have a preferred orientation of the platy graphite particles so that nearly all of the observed diffraction peaks are (*00l*) reflections. The calculated basal repeat distance, I_c, is 1.20 nm for stage 2 and ≈ 1.54-1.56 nm for stage 3, corresponding to d_i ≈ 0.86-0.89 nm. Powder XRD patterns and derived structure parameters are also shown in Figure 2.2 for the electrochemically prepared stage 2 GIC. The d_i value obtained (0.84 nm) is slightly less than those from chemical oxidation.

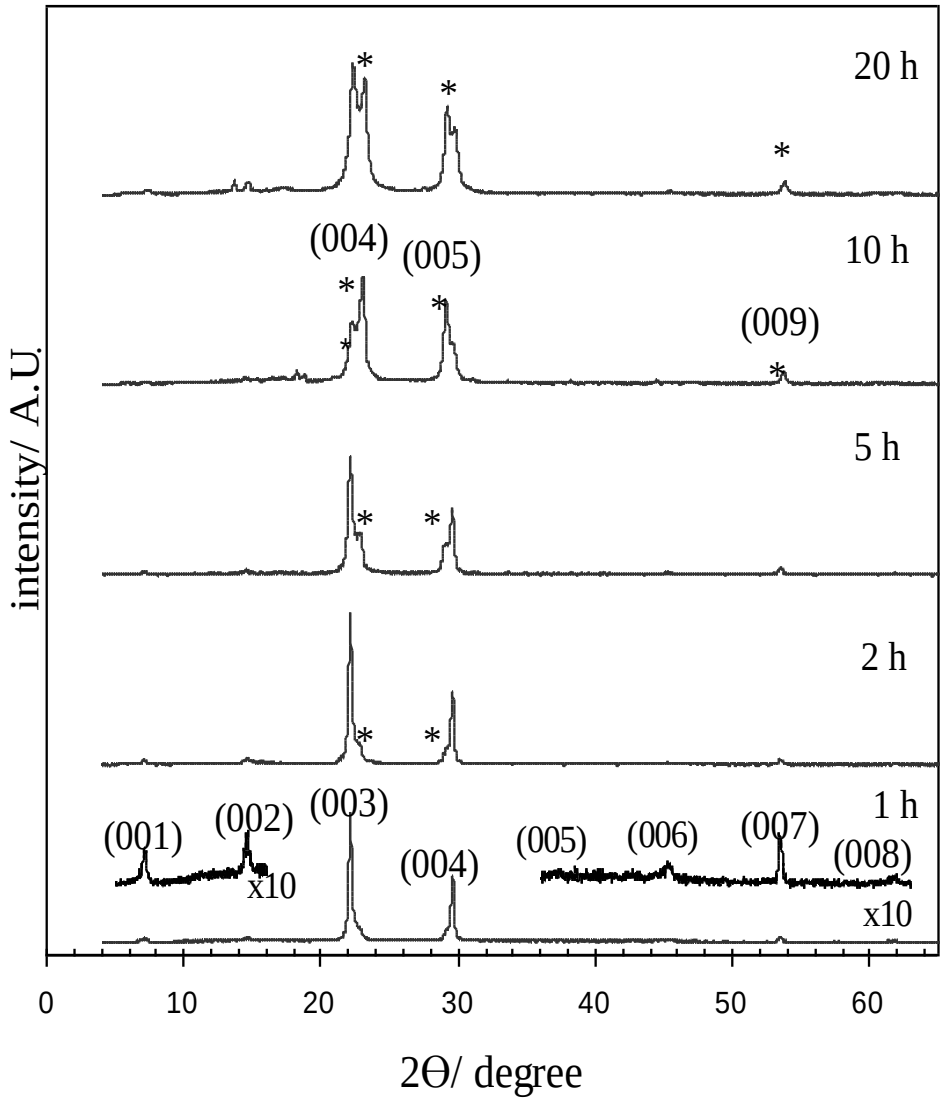

Figure 2.1 Powder XRD patterns for the GIC products after reaction times indicated. Some assigned (*00l*) indices are shown for the stage 2 product; diffraction peaks from the stage 3 product are indicated with an asterisk.

Table 2.1 Stage, basal repeat distance (I_c), and gallery height (d_i) for the GIC products at different reaction times as determined by powder XRD

Reaction time / h	Stage	I_c / nm	d_i / nm
1	2	1.20	0.87
2	2	1.20	0.87
5	2/3*	1.20 / 1.56	0.87 / 0.89
10	3/2*	1.55 / 1.19	0.87 / 0.86
20	3/2*	1.54 / 1.19	0.87 / 0.86

* the predominant stage is listed first

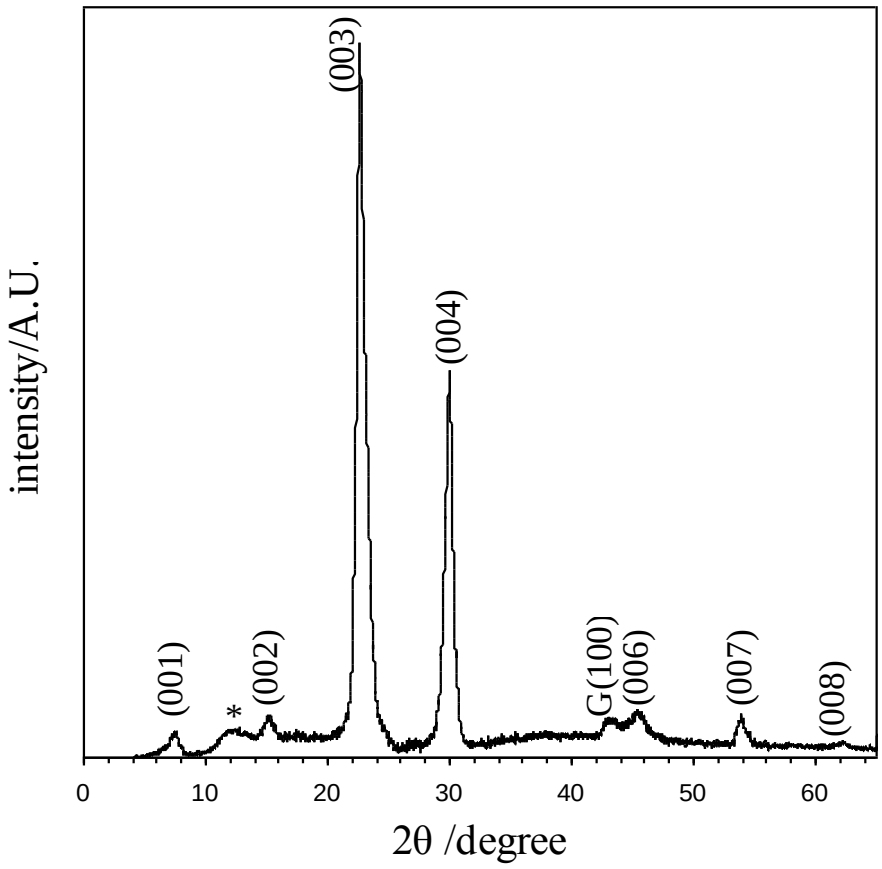

Figure 2.2 Powder XRD pattern of the electrochemically-prepared stage 2 GIC.

Figure 2.3 provides a structure model for the GICs galleries obtained. Gallery heights are larger than in $C_x[BF_4]$ (~0.79 nm) [17] and are also larger than in $C_xN(SO_2CF_3)_2$ (~ 0.81 nm) [29]. However, the observed dimensions sterically require that the long axes of $[FB(C_2F_5)_3]^-$ intercalate anions be parallel to the encasing graphene sheets.

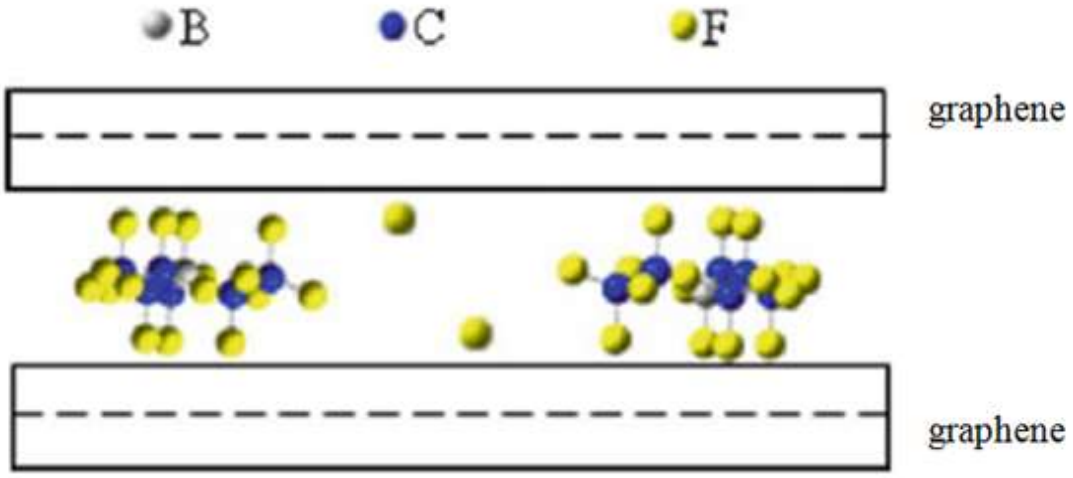

Figure 2.3 Structural model for $C_x[FB(C_2F_5)_3]\cdot\delta F$. The occupancy of fluoride anions is dependent on reaction time.

In aqueous or anhydrous hydrofluoric acid, the intercalation of fluoroanions is often accompanied by co-intercalation of fluoride [30]. The overall reaction in aqueous HF solvent is therefore provided in Equation 2.3:

$$C_x + [FB(C_2F_5)_3]^- + (1+\delta)/2\ [MnF_6]^{2-} \xrightarrow{\text{aqu. HF}} C_x[FB(C_2F_5)_3]\cdot\delta F + (1+\delta)/2\ Mn^{2+} + (3+2\delta)\ F^- \quad (2.3)$$

The electrochemical oxidation can be described by the following reaction:

$$C_x + [FB(C_2F_5)_3]^- \xrightarrow{CH_3NO_2} e^- + C_x[FB(C_2F_5)_3]\cdot\delta CH_3NO_2 \quad (2.4)$$

We previously reported δ values, which indicate the molar ratio of fluoride ion co-intercalate to larger anion intercalate for different GICs, and observed increases in the fluoride co-intercalate content for products with longer reaction times in hydrofluoric acid. Determining the detailed composition of the GICs is a prerequisite for understanding sheet charge densities. Compositional studies described below have provided both compositional parameters, *x* and δ, for the GIC products obtained here at different reaction times.

For $C_x[FB(C_2F_5)_3]\cdot\delta F$, both compositional parameters *x* and δ are obtained from F-ion probe and B analytical ICP data. Note that the methodology developed and described above in the experimental section provides the F content arising from fluoride co-intercalate, without detecting any fluoride from the borate anion. Therefore, simultaneously solving Equations 2.5 and 2.6 can be used to calculate the GIC compositions given in Table 2.2.

$$\text{mass \% B} = \frac{10.8}{12.0x + 386.9 + 19.0\delta} \quad 100 \qquad (2.5)$$

$$\text{mass \% F} = \frac{19.0\ \delta}{12.0x + 386.9 + 19.0\delta} \quad \text{x} \quad 100 \qquad (2.6)$$

Table 2.2 Compositional data for chemically-prepared $C_x[F(C_2F_5)_3B]\cdot\delta F$ at different reaction times. B and F mass pct from ICP are used to calculate *x*, δ, and borate anion mass pct. For comparison, the borate anion mass pct determined by thermogravimetry is provided.

Reaction time/ h	B / mass pct (by ICP)	F / mass pct (by F^- ion probe)	*x*	δ	$[F(C_2F_5)_3B]^-$ / mass pct (calc)	$[F(C_2F_5)_3B]^-$ / mass pct (by TGA)
1	1.07	0.086	52	0.05	38.5	36.2
2	1.07	0.062	52	0.03	38.5	37.2
5	1.06	0.90	52	0.48	38.9	38.3
10	0.99	3.1	56	1.8	38.6	36.3
20	1.05	2.4	51	1.3	40.2	37.3

Thermogravimetry can be used as a check on the compositions derived above. The GIC products show a mass loss at 180-200 ^{0}C, which is ascribed to intercalate decomposition and volatilization. (Figure 2.4) The GICs prepared with longer reaction times (10 and 20 h) have a higher fluoride content (see below), and also show a second mass loss near 300 ^{0}C. In both cases, intercalate anion decomposition begins at a much lower temperature, and occurs over a wider temperature range, than decomposition of the same anion in the potassium salt. The mass loss with onset at 550-570 ^{0}C is ascribed to decomposition and volatilization of the graphene sheets. These TGA data are used to determine the $[FB(C_2F_5)_3]^-$ content in the products (last column in Table 2.2), and the results agree well with the compositions derived from ICP data.

The decreased thermal stability of anion intercalates as compared to their alkali metal salts is a well-known phenomenon for GICs. In this case, $K[FB(C_2F_5)_3]$ shows a relatively sharp mass loss with onset at ≈ 360 ^{0}C. Most likely, the lower stability of the intercalated $[FB(C_2F_5)_3]^-$ anion results from the catalytic activity of the proximal graphene sheet surfaces. Another example of thermolytic catalysis by carbon surface is seen during methane decomposition on carbon [31].

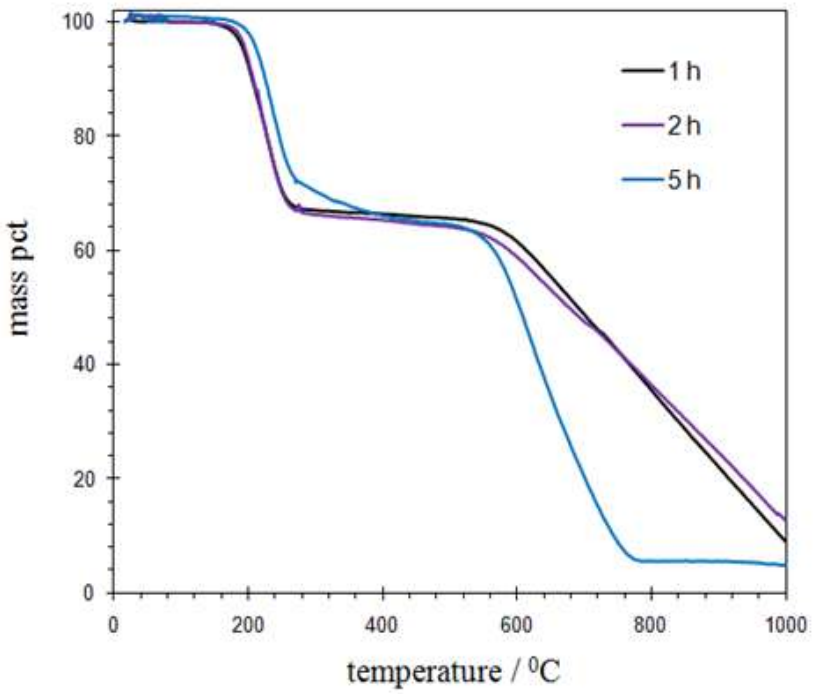
100
80
60
40
20
0
mass pct
0
200
400
600
800
1000
temperature / ^{0}C
1 h
2 h
5 h

(a)

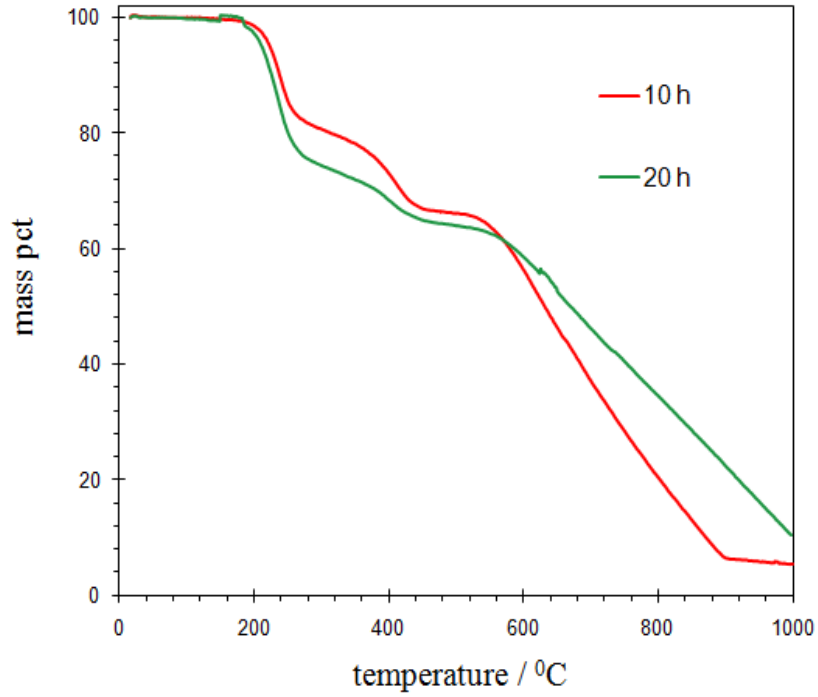
100
80
60
40
20
0
mass pct
0
200
400
600
800
1000
temperature / ^{0}C
10 h
20 h

(b)

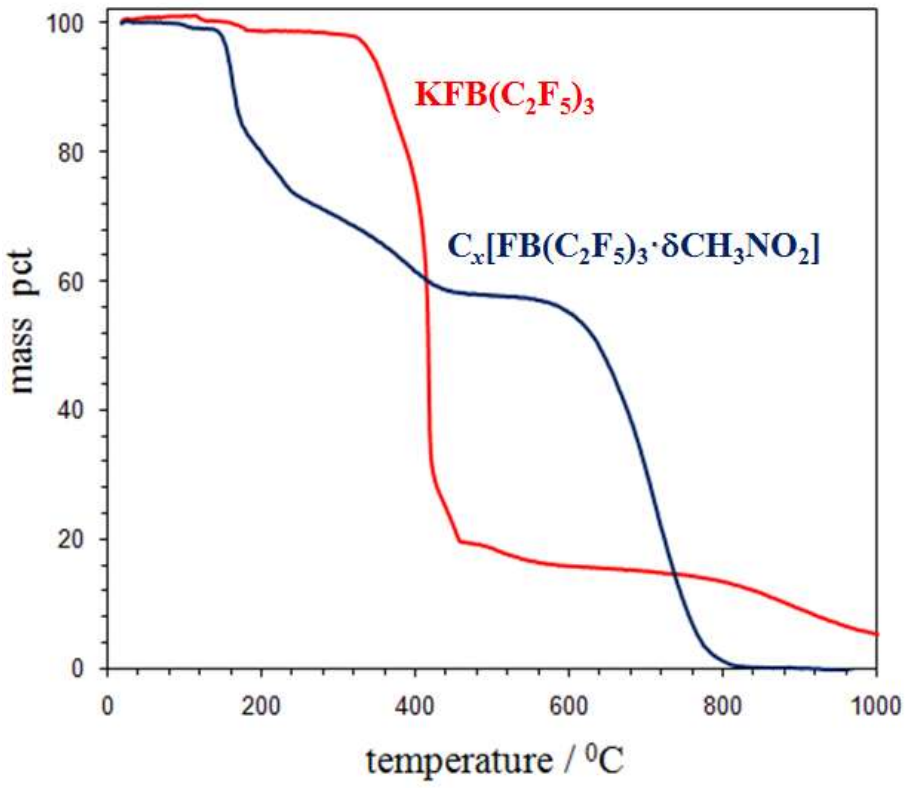

(c)

Figure 2.4 TGA data obtained for (a) the chemically prepared GICs for 1 h, 2 h, 5 h (b) the chemically prepared GICs for 10 h, 20 h (c) the electrochemically-prepared GIC (EC), and neat $K[FB(C_2F_5)_3]$.

Although the $[FB(C_2F_5)_3]^-$ anion intercalate content is nearly constant for the chemically-oxidized GICs (as reflected in the relatively constant value obtained for *x*), the co-intercalate fluoride content indicated by δ increases about 25-fold for the longer reaction times. An increase in the fluoride co-intercalate content with reaction time has been observed previously with GICs prepared in hydrofluoric acid [29]. $C_xN(SO_2CF_3)_2 \cdot \delta F$ was prepared in hydrofluoric acid and compositional ranges of *x*= 50-60 and δ= 0–1 were obtained, with δ increasing for longer reactions. That GIC has $d_i \approx$ 0.8 nm, similar to the GICs obtained in this study. For GICs with larger galleries, the fluoride co-intercalate contents can be significantly higher, for example $C_x[B(OC(CF_3)_2C(O)O)_2] \cdot \delta F$ (d_i= 1.5 nm, δ= 4.1), $C_x[B(OC(O)C(O)O)_2] \cdot \delta F$ (d_i= 1.4 nm, δ= 2.9) [21], and $C_xC_8F_{17}SO_3 \cdot \delta F$ (d_i= 2.7 nm, δ= 2.4) [32].

For the electrochemical product, the TGA mass loss below 110 ^{0}C (1.3 %) is ascribed to intercalated solvent (the normal b.p. of CH_3NO_2 is 101 ^{0}C). As above, mass losses below 550 ^{0}C are ascribed to intercalate decomposition and volatilization and the higher temperature mass loss is ascribed to decomposition of the graphene sheets. Combining B analysis and TGA mass loss gives a composition of *x*= 44 and δ= 0.37 for the $C_x[FB(C_2F_5)_3] \cdot \delta CH_3NO_2$ product obtained. The EC product has somewhat higher borate anion content than the chemically-oxidized GICs, but the x values obtained are similar to those observed for other small fluoro- or oxoanions. Previous studies showed that for smaller intercalate anions; GIC compositions generally have $x \approx 24n$, where n is the GIC stage [13]. For example, for stage 2 GICs, the following intercalate anion contents have been determined; $[PF_6]^-$(*x*= 48), $[AsF_6]^-$ (*x*= 45) [33], and HSO_4^- (*x*= 48) [13].

For large intercalate anions, steric interactions limit the packing density of intercalated species, and thus result in significantly larger values of *x* at a given GIC stage. For example, stage 1 $C_x[B(OC(CF_3)_2C(O)O)_2]$ (*x*= 51) [21], stage 1 $C_x[B(OC(CF_3)_2C(CF_3)_2O)_2]$ (*x*= 58) [20] stage 2 $C_x[B(OC(O)C(O)O)_2]$ (*x*= 110) [34] all show much lower intercalate contents than those expected using the *x*= 24n relation. These GICs can also have high fluoride co-intercalate contents. As has been noted previously, the fluoride co-intercalate content appears to depend both on synthetic conditions and the gallery dimensions [29].

The "standing-up" orientation for the borate chelate intercalates, i.e. with their long axes perpendicular to graphene sheets allow for closer packing [34]. In the present case, the borate anions are smaller and can adopt a "lying-down" orientation.

2.5 REFERENCES

1. Dresselhaus, M.S.; Dresselhaus, G., *Advances in Physics*, **2002**, 51(1), 1.

2. Zabel, H.; Solin, S.A., *Graphite Intercalation Compounds. Springer-Verlag, Berlin*, **1990**, 1.

3. Kharissova, O.V.; Kharisov, B.I., *The Open Inorganic Chemistry Journal*, **2008**, 2, 39.

4. Nicholas, R.J.; Mainwood, A.; Eaves, L., *Phil. Trans. R. Soc. A*, **2008**, 366, 189.

5. Yakovlev, A.V.; Finaenov, A.I.; Zabud'kov, S.L.; Yakovleva, E.V., *Russian Journal of Applied Chemistry*, **2006**, 79(11), 1741.

6. Stankovich, S.; Dikin, D.A.; Piner, R.D.; Kohlhaas, K.A.; Kleinhammes, A.; Jia, Y. et al. , *Carbon*, **2007**, 45(7), 1558.

7. Ka, B.H.; Oh, S.M., *Journal of the Electrochemical Society*, **2008**, 155(9), A685.

8. Wang, Z.M.; Hoshinoo, K.; Xue, M.; Kanoh, H.; Ooi, K., *Chem Commun*, **2002**, 1696.

9. Dillon, A.C.; Jones, K.M.; Bekkedahl, T.A.; Kiang, C.H.; Bethune, D.S.; Heben, M.J., *Nature (London)*, **1997**, 386(6623), 377.

10. Ruisinger, B.; Boehm, H., *Carbon*, **1993**, 31(7), 1131.

11. Zhang, X.; Lerner, M.M., *Chem Mater*., **1999**, 11(4), 1100.

12. Yan, W.; Lerner, M.M., *Carbon*, **2004**, 42(14), 2981.

13. Besenhard, J.; Wudy, E.; Moehwald, H.; Nickl, J.; Biberacher, W.; Foag, W., *Synth. Met*., **1983**, 7, 185.

14. Zhang, X.; Lerner, M.M., *Mol Cryst Liq Cryst Sci Technol Sect A: Molecular Crystals and Liquid Crystals*, **2000**, 340, 37.

15. Yan, W.; Lerner, M.M., *J. Electrochem. Soc*., **2001**, 148(6), D83.

16. Yan, W.; Lerner, M.M., *Carbon*, **2004**, 42(14), 2981.

17. Bilaud, D.; Pron, A.; Vogel, F.L.; Hérold, A., *Mat Res Bull*, **1980**,15,1627.

18. Chenite, A.; Billaud, D., *Carbon*, **1982**, 20(2), 120.

19. Barthel, J.; Schmidt, M.; Gores, H.J., *J. Electrochem. Soc*., **2000**, 147(1), 21.

20. Yan, W.; Lerner, M.M., *J. Electrochem. Soc*., **2003**, 150(9), D169.

21. Yan, W.; Lerner, M.M., *J. Electrochem. Soc*., **2004**, 151(2), J15.

22. Katinonkul, W.; Lerner, M.M., *Carbon*, **2007**, 45, 2672.

23. Frohn, H.J.; Bardin, V.V., *Z. Anorg. Allg. Chem*., **2001**, 627(1), 15.

24. Frohn, H.J.; Bardin, V.V., *Z. Anorg. Allg. Chem*., **2001**, 627, 2499.

25. Zhou, Z-B.; Matsumoto, H.; Tatsumi, K., *Chem. Eur. J*., **2006**, 12, 2196.

26. Pawelke, G.; Willner, H., *Z. Anorg. Allg. Chem*., **2005**, 631, 759.

27. Bode, H.; Jenssen, H.; Bandte, F., *Angew. Chem*., **1953**, 65, 304.

28. VWR International, Inc. Combination Fluoride Electrodes Instruction Manual. VWR.

29. Katinonkul, W.; Lerner, M.M., *Carbon*, **2007**, 45, 499.

30. Forsman, W.; Mertwoy, H., *Carbon*, **1982**, 20(3), 255.

31. Sun, R-Q,; Sun, L-B.; Chun, Y.; Xu, Q-H., *Carbon*, **2008**, 46, 1757.

32. Zhang, Z.; Lerner, M.M., *Chem. Mater*., **1996**, 8(1), 257.

33. Billaud, D.; Chenite, A., *J. Power Sources*, **1984**, 13, 1.

34. Katinonkul, W.; Lerner, M.M., *J. Physics and Chemistry of Solids*, **2007**, 68, 394.

CHAPTER 3

ELECTROCHEMICAL PREPARATION OF GRAPHITE INTERCALATION COMPOUNDS CONTAINING A CYCLIC AMIDE, $[CF_2(CF_2SO_2)_2N]^-$

Bahar Özmen-Monkul[a], Michael M. Lerner[a],

Rika Hagiwara[b]

[a] Department of Chemistry

Oregon State University

Corvallis, OR 97331-4003, USA

[b] Graduate School of Energy Science,

Kyoto University Sakyo-ku,

Kyoto, 606-8501, Japan

Journal of Fluorine Chemistry, **2009**, 130, 581-585

3.1 ABSTRACT

Graphite intercalation compounds (GICs) containing the cyclo-hexafluoropropane-1,3-bis(sulfonyl)amide anion, $[CF_2(CF_2SO_2)_2N]^-$, are prepared for the first time. Stage 2 and 3 GICs are obtained by electrochemical oxidation of graphite in a nitromethane electrolyte. Gallery heights of 0.85-0.86 nm are determined by powder X-ray diffraction, and the intercalate anion orientation within the intercalate galleries is modeled using an energy minimized anion structure. GIC compositions are determined by thermogravimetric, fluorine and nitrogen analyses. The chemical preparation and bifluoride displacement reactions are compared with a GIC containing the linear bis(trifluoromethanesulfonyl)amide anion, $[(CF_3SO_2)_2N]^-$.

3.2 INTRODUCTION

Graphite is a unique layered host in its ability to undergo either oxidative (acceptor-type) or reductive (donor-type) intercalation chemistry, and in the extent of ordering of the intercalate galleries known as staging [1]. Stage 2 indicates two graphene sheets between intercalate galleries, there are three graphene sheets separating the galleries in a stage 3 GIC, and etc. Hydrolysis or thermolysis treatment of the acceptor-type GICs graphite sulfate or graphite nitrate produces exfoliated graphite, which is an important commercial material [2]. Thermally exfoliated graphite (TEG) is used in applications as liners, adsorbents, catalysts, flexible heaters, and as part of multifunctional composites in fireproofing [3]. An oxidized form of graphite known as graphite oxide (GO) is also a layered material that has been proposed for many applications [3,4]. Individual graphene sheets and the thickness of a single carbon atom have been isolated recently; they have shown many novel properties [5, 6].

Aside from graphite sulfate and graphite nitrate, a broad chemistry of acceptor-type GICs has been developed. The known intercalate anions include fluoro-, chloro-, bromo- or oxometallates [1], trifluoroacetate [7], perfluoroalkyl-substituted sulfonylamides or methides [8, 9] and perfluoroalkylsulfonates [10,11]. Gallery heights of greater than 2 nm can be obtained for the latter class of GICs when the intercalates contain long fluoroalkyl groups [10]. Gallery heights refer to the distance (perpendicular to the sheet stacking direction) between carbon sheet centers encasing an intercalate gallery. The intercalation of larger anions opens the possibility of interesting new graphite chemistry such as selective sorption, catalysis, nanocomposite formation, and new routes to exfoliated graphene sheets.

Acceptor-type GICs can be prepared either by chemical or electrochemical oxidation, but reactions often require challenging synthetic conditions. The very high onset potential for graphite intercalation (which depends on the specific chemistry but is approximately +4.5 V vs. Li/Li^+) requires that intercalate anions be highly resistant to oxidation. Additionally, other reaction components, such as the solvent (for chemical reactions) or current collector, binder, and electrolyte (for electrochemical reactions) must also be oxidatively stable at the chemical or electrochemical potentials that are applied.

GICs containing the bis(trifluoromethanesulfonyl)amide anion, $C_x[(CF_3SO_2)_2N]$, were first reported by the oxidation of graphite with a solution of $[MnF_6]^{2-}$ dissolved in 48 % hydrofluoric acid [8]. The intercalation kinetics is remarkably fast; GICs are obtained from 100 μm particle diameter graphite within seconds without any trace of a bulk graphite phase remaining. The reported gallery height, d_i, for the products are 0.81 nm, and the stage 2 GIC has x= 37. Although stage 1 GICs cannot be obtained using an aqueous hydrofluoric acid solvent due to the limited oxidative stability of this solvent [11], a stage 1 $C_x[(CF_3SO_2)_2N]$ was subsequently prepared by electrochemical oxidation in nitromethane [12].

Much slower kinetics are observed for GICs prepared with the larger amides bis(pentafluoroethanesulfonyl)amide, $[(CF_3CF_2SO_2)_2N]^-$, trifluoromethanesulfonyl-n-nona-fluorobutanesulfonylamide, $[(CF_3SO_2)(CF_3(CF_2)_3SO_2)N]^-$, and tris(trifluoromethanesulfonyl)methide, $[(CF_3SO_2)_3C]^-$ [8, 9]. These syntheses require days or weeks using the $[MnF_6]^{2-}$ oxidant at ambient or elevated temperatures up to 70°C.

In this study, we report the first GIC containing a cyclic amide, cyclo-hexafluoropropane-1,3-bis(sufonyl)amide, $[CF_2(CF_2SO_2)_2N]^-$, by electrochemical oxidation using a nitromethane electrolyte. Although GICs containing the linear $[(CF_3CF_2SO_2)_2N]^-$ anion can be prepared by chemical oxidation in hydrofluoric acid as noted above, and are stable in that organic solvent, GICs containing $[CF_2(CF_2SO_2)_2N]^-$ cannot be prepared by that chemical method and undergo anion displacement reactions when placed in hydrofluoric acid. These chemical differences will be further described and discussed below.

3.3 EXPERIMENTAL

SP-1 grade graphite powder (Union Carbide, average particle diameter 100 μm), cyclohexane (Fisher Scientific, HPLC grade), hexane (Fischer Chem, certified grade), hydrofluoric acid (Mallinckrodt AR, 48 % w/o), anhydrous hydrofluoric acid (AHF) (Matheson, pure grade) and fluorine gas (Air Products, > 97 %) were used as received. Bright yellow $K_2[MnF_6]$ powder was synthesized according to a literature method [13] by the reduction of $K[MnO_4]$ (EM Science GR) with H_2O_2 (Mallinckrodt AR, 30 % aqueous solution). Potassium cyclo-hexafluoropropane-1,3-bis(sulfonyl)amide, $K[CF_2(CF_2SO_2)_2N]$ (Jemco Inc.) and lithium bis(trifluoromethanesulfonyl)amide, $Li[(CF_3SO_2)_2N]$ (3M) were dried by heating in *vacuo* at 100 ºC for 48 h. Nitromethane, CH_3NO_2 (Sigma-Aldrich, > 99 %) was stirred over 4A molecular sieve for 48 h and subsequently handled under an inert atmosphere.

For the electrochemical experiments, the working electrodes were prepared by painting cyclohexane slurries of SP-1 graphite powder (50-60 mg) and 10 wt % polymer

binder (EPDM) onto Ni mesh flags (nominal area 1 cm^2) welded to Ni wires. The coated electrodes were air dried to remove excess solvent. Counter electrodes were stainless steel (SS) mesh and reference electrodes were Ni wires. Cells were subsequently assembled and operated in an inert atmosphere glove box at ambient temperature. Two-compartment cells with glass-frit separators were filled with electrolyte solutions of 0.05 M $K[CF_2(CF_2SO_2)_2N]$ / CH_3NO_2 and 0.33 M $Li[(CF_3SO_2)_2N]$ / CH_3NO_2 for the syntheses of GICs of $C_x[(CF_2(CF_2SO_2)_2N]$ and $C_x[(CF_3SO_2)_2N]$, respectively. Galvanostatic oxidation was carried out for a set time at the working electrode, depending on the desired stage. At the same time, electrolyte reduction occurs at the counter electrode. Following the electrochemical oxidation reactions, working electrodes were removed from the electrolyte solutions and washed with 3-4 mL of nitromethane before being placed under dynamic vacuum for 0.25 h.

In the chemical displacement reactions, the electrochemically-obtained GICs were stirred at ambient temperature in 10 mL of 0.05 M $K_2[MnF_6]$ / HF (aq. 48 %) for ~70 h. The solids were isolated by filtration on hydrophilic polypropylene membranes (0.2 μm pore diameter), briefly rinsed with 4-5 mL hexane, and then dried overnight *in vacuo*. All GIC products were stored and handled under an inert atmosphere.

Powder X-ray diffraction (XRD) data were collected on a Rigaku MiniFlex II diffractometer with Ni-filtered Cu K_α radiation using a detector slit width of 3 mm. Data were collected at 0.02° 2Θ steps, between 4° and 65°.

TGA data were obtained using a Shimadzu, Inc. TGA-50. Samples were loaded into Pt pans and the sample chamber flushed with argon gas at a flow rate of 20 ml / min. Temperature was increased from ambient to 1000°C at 5°C / min.

The energy-minimized structure for the cyclic $[CF_2(CF_2SO_2)_2N]^-$ anion was calculated using the hybrid density functional method (B3LYP) with a 6-31G (d) basis set and GaussView 3.0 software. The energy-minimized structure of linear $[(CF_3SO_2)_2N]^-$ has been previously reported [12].

Elemental analyses of hydrogen, carbon, nitrogen and fluorine using a CHN coder and a fluoride ion selective electrode were performed at the Center for Organic Elemental Microanalysis of Kyoto University.

GIC compositions were calculated from the obtained fluorine and nitrogen mass percentages according to equations (3.1) and (3.2), with *F* or *N* being the number of fluorine or nitrogen atoms, and *x* the number of graphene carbons, per formula unit:

$$\text{mass pct F} = 100 * [19.0\,F \,/\, (12.0\,x + \text{MW of anion})] \quad (3.1)$$

$$\text{mass pct N} = 100 * [14.0\,N \,/\, (12.0\,x + \text{MW of anion})] \quad (3.2)$$

3.4 RESULTS AND DISCUSSION

Powder XRD data for electrochemically-prepared $C_x[CF_2(CF_2SO_2)_2N]$ are shown in Figure 3.1 GIC products were obtained after oxidation for 13 h at 7 mA / g and 5 h at 17 mA / g; these were subsequently indexed as stage 2 and 3 GICs, respectively. Fits of the indexed peaks provide basal plane repeat distances (I_c) of 1.186 nm for stage 2 and

1.530 nm for stage 3 products. Using the relation of gallery height, repeat distance, and stage indicated in equation 3.3:

$$I_c = d_i + 0.335 \text{ nm } (n-1) \quad (3.3)$$

gives d_i= 0.85 nm for stage 2 and d_i= 0.86 nm for stage 3.

For comparison, GICs containing the linear $[(CF_3SO_2)_2N]^-$ anion have been prepared by both electrochemical and chemical methods with d_i= 0.80-0.81 nm for all stages obtained [8, 12]. The gallery heights impose steric restrictions on possible intercalate anion orientations, as shown in Figure 3.2.

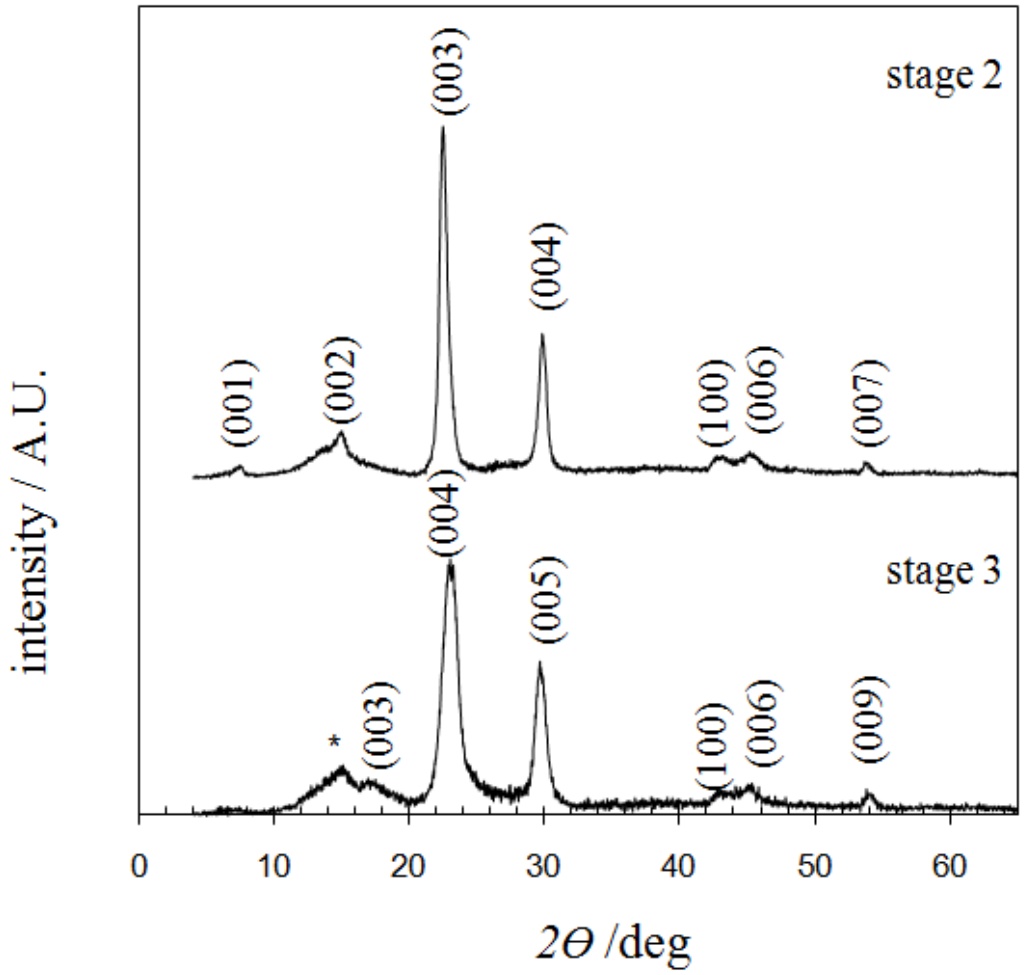

Figure 3.1 Powder XRD patterns of stage 2 and stage 3 $C_x[CF_2(CF_2SO_2)_2N]$. Some assigned indices are shown. The starred peak corresponds an impurity.

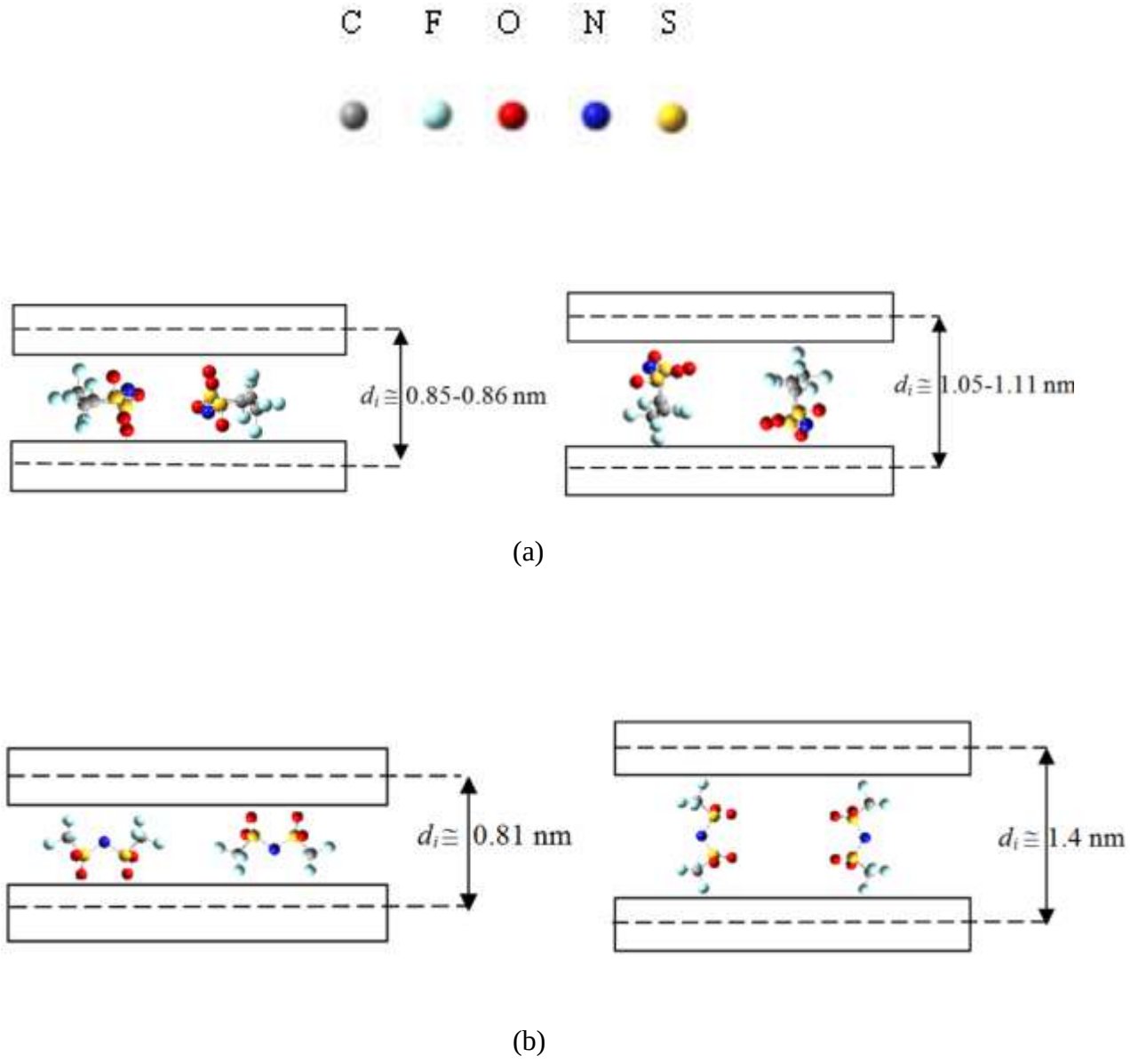

Figure 3.2 Structure models for $C_x[CF_2(CF_2SO_2)_2N]$ with intercalate lying down or standing up (a), and $C_x[(CF_3SO_2)_2N]$ with intercalate lying down or standing up (b). Intercalate dimensions suggest the lying down orientation occurs in both GICs.

Due to these steric restrictions, the pseudo-cylindrical linear amide must be oriented with long axes parallel to the encasing graphene sheets (called a "lying-down" orientation) [12]. A model structure with this intercalate orientation also agrees well with the one-dimensional structure refinement of powder XRD data [8]. Similarly, the gallery heights obtained for the cyclic amide found in this study require that long axes be parallel to the graphene sheets. As further indicated in Figure 3.2, the lying-down orientation has two possibilities, i.e. the nitrogen may point toward either of the graphene sheets. Figure 3.3 shows the calculated surface charge density of the cyclic amide. The most negatively charged surface is around the N atom, which can orient towards either of the adjacent positive graphene sheets surfaces.

The molar ratios of graphene carbon to anion, i.e. the compositional x value in $C_x[CF_2(CF_2SO_2)_2N]$ as determined by the N and F elemental analyses data are $x = 45$, $x = 52$ for the stage 2 and 3 products, respectively (see Table 3.1).

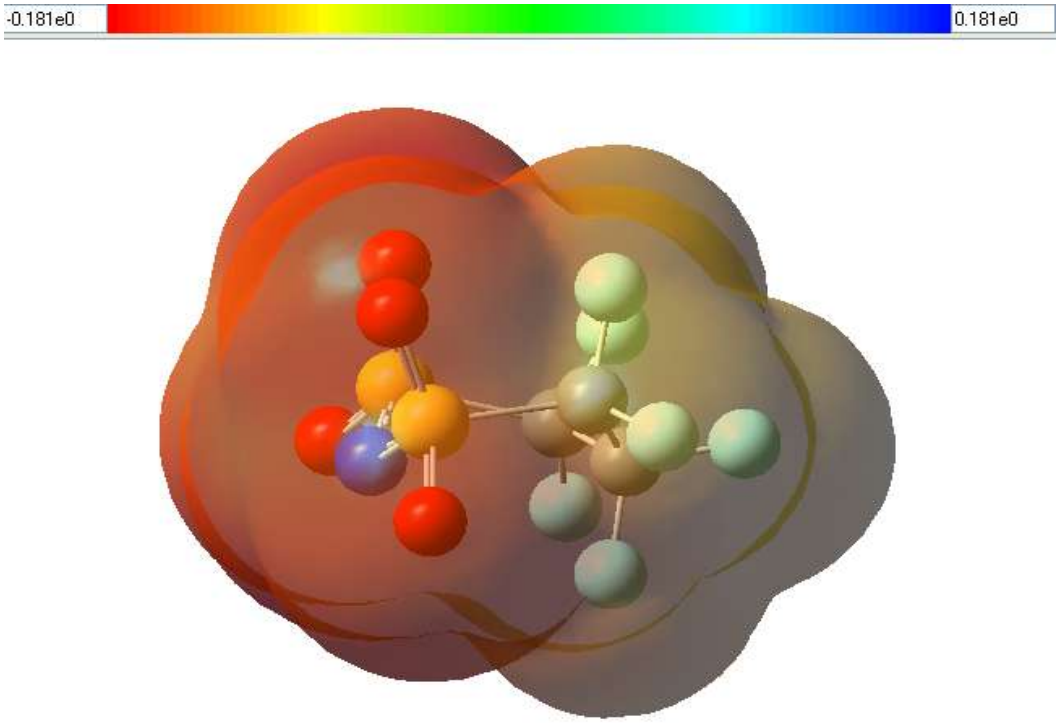

Figure 3.3 Calculated surface charge density of the $[CF_2(CF_2SO_2)_2N]^-$ anion.

Table 3.1 Calculated and observed mass percents of N, F in stage 2 $C_{45}[CF_2(CF_2SO_2)_2N]$ and stage 3 $C_{52}[CF_2(CF_2SO_2)_2N]$.

	N /mass pct		F /mass pct	
	(calc)	(obs)	(calc)	(obs)
Stage 2	1.67	1.72	13.59	13.25
Stage 3	1.54	1.57	12.51	12.29

Thermogravimetric analysis (TGA) of the two $C_x[CF_2(CF_2SO_2)_2N]$ products and the corresponding potassium salt of the amide anion are shown in Figure 3.4. Three mass loss regions are observed for the GICs, from 105-205 °C, from 410-480 °C, and from 600-800 °C. The small mass loss below 100 °C (solvent b.p.= 101 °C) shows that any CH_3NO_2 solvent co-intercalate is effectively removed during evacuation. The first two mass losses are ascribed to intercalate anion decomposition and volatilization. The anion decompositions for the GICs initiate at a much lower temperature, and occur over a wider temperature range, than that for the corresponding potassium salt. The decreased thermal stability for GICs relative to related alkali or alkaline earth salts of the same anions is commonly observed and likely results from the accelerated kinetics due to catalytic activity of the graphene sheets on the thermolysis of organic molecules [14, 15].

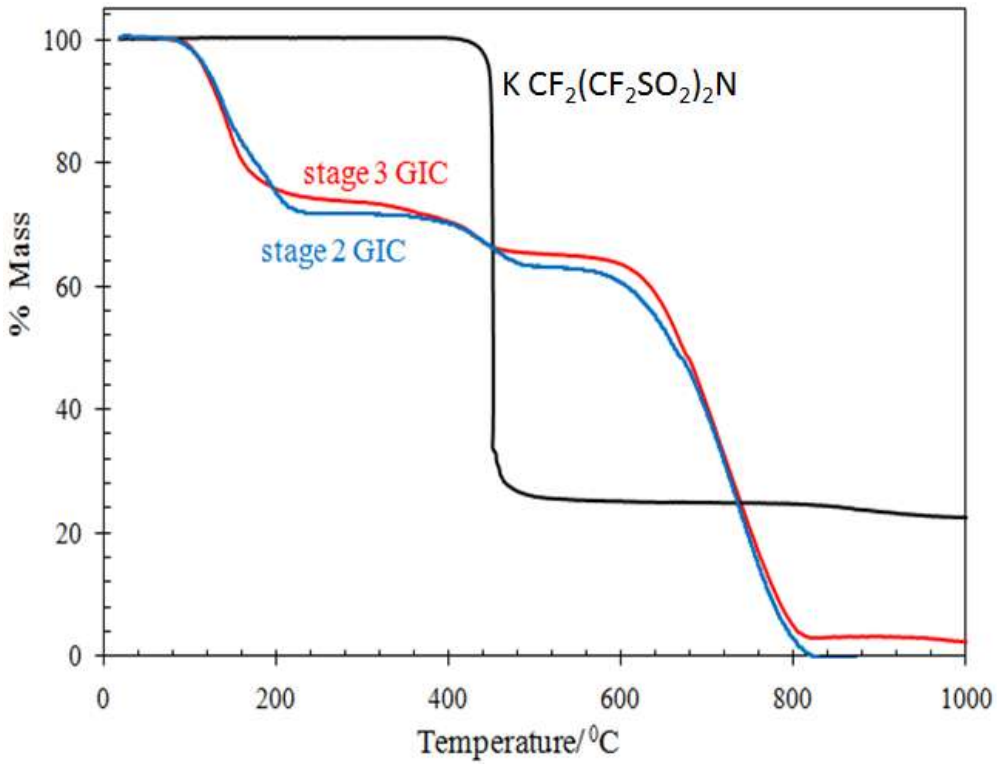

Figure 3.4 TGA data for stage 2 and stage 3 GICs of $C_x[CF_2(CF_2SO_2)_2N]$ and for $K[CF_2(CF_2SO_2)_2N]$.

The final mass loss above 600 °C is ascribed to the decomposition and volatilization of the graphene sheets. In the case of $K[CF_2(CF_2SO_2)_2N]$, the observed 22 % mass residual at 1000 °C may arise from one or more of the following species (with theoretical mass percent residuals indicated): KF (18 %), K_2O (14 %), or K_2S (17 %). The specific decomposition product(s) for the salt are not identified in this study. From the elemental analyses described above, mass percents due to graphene carbon are calculated to be 65 and 68 % for the stage 2 and stage 3 GICs respectively. The observed mass losses for two low temperature regions total 63 and 62 % (from TGA) for stage 2 and 3, respectively, and are therefore in good agreement with these compositions.

The obtained x= 45 value for a stage 2 $C_x[CF_2(CF_2SO_2)_2N]$ conforms to the long established observation of C_x[Anion], x= 24n, where n is the stage [16]. The obtained x= 52 for stage 3 GIC is relatively low and suggests that some stage 2 is present. The broader PXRD peaks observed further support this conclusion.

Although the gallery heights and GIC compositions for the linear and cyclic amide are similar, there is nevertheless a marked difference in their relative chemical stabilities. Repeated attempts to form GICs with the cyclic amide using chemical oxidation in either hydrofluoric acid or anhydrous HF were unsuccessful; these reactions always resulted in the generation of graphite bifluoride. In contrast, as described above, the GIC containing the linear amide is readily synthesized under these conditions. We have proposed previously that graphite intercalation in hydrofluoric acid or anhydrous HF proceeds by the initial generation of graphite bifluoride, and subsequent displacement of the bifluoride intercalate with the target anion [17]. To test this model, stage 3 GICs of the cyclic amide GIC and the linear amide were prepared electrochemically and then

separately placed for 70 h in identical $K_2[MnF_6]$ / HF (aq. 48 %) solutions containing a large molar excess of bifluoride. The presence of $[MnF_6]^{2-}$ is required to prevent GIC reduction in the aqueous solvent. Powder XRD patterns of the isolated solids from these studies are shown in Figure 3.5. The GIC containing the linear amide shows no change, it is not displaced by bifluoride. This is consistent with the formation of the linear amide GIC in this solution. For the cyclic amide, however, the observed product after reaction (Figure 3.5 d) is only graphite or high-stage graphite bifluoride (d_i= 0.65 nm); i.e. bifluoride displaces the larger intercalate anion in this case.

The dramatic difference in GIC stabilities could be related to the different charge density distributions in the intercalate anions. The cyclic amide appears to present more charged surface within the gallery interior, while the negative anion surface is more effectively placed adjacent to graphene sheets for the linear amide. This could provide greater lattice stabilization energy for the linear amide GIC. Alternately, it may be that a more polar gallery interior facilitates co-intercalation and eventual displacement by bifluoride. Further work and more chemical comparisons will likely clarify the underlying cause of the observed difference in stabilities.

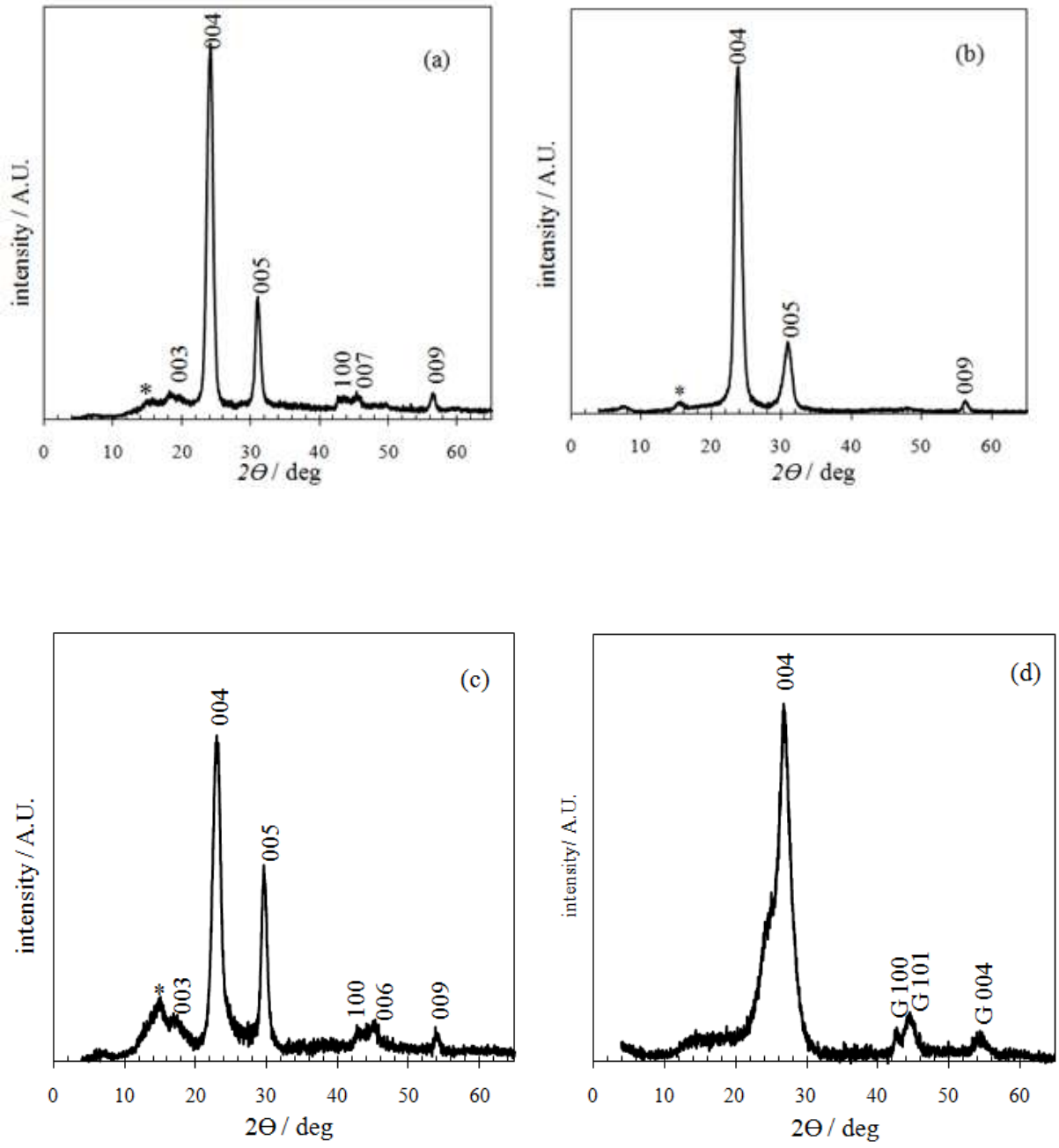

Figure 3.5 PXRD patterns of a stage 3 $C_x[(CF_3SO_2)_2N]$ before (a) and after (b) reaction with $K_2[MnF_6]$ / aq HF, and a stage 3 $C_x[CF_2(CF_2SO_2)_2N]$ before (c) and after (d) reaction with $K_2[MnF_6]$ / aq HF. Some indices are shown, those labeled G correspond to graphite. The starred peak corresponds to an impurity.

3.5 REFERENCES

1. Dresselhaus, M.S.; Dresselhaus, G., *Advances in Physics*, **2002**, 51(1), 1.

2. Sorokina, N.E.; Nikol´skaya, I.V.; Ionov, S.G.; Avdeev, V.V., *Russian Chemical Bulletin, International Edition*, **2005**, 54(8), 1749.

3. Yakovlev, A.V.; Finaenov, A.I.; Zabud'kov, S.L.; Yakovleva, E.V., *Russian Journal of Applied Chemistry*, **2006**, 79(11), 1741.

4. Kovtyukhova, N.I.; Ollivier, P.J.; Martin, B.R.; Mallouk, T.E.; Chizhik, S.A.; Buzaneva, E.V.; Gorchinskiy, A.D., *Chem. Mater*., **1999**, 11, 771.

5. Stankovich, S. ; Dikin, D.A.; Dommett, G.H.B.; Kohlhaas, K.M.; Zimney, E.J.; Stach, E.A.; Piner, R.D.; SonBinh, T.N.; Ruoff, R.S., *Nature*. **2006**, 442, 282.

6. Cassagneau, T.; Guerin, F.; Fendler, J.H., *Langmuir*, **2000**, 16, 7318.

7. Bourelle, E.; Douglade, J.; Metrot, A., *Mol. Cryst. Liq. Cryst. A.*, **1994**, 244 227.

8. Zhang, X.; Sukpirom, N.; Lerner, M.M., *Mater. Res. Bull*., **1999**, 34(3), 363.

9. Zhang, X.; Lerner, M.M., *Mol. Cryst. Liq. Cryst. Sci. Technol. Sect A: Molecular Crystals and Liquid Crystals*, **2000**, 340, 37.

10. Zhang, Z.; Lerner, M.M., *Chem. Mater*., **1996**, 8(1), 257.

11. Zhang, X.; Lerner, M.M., *Chem. Mater*., **1999**, 1, 1100.

12. Yan, W.; Lerner, M.M., *J. Electrochem. Soc*., **2001**, 148(6), D83.

13. Bode, H.; Jenssen, H.; Bandte, F., *Angew. Chem*., **1953**, 65, 304.

14. Muradov, N.; Smith, F.; T-Raissi, A., *Catal. Today*, **2005**, 102-103, 225.

15. Sun, R-Q.; Sun, L-B.; Chun, Y.; Xu, Q-H., *Carbon*, **2008**, 46, 1757.

16. Hofmann, U.; Rüdorff, W., *Transactions of the Faraday Society*. **1938**, 34, 1017.

17. Katinonkul, W.; Lerner, M.M. , *Journal of Physics and Chemistry of Solids*, **2007**, 68, 394.

CHAPTER 4

THE FIRST GRAPHITE INTERCALATION COMPOUNDS CONTAINING TRIS(PENTAFLUOROETHYL)TRIFLUOROPHOSPHATE

Bahar Özmen-Monkul, Michael M. Lerner

Department of Chemistry

Oregon State University

Corvallis, OR 97331-4003, USA

Carbon, accepted

4.1 ABSTRACT

Graphite intercalation compounds (GICs) containing the tris(pentafluoroethyl)trifluorophosphate anion, $[(C_2F_5)_3PF_3]^-$ are prepared for the first time by electrochemical oxidation of graphite in a nitromethane electrolyte. Powder X-ray diffraction (PXRD) data indicate that products are of stages 2-4 with gallery heights of 0.82-0.86 nm. Intercalate orientation is determined by using a structure model containing an energy minimized anion. GIC compositional parameters are obtained by microwave digestion followed by F elemental analysis, in combination with thermogravimetric analyses.

4.2 INTRODUCTION

Graphite can incorporate a wide range of intercalate guests between planar graphene sheets to form Graphite Intercalation Compounds (GICs). GICs can be either acceptor-type or donor- type; in the former case graphite is oxidized to accept anionic intercalates, whereas in the latter case graphite is reduced to accept cationic intercalates. Ordered sequences of graphene sheets and intercalate are known as "stages", this phenomena is observed extensively with the graphite host. Stage 1 (n=1) indicates that intercalate is present between all the graphene sheets; stage 2 (n=2) indicates the presence of intercalate between alternate graphene sheets, and etc.

The removal of valence band electrons to form acceptor-type GICs requires strong oxidants, while the input of electrons into the conduction band to form donor-type GICs requires strong reductants [1]. LiC_x compound is the most commercially important donor-type GIC; the LiC_x / C_x redox couple is the active component in the negative electrodes in Li-ion cells [2, 3]. Acceptor-type GICs have found application in exfoliated form as gas or oil adsorbents, and when pressed into sheets these materials are used as high-temperature gaskets or seals, and as packing materials [4, 5]. Exfoliated graphite is produced by the rapid volatilization of anionic intercalates at elevated temperatures. Related methods can form graphene nanoplatelets [6]. Graphene-based nanoscale materials have extraordinary mechanical, electronic and thermal properties and have been proposed for a range of applications including electronically-conducting composites [7], transparent electrodes [8] and photovoltaic devices [9, 10].

GICs with hexafluoride intercalates (PF_6^-, SbF_6^-, AsF_6^-) have been investigated previously [11, 12]. For example, direct reaction of solutions containing the nitronium

salts, NO_2PF_6 or NO_2SbF_6 with graphite can produce stage 1-2 GICs [12]. MF_6^- (M= P, As, Sb) anions have also been intercalated into graphite by electrochemical oxidation in oxidatively-stable solvents such as propylene carbonate [13] or nitromethane [14]. The tetrahedral $[BF_4]^-$ and octahedral $[PF_6]^-$, $[SbF_6]^-$, $[AsF_6]^-$ fluoroanions form GICs with gallery heights (d_i) of 0.77-0.81 nm [11, 12].

Substitution of some of the fluoro groups on fluorometallate anions such as BF_4^- with strong electron-withdrawing fluoroalkyl groups can produce new candidates for intercalation. We have recently reported the intercalation of the GICs containing $[FB(C_2F_5)_3]^-$ anion using both chemical and electrochemical methods [15].

The starting materials for intercalate anions can be present in different forms. For example, gaseous molecules, dissolved anions, or ionic liquids (ILs) are all potential sources of intercalate anions. Syntheses that involve ionic liquids can be advantageous in that they involve a liquid-solid interaction but there is no need for an added solvent that may co-intercalate. Ionic liquids have found applications as nonvolatile, nonflammable and environmentally friendly solvents [16]. Some other useful features of ILs include their excellent hydrolytic, thermal, and electrochemical stability and they have been employed in organic synthesis [17], electrosynthesis [18], gas absorption [19-21] and batteries [22].

ILs containing hexafluorophosphate are relatively hydrophobic but are hydrolytically unstable at high temperatures [23]. The instability of the PF_6^- anion towards hydrolysis is due to the formation of HF following the reaction with water. The stability can be increased by the replacement of some fluorine atoms by hydrophobic perfluoroalkyl-groups. Tris(pentafluoroethyl)trifluorophosphoric acid, $H[(C_2F_5)_3PF_3]$

(HFAP) or alkali metal salts of this acid are used as starting materials to synthesize the IL containing tris(pentafluoroethyl)trifluorophosphate anion, $[(C_2F_5)_3PF_3]^-$ [24]. The water uptake of fluoroalkylphosphate (FAP)-based ILs is much less than that of ILs containing the bis[(trifluoromethyl)sulfonyl]amide anion and is more than 10 times less than that of ILs consisting of the PF_6^- anion [25]. FAP-based ILs possess an electrochemical stability comparable to that of bis[(trifluoromethyl)sulfonyl]amide-based ILs and even higher than ILs containing tetrafluoroborate. As an example, tetrabutylammonium FAP is reported to exhibit an oxidation potential of + 3.7 V vs ferrocene and an electrochemical window as large as 7.0 V [25, 26]. 1-ethyl-3-methylimidazolium tris(pentafluoroethyl)trifluorophosphate (EMIM TFP) (see Figure 4.1) is an ionic liquid with a high conductivity of 3.6 $mScm^{-1}$ (at 20 ^0C) as well as high thermal stability (up to 300 ^0C) (EMD technical data).

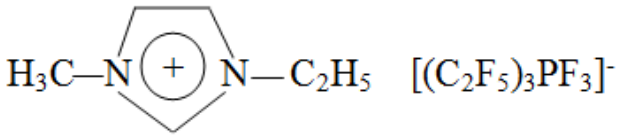

Figure 4.1 1-ethyl-3-methylimidazolium tris(pentafluoroethyl)trifluorophosphate

There are relatively few GICs containing compounds of phosphorus. GICs containing phosphate were first reported in the 1930s. Second stage GICs with H_3PO_4 and $H_4P_2O_7$ were prepared under relatively forcing conditions (80-100 ^0C, CrO_3, 150 h) [27, 28]. The co-intercalation of H_3PO_4 together with HNO_3 or H_2SO_4 has also been reported [29-33] Sorokina et al. reported ternary GICs in C-HNO_3-H_3PO_4 system (stage=

2-4, d_i= 0.82-0.84 nm) [31]. Galvanostatic intercalation at 80 ^{0}C produced stage 1 ternary GICs in C-H_2SO_4-H_3PO_4 system with d_i= 0.81 nm [33]. In these ternary GIC systems, the first step is the rapid formation of graphite nitrate or graphite bisulfate, followed by the partial replacement of solvated HNO_3 or H_2SO_4 intercalate by H_3PO_4. The second step is slow and requires high temperatures, high H_3PO_4 concentrations, and long reaction times [31].

There are reported covalent GICs where phosphate esters are incorporated into graphite oxide or graphite fluoride [34-37], the use of phosphates in graphite exfoliation is known [38, 39]. Also, ternary donor-type GICs containing graphite-phosphorus-alkali metal are reported, for example stage 1 $C_{3.2}KP_{0.3}$ has a gallery height of 0.886 nm [40]. The solutions of Li and Na metals in hexamethylphosphoramide solvent are reported to produce blue colored, ternary stage 1 GICs of $C_{32}LiX$ and $C_{27}NaX$ (X= $[(CH_3)_2N]_3PO$) with 0.762 nm gallery heights [41].

In this report, we describe the electrochemical intercalation of $[(C_2F_5)_3PF_3]^-$ into graphite and the details of electrochemical and structural properties of this new GIC.

4.3 EXPERIMENTAL

SP-1 grade graphite (Union Carbide, 100 μm average particle diameter), cyclohexane (Fisher Scientific, HPLC grade), glacial acetic acid (EM Science, 99.7 %), NaCl (Mallinckrodt, AR grade), NaOH (Mallinckrodt, ACS grade), NaF (J.T. Baker, ACS grade), and 1-ethyl-3-methylimidazolium tris(pentafluoroethyl)trifluorophosphate (EMD, ≥ 98 %) were used as received. Nitromethane (Sigma-Aldrich, > 99 %) was stirred over 4Å molecular sieve for 48 h prior to use. Ultrapure water (resistivity= 18

MΩ.cm at 25 ^{0}C) from a Milli-Q Labo system (Millipore, Milford, MA) was used throughout the experiments.

The reagents were handled and the electrochemical cell was assembled and operated under an inert atmosphere at ambient temperature. One-compartment glass cells were filled with a 0.06 M, 5 mL EMIM TFP / CH_3NO_2 electrolyte. Working electrodes were prepared by painting a cyclohexane slurry of SP-1 graphite powder (40-80 mg) and 8 wt % polymer binder (EPDM) onto a Pt mesh flag (area= 1 cm^2) welded to a Pt wire. Counter electrodes were stainless steel mesh, and reference electrodes were Pt wire. Current was applied at 30-66 mA/g carbon for 0.3-4 h. Following the electrochemical oxidation, the working electrode was removed and dried *in vacuo* for several minutes.

Powder X-ray diffraction data were collected on a Rigaku MiniFlex II diffractometer with Ni-filtered Cu K_α radiation using a detector slit width of 3 mm. Data were collected at a scan rate of 1^0 2θ / min, between 4^0 and 90^0 2θ.

TGA data were obtained using a Shimadzu, Inc. TGA-50 thermogravimetric analyzer. Samples were loaded into a platinum pan; the sample chamber was flushed with Ar gas. Thermal scans from ambient to 800 ^{0}C were performed under flowing Ar at a rate of 5 ^{0}C / min.

GIC products of samples (20–30 mg) were digested with 0.1 M NaOH (1 ml) using a microwave digester (CEM Corporation, MDS 2000) at 50 psi and then 100 psi for 0.12 h and 0.25 h, respectively. The resulting solutions were diluted to 10.0 ml and stored in Nalgene plastic bottles.

Low level total ionic strength adjustment buffer (LLTISAB) was prepared by addition of glacial acetic acid (57 ml) and NaCl (58 g) to 500 ml water, followed by the

slow addition of 5 M NaOH until the pH was between 5.0 and 5.5, and then dilution to 1.00 L total volume. Digested sample solutions were added to equal volumes of LLTISAB prior to analyses. Fluoride analyses were performed using an ion-selective fluoride combination electrode with a standard single-junction sleeve-type reference electrode and a mV scale voltmeter (VWR International, Inc.). A calibration curve was obtained using fluoride standards prepared by dilution of a standard solution (10 μg F/1.00 ml). Below pH 5, the formation of HF or HF_2^-, which are not detected by the fluoride electrode, can result in inaccurate F^- analyses. Additionally, the total ionic strength of the sample solutions must be maintained with the specification range of the electrode. The procedures adopted above provided the required ranges of both pH and ionic strength. As a control experiment, approx. 24 mg of NaF was subjected to the digestion procedure above and the fluoride mass percentage was accurately determined to within 0.1 %.

Since the hot ionic liquid itself damaged the Teflon vessels, it could not be digested by the same microwave digestion method described for GICs. The IL was digested by reaction in an NaOH solution heated to below the boiling point for 1 h, 2 h and 4 h durations. Subsequent fluoride analyses show that < 1 mass pct of the fluoride contained in the IL is present as fluoride due to decomposition of the IL under these conditions.

The energy-minimized structure of the $[(C_2F_5)_3PF_3]^-$ anion was calculated using the hybrid density functional method (B3LYP) with a 6-31G (d) basis set and GaussView 3.0 software.

4.4 RESULTS AND DISCUSSION

Electrolyte stability above 4.5 V vs Li/Li^+ is necessary for the formation of low-stage GICs. In this study, an electrolyte comprising a solution of EMIM TFP in nitromethane is employed. Although EMIM TFP is hydrophobic, and is immiscible with water, it is miscible with many organic solvents (toluene, acetonitrile, nitromethane). Nitromethane is selected as the solvent in this study due to its high oxidative stability limit (≈ 5.5 V vs. Li/Li^+) [14].

The potential-charge curves obtained for a graphite electrode oxidized in an EMIM TFP / CH_3NO_2 electrolyte shows reproducible transition points (Figure 4.2, labeled a-e) that indicate stage transitions during the intercalation of the graphite electrode according to Equation 4.1.

$$x\mathrm{C} + [(\mathrm{C_2F_5})_3\mathrm{PF_3}]^- (\mathrm{sol}) \longrightarrow \mathrm{C}_x[(\mathrm{C_2F_5})_3\mathrm{PF_3}]\cdot\delta\mathrm{F} + \mathrm{e}^- \qquad (4.1)$$

In the above product, x is the mole ratio of graphene carbon to TFP intercalate, and δ is the mole ratio of co-intercalated fluoride to TFP (see below).

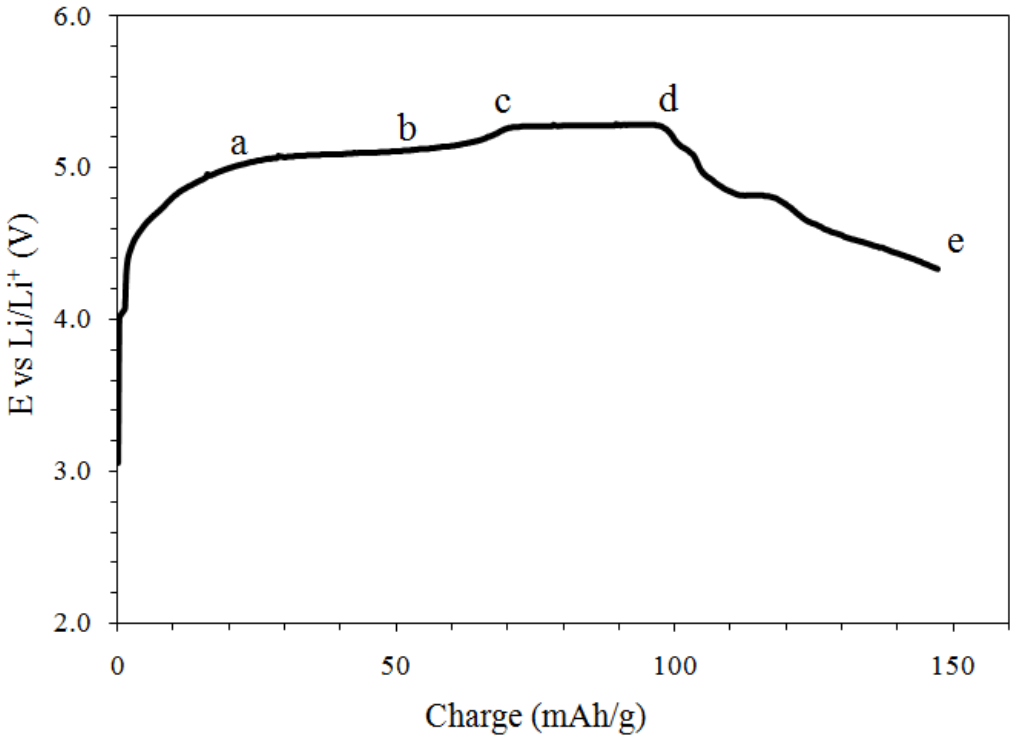

Figure 4.2 Galvanostatic potential-charge plot for a graphite electrode oxidized in 0.07 M EMIM TFP / CH_3NO_2 electrolyte.

In an idealized potential-charge curve, rising potential regions correspond to oxidation of a single-stage GIC, whereas the plateau regions represent the conversion of a higher stage to a lower stage. In Figure 4.2, plateaus are observed between points a-b and c-d. There is an unusual but reproducible decrease in the electrode potential on continued charging after the second plateau. The obtained GIC products are characterized by PXRD which is collected *ex situ* in separate experiments at each of the indicated transition points (Figure 4.3). Because of the preferred orientation of GICs only *(00l)* reflections are seen in the diffraction data. The correlation between unit cell repeat distance, I_c, and gallery height, d_i, which is the distance between intercalated repeating graphene sheets along the stacking direction, is given in Equation (4.2).

$$I_c = d_i + (n-1)\ 0.335\ \text{nm} \qquad (4.2)$$

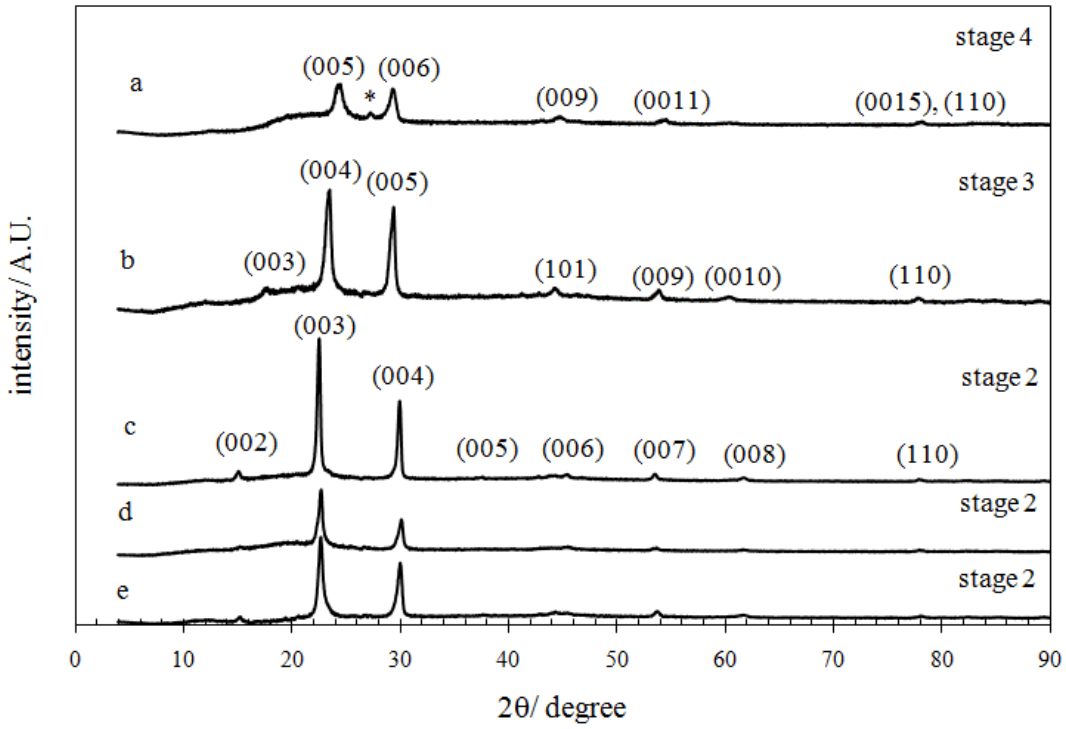

Figure 4.3 PXRD data for the $C_x[PF_3(C_2F_5)_3]$ products obtained at transitions a-e in Figure 4.2. The assigned stages and *(00l)* indices are shown for each GIC. The (*) indicates the *(002)* peak of graphite.

Table 4.1 provides the potential and applied charge at each of the labeled transition points. The plateau observed between a and b corresponds to the conversion of stage 4 to 3. No stage transition is observed, however, on charging from point c to d. The decreasing potential after point d (Figure 4.2) does not relate to a stage change in the GIC obtained (see Figure 4.3), and has not been observed previously in electrochemical experiments using a nitromethane electrolyte [42]. This potential decrease is therefore attributed to the decomposition of the organic cation present in the ionic liquid. Supporting this assignment, it is observed that the stage 2 GIC obtained at point e is not stable in the electrolyte. While at open circuit, a potential decrease is observed and after 3 h in the electrolyte the product is reduced back to graphite, as seen in the galvanostatic potential-time curve in Figure 4.4.

Table 4.1 Electrochemical and diffraction data for products obtained at transition points a-e in Figure 4.2 during galvanostatic oxidation of graphite in 0.07 M EMIM TFP / CH_3NO_2 electrolyte.

Transition point	a	b	c	d	e
V vs. Li	5.10	5.14	5.26	5.28	4.34
$Q_{applied}$ (mAh/g)	23	47	64	116	147
Stage	4	3	2	2	2
d_i (nm)	0.823	0.850	0.857	0.853	0.853

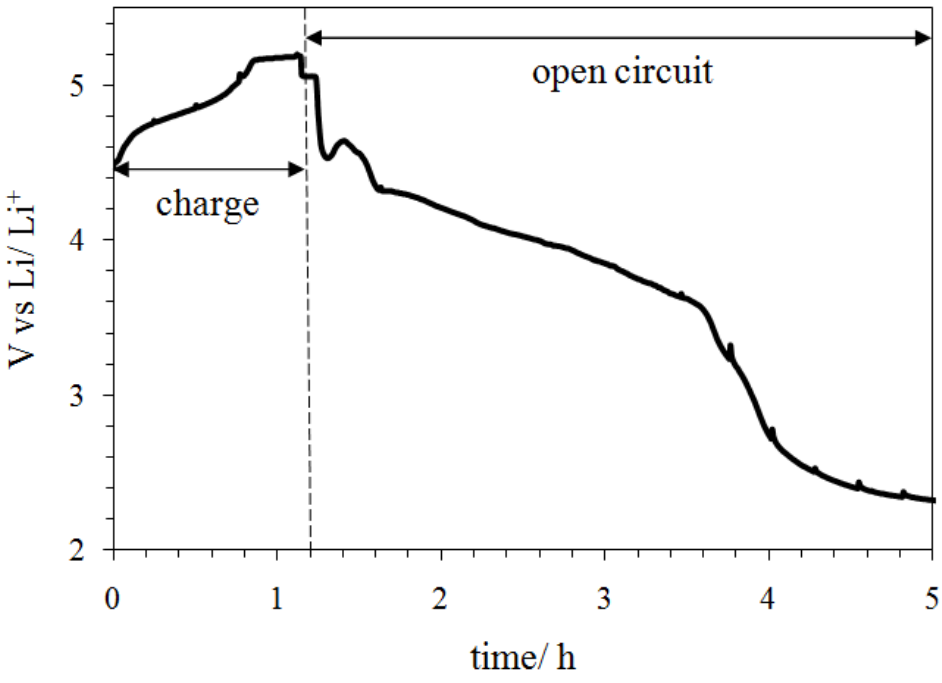

Figure 4.4 Galvanostatic potential-time (charge and open circuit) curve for a graphite electrode oxidized in 0.062 M EMIM TFP / CH_3NO_2 electrolyte.

The oxidation potentials required to form a GIC stage vary for different intercalate anions and reaction conditions. Where reaction conditions are controlled, these compositional differences can be related to the thermodynamics of GIC formation. In a simple model, where similar intercalate packing densities are assumed, lattice enthalpies for these two-dimensional ionic structures are inversely proportional to the separation of ionic charges, and thus inversely proportional to the gallery heights. Figure 4.5 shows a plot of the oxidation potentials for electrochemically-prepared stage 2 GICs vs $1/d_i$. The approximately linear relation confirms the utility of this simple model and also underscores the very high potentials that will be required for the intercalation of larger anions. The observed oxidation potential for the preparation of stage 2 $C_xPF_3(C_2F_5)_3$ (d_i = 0.85-0.86 nm) is in good agreement with this trend.

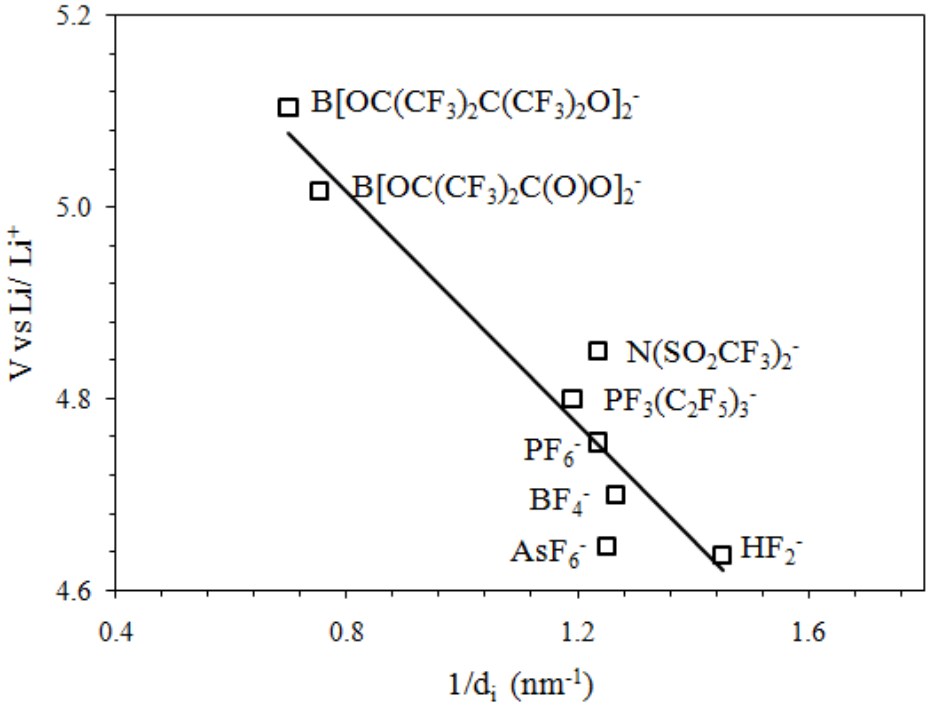

Figure 4.5 Relationship between oxidation potentials for stage 2 GICs and $1/d_i$

There are two geometric isomers of $[(C_2F_5)_3PF_3]^-$, facial (fac) and meridional (mer), with pseudo C_{3v} and C_s symmetries, respectively. The $H[(C_2F_5)_3PF_3]$ precursor in the preparation of ILs, contains predominantly mer- isomer, with the fac- isomer present at approximately 15 mol %, as determined by ^{19}F NMR spectroscopy [25]. A similar isomer ratio is presumed to exist in EMIM TFP [24, 25]. Since the anion present in the electrolyte is in large excess to that intercalated into the GIC, however, there are sufficient concentrations of both isomer to form the GIC products obtained.

The energy-minimized structures for the $[(C_2F_5)_3PF_3]^-$ anion for both fac- and mer- isomers, oriented to generate minimum gallery heights, are shown in Figure 4.6. In Figure 4.6, the intercalate anions are oriented within galleries to minimize the gallery heights, and therefore allow the most favorable lattice enthalpy. For the mer isomer, the F-P-F axis containing trans fluoride substituents on the central P, is perpendicular to the graphene sheets. For the fac isomer, the triangular face containing 3 F substituents is oriented parallel to the graphene sheets. Anion orientations that minimize gallery height are observed for most GIC products [43, 44], although exceptions are known [42].

The GIC galley heights are calculated by summing the anion heights, the van der Waals radii of two outer fluorine atoms (0.135 nm) and one graphene sheet thickness. The calculated gallery heights of fac- and mer- isomers thus obtained are 0.88 nm and 0.96 nm, respectively. The observed gallery height for a stage 2 GIC by PXRD is 0.85-0.86 nm, suggesting that the fac isomer predominates in the GIC products.

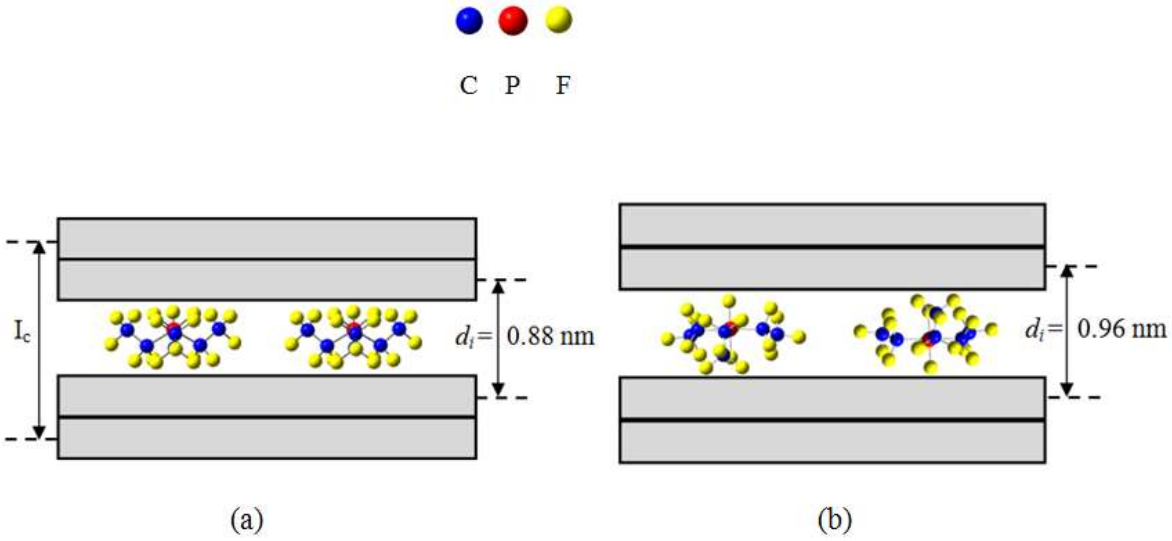

Figure 4.6 Structural models for stage 2 GICs of $C_x[PF_3(C_2F_5)_3]$ (a) fac- isomer (b) mer- isomer which indicate two equivalent orientations for each isomer. The gallery heights (d_i) and the identity period (I_c) are also indicated

Table 4.2 provides the compositional parameters of $C_x[PF_3(C_2F_5)_3]$ obtained at transition points from a to e. Note that the compositional parameter *x* cannot be accurately determined by coulometry due to the inefficiency of the electro-oxidation. Therefore, composition is determined by combining TGA data (which provide the total mass of phosphate and fluoride intercalates) with ion-selective fluoride analysis (which provides the fluoride intercalate content) in order to determine the composition of $C_x[PF_3(C_2F_5)_3]\cdot\delta F$. Since fluoride can be generated by electrolyte decomposition during the electro-oxidation, and fluoride ion co-intercalates are well known in fluoroanion-containing GICs, the fluoride co-intercalate content was evaluated for each GIC product obtained.

Table 4.2 Compositional data for electrochemically prepared GICs of $C_x[PF_3(C_2F_5)_3].\delta F$ at different transition points (a-e). The measured mass pct for F (ion-selective electrode) and graphene C mass pct (TGA) are used to calculate *x* and δ.

Transition point	C/mass pct (TGA)	F/mass pct (ion probe)	*x*	δ
a	69.5	0.45	85.9	0.4
b	67.8	0.17	78.6	0.1
c	59.8	3.53	60.6	2.3
d	59.6	3.80	53.1	2.3
e	52.0	3.01	43.0	1.6

Graphene carbon mass losses observed from TGA graphs above temperatures of 600 ^{0}C (Figure 4.7) are used to calculate x and δ by solving Equations 4.3 and 4.4 simultaneously. The F mass pct and C mass pct values shown in Table 4.2 are calculated after the subtraction of the EPDM (binder) masses that were added to form the graphite electrodes.

$$\% \text{ mass of co-intercalated } F^- = [19\delta / (12x + 445.011 + 19\delta)] * 100 \quad (4.3)$$

$$\% \text{ mass of graphene C} = [12x / (12x + 445.011 + 19\delta)] * 100 \quad (4.4)$$

where molecular weight of the TFP anion is 445.01 g/mole.

GIC compositions for smaller intercalates are generally close to x = 24n, where n is the GIC stage [45]. For example, for stage 2 GICs, the following intercalate anion contents have been determined; $[PF_6]^-$ (x= 48), $[AsF_6]^-$ (x= 45) [46], and HSO_4^- (x= 48) [45]. In Table 4.2, the x values are reported as 43-60, 78 and 86 for stage 2, 3 and 4 GICs respectively. These compositional values are therefore consistent with those previously seen. The calculated x values shown in Table 4.2 are larger for stage 4 GIC (at point a) compared to stage 3 and stage 2 GICs (at points b and c, d, e) respectively which explains that there is more intercalate present for stage 2 GICs. This is also noticeable from the TGA curves in Figure 4.7; the mass loss is increasing for longer electro-oxidation times. The δ values obtained are smaller for higher stage GICs compared to those after longer oxidation times.

According to the TGA data shown in Figure 4.7, all the GIC products show mass losses within three main regions. The first region starts at ambient temperatures and ends at about 180 ^{0}C, and is ascribed to the intercalate decomposition and volatilization, the second mass loss is between 215-580 ^{0}C and is assigned to the decomposition of the EPDM polymer binder. The last mass loss occurs above 600 ^{0}C and is ascribed to the decomposition of the graphene sheets.

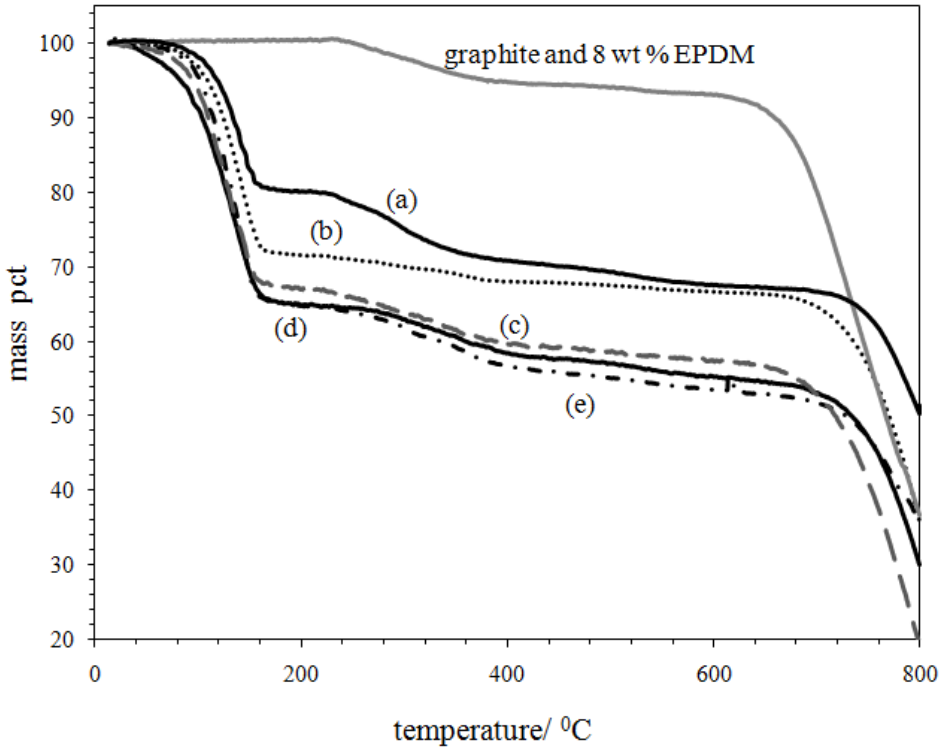

Figure 4.7 TGA data obtained for GICs of $C_x[(C_2F_5)_3PF_3]$ at breakpoints a-e. Data for graphite with 8 wt % EPDM is also shown.

4.5 REFERENCES

1. Bartlett, N.; McQuillan, B., *In intercalation chemistry*. New York: Academic Press. **1982**.
2. Tirado, J.L., *Mater Sci & Eng, R: Reports*, **2003**, R40(3), 103.
3. Kaskhedikar, N.A.; Maier, J., *Adv. Mater.*, **2009**, 21(25-26), 2664.
4. Enoki, T.; Suzuki, M., Endo, M., *Graphite intercalation compounds and applications*, Oxford: University Press, **2003**, p. 9-55.
5. Yakovlev, A.V.; Finaenov, A.I.; Zabud'kov, S.L.; Yakovleva, E.V., *Russ. J. Appl. Chem.*, **2006**, 79(11), 1741.
6. Stankovich, S.; Dikin, D.A.; Piner, R.D.; Kohlhaas, K.A.; Kleinhammes, A.; Jia, Y.; Wu, Y.; Nguyen, S.T.; Ruoff, R.S., *Carbon*, **2007**, 45(7), 1558.
7. Stankovich, S.; Dikin, D.A.; Dommett, G.H.B.; Kohlhaas, K.M.; Zimney, E.J.; Stach, E.A.; Piner, R.D.; Nguyen, S.T.; Ruoff, R.S., *Nature*, **2006**, 442(7100), 282.
8. Watcharotone, S.; Dikin, D.A.; Stankovich, S.; Piner, R.; Jung, I.; Dommett, G.H.B.; Evmenenko, G.; Wu, S-E.; Chen, S-F.; Liu, C-P.; Nguyen, S.T.; Ruoff, R.S., *Nano Lett.*, **2007**, 7(7), 1888.
9. Liu, Z.; Liu, Q.; Huang, Y.; Ma, Y.; Yin, S.; Zhang, X.; Sun, W.; Chen, Y., *Adv. Mater.*(Weinheim, Germany), **2008**, 20, 3924.
10. Wang, X.; Zhi, L.; Mullen, K., *Nano Lett.*, **2008**, 8(1), 323.
11. Bartlett, N.; McQuillan, B.; Robertson, A.S., *Mater. Res. Bull.*, **1978**, 13(12), 1259.
12. Billaud, D.; Pron, A.; Vogel, F.L., *Synth. Met.*, **1980**, 2(3-4), 177.
13. Jobert, A.; Touzain, P.; Bonnetain, L., *Carbon*, **1981**, 19(3), 193.
14. Zhang, Z.; Lerner, M.M., *J. Electrochem. Soc.*, **1993**, 140(3), 742.
15. Özmen-Monkul, B.; Lerner, M.M.; Pawelke, G.; Willner, H., *Carbon*, **2009**, 47, 1592.
16. O'Mahony, A.M.; Silvester, D.S.; Aldous, L.; Hardacre, C.; Compton, R.G., *J. Chem. Eng. Data*, **2008**, 53(12), 2884.
17. Freemantle, M., *Chem & Eng News*, **2004**, 82(45), 44**.**
18. Zein El Abedin, S.; Borissenko, N.; Endres, F., *Electrochem. Commun.*, **2004**, 6(4), 422.

19. Muldoon, M.J.; Aki, S.N.V.K.; Anderson, J.L.; Dixon, J.K.; Brennecke, J.F., *J Phys. Chem. B*, **2007**, 111(30), 9001.

20. Chrobok, A.; Swadzba, M.; Baj, S., *Pol. J. Chem*., **2007**, 81(3), 337.

21. Dyson, P.J.; Laurenczy, G.; Ohlin, A.; Vallance, J.; Welton, T., *Chem. Commun*., **2003**, 19, 2418.

22. Endres, F.; MacFarlane, D.; Abbott, A., *Electrodeposition from ionic liquids*. New York: Wiley-VCH, **2008**.

23. Swatloski, R.P.; Holbrey, J.D.; Rogers, R.D., *Green Chem*., **2003**, 5(4), 361.

24 Ignat'ev, N.V.; Willner, H.; Sartori, P., *J. Fluorine Chem*., **2009**, 130, 1183.

25. Ignat'ev, N.V.; Welz-Biermann, U.; Kucheryna, A.; Bissky, G.; Willner, H., *J. Fluorine Chem.*, **2005**, 126, 1150.

26. Oesten, R.; Heider, U.; Schmidt, M., *Solid State Ionics*, **2002**, 148, 391.

27. Rudorff, W.; Hofmann, U., *Z. Anorg. Allg. Chem*., **1938**, 238(1), 1.

28. Rudorff, W., *Z. Phys. Chem*., **1939**, B45, 42.

29. Bottomley, M.J.; Parry, G.S.; Ubbelohd, A.R.; Young, D.A., *J. Chem. Soc*., **1963**, 5674.

30. Herold, A., *Les carbons par le groupe fransaise d'etude des carbons.* Masson et Cie. Editor. vol 2, Paris, **1965**, p.356-376.

31. Sorokina, N.E.; Maksimova, N.V.; Avdeev, V.V., *Inorg. Mater*., **2002**, 38(6), 564.

32. Sorokina, N.E.; Leshin, V.S.; Avdeev, V.V., *J. Phys. Chem. Solids*, **2004**, 65, 185.

33. Leshin, V.S.; Sorokina, N.E.; Avdeev, V.V., *Russ. J. Electrochem*., **2005**, 41(5), 572.

34. Paasonen, V.M., Nazarov, A.S., *Zhurnal Neorganicheskoi Khimii*, **1998**, 43(8), 1280.

35. Banares-Munoz, M.A.; Flores-Gonzales, L.V.; Perez-Bernal, M.E.; Ruano-Casero, R.J.; Sanchez-Escribano, V., *J. Inclusion Phenomena*, **1984**, 1(4), 411.

36. Iskander, B.; Vast, P., *Carbon*, **1980**, 18(4), 299.

37. Zhang, D.; Wu, Z.; Zhang, X., *Huaxue Gongchengshi*, **2007**, 21(2), 8.

38. Yin, W.; Jin, W.; Quan, X.; Li, Y.; Cui, X., *Feijinshukuang*, **2006**, 29(1), 35.

39. Han, Z.D.; Zhang, D.W.; Dong, L.M.; Zhang, X.Y., Wui Huaxue Xuebao, **2007**, 23(2), 286.

40. Hérold, C.; Goutfer-Wurmser, F.; Marêché, J.F.; Lagrange, P., *Mol. Cryst. Liq. Cryst.*, **1998**, 310, 57.

41. Ginderov, D.; Setton, R., *Carbon*, **1968**, 6, 81.

42. Yan, W.; Lerner, M.M., *J. Electrochem. Soc*., **2004**, 151(2), J15-J20.

43. Zhang, X.; Sukpirom, N.; Lerner, M.M., *Mat. Res. Bull*., **1999**, 34(3), 363.

44. Özmen-Monkul, B.; Lerner, M.M.; Hagiwara, R., *J. Fluorine Chem*., **2009**, 130, 581.

45. Besenhard, J.; Wudy, E.; Moehwald, H.; Nickl, J.; Biberacher, W.; Foag, W., *Synth. Met*., **1983**, 7, 185.

46. Billaud, D.; Chenite, A., *J. Power Sources*, **1984**, 13, 1.

CHAPTER 5

CONCLUSION

A new acceptor-type graphite intercalation compound (GIC) containing the fluoro-tris(pentafluoroethyl)borate anion, $[FB(C_2F_5)_3]^-$, is obtained for the first time by chemical oxidation of graphite with $K_2[MnF_6]$ in aqueous (48 %) hydrofluoric acid. GICs up to stage 2 with gallery heights of d_i= 0.86 nm can be obtained. In addition, electrochemical method is used to prepare stage 2 GIC of $C_x[FB(C_2F_5)_3]\cdot\delta CH_3NO_2$ having d_i= 0.84 nm in a nitromethane electrolyte. Energy minimized structure for the isolated anion show that, the borate anions adopt a "lying-down" orientation where the long axes of $[FB(C_2F_5)_3]^-$ intercalate anions be parallel to the encasing graphene sheets. The gallery height calculated was consistent with the one observed with powder XRD data. The compositional *x* and δ parameters are determined by both thermogravimetric and elemental analyses. A newly-developed digestion method is used in combination with an ion-selective electrode and potentiometer. Results indicate that for chemically prepared GICs there are less than two fluoride cointercalate per borate anion in the galleries. Combining B analysis and TGA mass loss give a composition of *x*= 44 and δ= 0.37 for the $C_x[FB(C_2F_5)_3]\cdot\delta CH_3NO_2$ product obtained.

Stage 2 and stage 3 of new GICs including cyclo-hexafluoropropane-1,3 bis(sulfonyl)amide anion, $[CF_2(CF_2SO_2)_2N]^-$ are obtained for the first time using electrochemical oxidation. The gallery heights, d_i, for these GIC's are 0.85-0.86 nm are obtained for stage 2 and 3 products respectively. The compositional parameter, *x* is determined as 45 and 52 by using elemental analyses and TGA data for stage 2 and stage

3 GICs respectively. The prepared GIC stability is compared with the one including a linear amide and concluded that the electron density closer to the positively charged graphene sheet would bring a more stable GIC with respect to displacement.

The first time synthesis of GICs including (pentafluoroethyl)trifluorophosphate anion, $[(C_2F_5)_3PF_3]^-$ are performed by electrochemical method in nitromethane electrolyte. Stages 2 and 4 with gallery heights of 0.86 and 0.82 nm are obtained respectively. Energy minimized anion model and PXRD data confirmed a lying down orientation. The GICs are characterized by using TGA and F ion-selective probe analyses in order to find out *x* and δ values for $C_x[(C_2F_5)_3PF_3]\cdot\delta F$ where δ represents the free-fluoride (due to anion decomposition) in the galleries. The *x* values decreased as the stage number decreases where the δ values increased up to 2.26.

BIBLIOGRAPHY

1. Aksenov, V.V.; Vlasov, V.M.; Danilkin, V.I.; Rodionov, P.P.; Shnitko, G.N., *J. Fluorine Chem.*, **1990**, 46(1), 57.

2. (a) Akuzawa, N.; Sakamoto, T.; Fujimoto, H.; Kasuu, T; Tkahashi, Y., *Synth. Met*., **1995**, 73(1), 41. (b) Akuzawa, N; Kamoshita, T; Tsuchiya, K; Matsumoto, R, *Tanso*, **2006**, 222, 107.

3. Alheid, H.; Schwarz, M.; Stumpp, E., *Molecular Cryst. and Liq. Cryst. Science and Tech. Sec. A-Molecular Cryst. and Liq. Cryst.*, **1994**, 244, 191.

4. Allen M.J.; Tung, V.C.; Kaner, R.B., *Chem. Rev*., **2010**, 110, 132.

5. Allied Business Intelligence, Fuel Cell Supply Chain: A Global Market Analysis, Potential and Forecasts March, 2003.

6. Amatucci, G.G.; Pereira, N., *J. Fluorine Che*m., **2007**, 128, 243.

7. (a) Amine, K.; Tressaud, A.; Imoto, H.; Fargin, E.; Hagenmuller, P.; Touhara, H., *Mater. Res. Bull*., **1991**, 26, 337. (b) Amine, K.; Nakajima, T., *Carbon*, **1993**, 31, 553.

8. (a) Avdeev, V.V.; Sorokina, N.E.; Maksimova, N.V.; Martynov, I.Yu.; Sezemin, A.V., *Inorg. Mater*., **2001**, 37(4), 366. (b) Avdeev, V.V.; Nalimova, V.A.; Semenenko, K. N., *High Pressure Res.* **1990**, *6*, 11. (c) Avdeev, V.V.; Nalimova, V. A.; Semenenko, K.N., *Synth. Met.* **1990**, *38*, 363.

9. Badaire, S.; Poulin, P.; Maugey, M.; Zakri, C., *Langmuir*, **2004**, 20, 10367.

10. Balandin, A.A.; Ghosh, S.; Bao, W.; Calizo, I.; Teweldebrhan, D.; Miao, F.; Lau, C.N., *Nano Lett*., **2008**, 8, 902.

11. Banares-Munoz, M.A.; Flores-Gonzales, L.V.; Perez-Bernal, M.E.; Ruano-Casero, R.J.; Sanchez-Escribano, V., *J. Inclusion Phenomena*, **1984**, 1(4), 411.

12. Banerjee, S.K.; Register, L.F.; Tutuc, E.; Reddy, D.; MacDonald, A.H., *IEEE Electron Device Lett*, **2009**, 30 (2), 158.

13. (a) Bartlett, N.; McQuillan, B.; Robertson, A.S., *Mater. Res. Bull*., **1978**, 13(12), 1259. (b) Bartlett, N.; McCarron, E.M.; McQuillan, B.W.; Thompson, T.E., *Synth. Metals*, **1979/1980,** 1(3), 221. (c) Bartlett, N.; McQuillan, B., *In intercalation chemistry*. New York: Academic Press. **1982**. (d) Bartlett, N; Okino, F.; Mallouk, T.E.; Hagiwara, R.; Lerner, M.; Rosenthal, G.L.; Kourtakis, K., *Oxidative intercalation of graphite by fluoroanionic species, Advances in Chemistry* Series No. 226, (Johnson, M.K.; King, R.B.; Kurtz, D.M.; Kutal, C.; Norton, M.L.; Scott, R.A.,

eds) ACS, Washington, D.C., **1990**, p391. (e) Bartlett, N.; Biagioni, R.N.; McQuillan, B.W.; Robertson, A.S.; Thompson, A.C., *J. Chem. Soc. Chem. Commun.*, **1978**, 5, 200.

14. Barthel, J.; Schmidt, M.; Gores, H.J., *J. Electrochem. Soc*., **2000**, 147(1), 21

15. Beguin, F.; Pilliere, H, *Carbon*, **1998**, 36(12), 1759.

16. Berger, C.; Song, Z.; Li, X.; Wu, X.; Brown, N.; Naud, C.; Mayou, D.; Li, T.; Hass, J.; Marchenkov, A.N.; Conrad, E.H.; First, P.N.; de Heer, W.A., *Science*, **2006**, 312, 1191.

17. (a) Besenhard, J.; Wudy, E.; Moehwald, H.; Nickl, J.; Biberacher, W.; Foag, W., *Synth. Met*., **1983**, 7, 185. (b) Besenhard, J.O., *Carbon*, **1976**, 14, 111. (c) Besenhard, J.O.; Fritz, H.P., *Naturforsc*h, **1972**, 27B, 1294.

18. (a) Billaud, D.; Pron, A.; Vogel, F., *Synth. Met*., **1980**, 2(3-4), 177. (b) Billaud, D.; Pron, A.; Vogel, F.; Herold, A., *Mater. Res. Bull*., **1980**, 15, 1627. (c) Billaud, D.; Chenite, A.; Metrot, A., *Carbon*, **1982**, 20, 493. (d) Billaud, D.; Chenite, A., *J. Power Sources*, **1984**, 13, 1.

19. Binenboym, J.; Selig, H.; Sarig, S., *J. Inorg. Nucl. Chem*., **1976**, 38, 2313.

20. Bode, H.; Jenssen, H.; Bandte, F., *Angew. Chem*. **1953**, 65, 304.

21. Boeck, A.; Rüdorff, W., *Z. Anorg. Allgem. Chem*., **1971**, 384, 169.

22. Boehm, H.P.; Helle, W.; Ruisinger, B., *Synth. Met*., **1988**, 23, 395.

23. Bottomley, M.J.; Parry, G.S.; Ubbelohd, A.R.; Young, D.A., *J. Chem. Soc*., **1963**, 5674.

24. Boukhvalov, D.W.; Katsnelson, M.I., *J. Am. Chem. Soc.*, **2008**, 130, 10697.

25. Bourelle, E.; Douglade, J.; Metrot, A., *Mol. Cryst. Liq. Cryst. A.*, **1994**, 244 227.

26. Brodie, B., *Ann. Chim. Phys.* **1855**, *45*, 351.

27. Buscarlet, E.; Touzain, P., Bonnetain, L, *Carbon*, **1976**, 14, 75.

28. Cassagneau, T.; Guerin, F.; Fendler, J.H., *Langmuir*, **2000**, 16, 7318.

29. Cheng, H; Sha, X; Chen, L; Cooper, A.C; Foo, M-L; Lau, G.C.; Bailey III, W.H.; Pez, G.P., *J. Am. Chem. Soc*., **2009**, 131(49), 17732.

30. Chenite, A.; Billaud, D., *Carbon*, **1982**, 20(2), 120.

31. Chernysh, I.G.; Buraya, I.D., *Khim. Tverd. Topliva* (*Solid Fuel Chemistry*), **1990**, 1, 123.

32. Chrobok, A.; Swadzba, M.; Baj, S., *Pol. J. Chem*., **2007**, 81(3), 337.

33. Croft, R.C.; Thomas, R.G., *Nature*, **1951**, 168, 32.

34. Cohen, A.D., Fr. Pat. **1975**, 2 291 151.

35. (a) Dato, A.; Radmilovic, V.; Lee, Z.; Phillips, J.; Frenklach, M., *Chem. Commun*., **2008**, 8, 2012. (b) Dato, A.; Lee, Z.; Jeon, K-J.; Erni, R.; Radmilovic, V.; Richardson, T. J.; Frenklach, M., *Chem. Commun*., **2009**, 6095.

36. Daumas, N.; Herold, A., *C.R. Acad. Sci*., Paris., **1969**, C286, 373.

37. Dillon, A.C.; Jones, K.M.; Bekkedahl, T.A.; Kiang, C.H.; Bethune, D.S.; Heben, M.J., *Nature (London)*, **1997**, 386(6623), 377.

38. (a) Dresselhaus, M.S.; Dresselhaus, G., *Adv. Physics* **1981**, 30, 139. (b) Dresselhaus, M.S.; Dresselhaus, G., *Advances in Physics*, **2002**, 51(1), 1.

39. Dunaev, A.V.; Sorokina, N.E.; Maksimova, N.V.; Avdeev, V.V., *Inorganic Materials*, **2005**, 41(2), 127.

40. Dyson, P.J.; Laurenczy, G.; Ohlin, A.; Vallance, J.; Welton, T., *Chem. Commun*., **2003**, 19, 2418.

41. (a) Ebert, L.B.; Selig, H., *Mater. Sci. Eng*., **1977**, 31, 177. (b) Ebert, L.B., Annu. Rev. *Mater. Sci*., **1976**, 6, 181. (c) Ebert, L.B.; Selig, H., *Synth. Met*., **1981**, 3, 53.

42. Emery, N.; Hérold, C.; Marêché1, J.F., Lagrange, P., *Sci. Technol. Adv. Mater*., **2008**, 9**,** 044102.

43. Endres, F.; MacFarlane, D.; Abbott, A., *Electrodeposition from ionic liquids*. New York: Wiley-VCH, **2008**.

44. Enoki, T.; Suzuki, M.; Endo, M., *Graphite Intercalation Compounds and Applications*, Oxford University Press, New York, **2003**.

45. Falardeau, E.R.; Hanlon, L.R.; Thompson, T.R., *Inorg. Chem*., **1978**, 17(2), 301.

46. Flandrois, S.; Grannec, J.; Hauw, C.; Hun, B.; Lozano, L.; Tressaud, T., *J. Solid State Chem*., **1988**, 77, 264.

47. Fouletier, M.; Armond, M., *Carbon*, **1979**, 17, 427.

48. Forsman, W.; Mertwoy, H., *Carbon*, **1982**, 20(3), 255.

49. Freemantle, M., *Chem & Eng News*, **2004**, 82(45), 44**.**

50. (a) Frohn, H.J.; Bardin, V.V., *Z. Anorg. Allg. Chem*., **2001**, 627(1), 15. (b) Frohn, H.J.; Bardin, V.V., *Z. Anorg. Allg. Chem*., **2001**, 627, 2499.

51. Fujimoto, K.; Sugiura, T.; Iijima, T.; Sato, M., *Hyomen*, **1992**, 30, 310.

52. Gao, W.; Alemany, L.B.; Ci, L.; Ajayan, P.M., *Nat. Chem*., **2009**, 1(5),403.

53. Geim, A.K.; Novoselov, K.S., *Nature Mater*., **2007**, 6, 183.

54. Ginderov, D.; Setton, R., *Carbon*, **1968**, 6, 81.

55. Giraudet, J.; Claves, D.; Hamwi, A., *Synthetic Metals*, **2001**, 118, 57.

56. Grannec, J.; Lozano, L., *Preparation Methods, in Inorganic Solid Fluorides*, P. Hagenmuller, Ed., Academic Press, New York, **1985**, p18.

57. Guérard, D.; Chaabouni, M.; Langrange, P.; El Makrini, S.; Hérold, A, *Carbon*, **1980**, 18, 257.

58. (a) Hamwi, A.; Touzain, P., Bonnetain, L., *Mater. Sci. Eng*., **1977**, 31, 95. (b) Hamwi, A.; Touzain, P., *Rev. Chim. Minér*., **1982**, 19, 432. (c) Hamwi, A.; Mouras, S.; Djurado, D.; Cousseins, J.C., Proceedings Carbon ’86, Baden-Baden, Germany, **1986**, p454. (d) Hamwi, A.; Daoud, M.; Cousseins, J.C., *Synth. Metals*, **1988,** 26, 89.

59. Han, Z.D.; Zhang, D.W.; Dong, L.M.; Zhang, X.Y., Wui Huaxue Xuebao, **2007**, 23(2), 286.

60. Hattori, Y.; Kurihara, M.; Kawasaki, S.; Okino, F.; Touhara, H., *Synthetic Metals*, **1995**, 74, 89.

61. (a) Herold, A., *Les carbons par le groupe fransaise d’etude des carbons.* Masson et Cie. Editor. vol 2, Paris, **1965**, p.356-376. (b) Herold, A.; Furdin, G.; Guerard, D.; Hachim, L.; Nadi, N.; Vangelisti, R., *Ann. Phys*., **1986**, 11, 3. (c) Herold, A., *NATO ASY, Ser. B*, **1987**, 172, 3. (d) Hérold, A.; Lelaurain, M.; Maréche J.F.; Mc Rae E., *CR Acad Sci Paris*, **1995**, 321(2), 61 (Serie IIb). (e) Hérold, A.; Mareˆche´, J.-F.; Lelaurin, M., *Mol. Cryst. Liquid. Cryst. A*, **1998**, 310, 43. (f) Hérold, A.; Maréche J.F.; Lelaurain, M., *Carbo*n, **2000**, 38, 1955.

62. Hérold, C.; Goutfer-Wurmser, F.; Marêché J.-F.; Lagrange, P., *Mol. Cryst. Liq. Cryst*., **1998**, 310, 43.

63. Hennig, G.R., *Prog. Inorg. Chem*., **1959**, 1, 125.

64. Higashika, S.; Kimura, K.; Matsuo, Y.; Sugie, Y., *Carbon*, **1999**, 37(2), 351.

65. Hirata, M.; Gotou, T.; Horiuchi, S.; Fujiwara, M.; Phba, M., *Carbon*, **2005**, 43, 503.

66. (a) Hoffmann, U.; Rüdorff, W., *Transactions of the Faraday Society*. **1938**, 34, 1017. (b) Hoffmann, U.; Frenzel, A., **1931**, *Z. Elektrochem*., 37, 613.

67. (a) Horn, D.; Boehm, H.P., *Mater. Sci. Eng*., **1977**, 31, 87. (b) Horn, D.; Boehm, H.P., *Mater. Sci. Eng*., **1972**, 31, 87.

68. Horowitz, H.H.; Haberman, J.I.; Klemann, L.P.; Newman, C.H.; Stogryn, E.L.; Whitney, T.A., *Proceedings-Electrochem. Soc*., **1981**, 81-4, 131.

69. Housecroft, C.E.; Sharpe, A.G., *Inorganic Chemistry*, Pearson Education Ltd., England, **2001**.

70. Hui, R.; Kang, F.Y.; Jiao, Q.J.; *New Carbon Materials*, **2009**, **24(1), 18.**

71. Hummers, W.S.; Offeman, R.E., *J. Am. Chem. Soc*., **1958**, 80, 1339.

72. (a) Ignat'ev, N.V.; Welz-Biermann, U.; Kucheryna, A.; Bissky, G.; Willner, H., *J. Fluorine Chem.*, **2005**, 126, 1150. (b) Ignat'ev, N.V.; Willner, H.; Sartori, P., *J. Fluorine Chem*., **2009**, 130, 1183.

73. (a) Inagaki, M, Wang, Z.D.; Okamoto, Y.; Ohira, M., *Synth. Met*., **1987**, 20, 9. (b) Inagaki, M., *J. Mater. Res*., **1989**, 4, 1560. (c) Inagaki, M., *J. Jpn. Inst. Energy*, **1998**, 77, 849. (d) Inagaki, M.; Kang, F.; Toyoda, M., *Chemistry and Physics of Carbon*, **2004**, 29, 1.

74. Interrante, L.V.; Markiewiz, R.S.; Mckee, D.W., *Synth. Metals*, **1979**, 1, 287.

75. Iskander, B.; Vast, P., *Carbon*, **1980**, 18(4), 299.

76. Jobert, A.; Touzain, P.; Bonnetain, L., *Carbon*, **1981**, 19(3), 193.

77. Johnson, D.A., *Some thermodynamic aspects of inorganic chemistry*, 2nd Ed., Cambridge University Press, Cambridge, **1982**.

78. Ka, B.H.; Oh, S.M., *J. Electrochem. Soc*., **2008**, 155(9), A685.

79. Kang, F.; Zhang, T.Y., Leng, Y., *Carbon*, **1997**, 35(8), 1167.

80. Kaskhedikar, N.A.; Maier, J., *Adv. Mater.*, **2009**, 21(25-26), 2664.

81. Katinonkul, W.; Lerner, M.M., *Carbon*, **2007**, 45, 2672. (b) Katinonkul, W.; Lerner, M.M., *J. Phys. Chem. Sol.* **2007**, *68*, 394.

82. Kharissova, O.V.; Kharisov, B.I., *The Open Inorg. Chem. J.*, **2008**, 2, 39.

83. Kim, K.S.; Zhao, Y.; Jang, H.; Lee, S.Y.; Kim, J.M.; Kim, K.S.; Ahn, J.-H.; Kim, P.; Choi, J.-Y.; Hong, B.H., *Nature*, **2009**, 457, 70.

84. Kim, S.; Nah, J.; Jo, I.; Shahrjerdi, D.; Colombo, L.; Yao, Z.; Tutuc, E.; Banerjee, S.K., *Appl. Phys. Lett.*, **2009**, 94, 062107.

85. Kita, F.; Kawakami, A.; Sonoda, T.; Kobayashi, H., *Proceedings-Electrochem. Soc*., **1993**, 93-23, 321.

86. Kobayashi, T.; Kurata, H.; Uyeda, N., *J. Phys* Chem., **1986**, 90(10), 2231.

87. Kovtyukhova, N.I.; Ollivier, P.J.; Martin B.R.; Mallouk T.E.; Chizhik, S.A.; Buzenava E.V.; Gorchinskiy, A.D., *Chem. Mater*., **1999**, 11, 771.

88. Kudin, K.N.; Ozbas, B.; Schniepp, H.C.; Prud'homme, R.K.; Aksay, I.A.; Car, R., *Nano Lett.* **2008**, 8, 36.

89. Lemmon, J.P.; Lerner, M.M., *Carbon*, **1993**, 31, 437.

90. Lerf, A.; He, H.; Forster, M.; Klinowski, J., *J. Phys. Chem. B*, **1998**, 102(23), 4477.

91. Lerner, M.; Hagiwara, R.; Bartlett, N., *J. Fluorine Chem*., **1992**, 57, 1.

92. Leshin, V.S.; Sorokina, N.E.; Avdeev, V.V., *Russ. J. Electrochem*., **2005**, 41(5), 572.

93. Levy, F., *Intercalated Layered Materials,* Reidel, Dordrecht, the Netherlands, **1979**.

94. Li, D.; Muller, M.B.; Gilje, S.; Kaner, R.B.; Wallace, G.G., *Nat. Nano.*, **2008**, 3, 101.

95. Li, H.; Wang, Z.; Chen, L.; Huang, X., *Adv. Mater.*, **2009,** 21, 4593.

96. Li, X.; Zhang, G.; Bai, X.; Sun, X.; Wang, X.; Wang, E.; Dai, H., *Nature Nanotechnology*, **2008**, 3, 538.

97. Liu, P.; Gong, K., *Carbon*, **1999**, 37, 701.

98. (a) Liu, Z.; Wang, Z.; Yang, X.; Ooi, K., *Langmuir*, **2002**, 18, 4926. (b) Liu, Z.; Liu, Q.; Huang, Y.; Ma, Y.; Yin, S.; Zhang, X.; Sun, W.; Chen, Y., *Adv. Mater.*(Weinheim, Germany), **2008**, 20, 3924.

99. Lope-Gonzales, J.D.; Rodriguez, A.M.; Vega, F.D., *Carbon*, **1969**, 7, 583.

100. Makrini, M.E.; Guérard, D.; Lagrange, P.; Hérold, A., *Physica*, **1980**, B99, 481.

101. (a) Mastalir, A.; Kiraly, Z.; Dekany, I.; Bartok, M., *Colloids Surf. A*, **1998**, 141, 397. (b) Mastalir, A.; Kiraly, Z.; Patzko, A.; De´ka´ny, I.; L'Argentiere, P., *Carbon*, **2008**, 46, 1631.

102. Matsumoto, R; Hoshina, Y; Akuzawa, N, *Materials Transactions*, **2009**, 50(7), 1607. Matsumoto, R.; Akuzawa, N., *Recent Research Activities of Micro- and Nano-Scale Carbon Related Materials*, Ed. Miyagawa, H., **2008**, 145.

103. (a) Matsuo, Y.; Sakai, Y.; Fukutsuka, T.; Sugie, Y., *Carbon*, **2009**, 47, 804. (b) Matsuo, Y.; Miyabe, T.; Fukutsuka, T.; Sugie, Y., *Carbon*, **2007**, 45, 1005. (c) Matsuo, Y.; Niwa, T.; Sugie, Y., *Carbon*, **1999**, 37, 897.

104. McCarron, E.M.; Grannec, Y.J.; Bartlett, N., *J. Che. Soc. Chem Commun*., **1980**, 890.

105. (a) Métrot, A.; Fischer, J.E., *Synth. Metals*, **1981**, 3, 201. (b) Métrot, A.; Guérard, D.; Billaud D.; Hérold, A., *Synth. Metals*, **1979/1980**, 1, 363.

106. Meyer, J.C.; Kisielowski, C.; Erni, R.; Rossell, M.D.; Crommie, M.F.; Zettl, A., *Nano Lett*., **2008**, 8(11), 3582.

107. Mizutani, Y.; Ihara, E.; Abe, T.; Asano, M.; Harada, T.; Ogumi, Z.; Inaba, M., *J. Phys. Chem. of Solids*, **1996**, 57(6-8), 799.

108. Mouras, S.; Hamwi, A.; Djurado, D.; Cousseins, J.C, *Re. Chem. Miner*., **1987**, 24, 572.

109. Muldoon, M.J.; Aki, S.N.V.K.; Anderson, J.L.; Dixon, J.K.; Brennecke, J.F., *J Phys. Chem. B*, **2007**, 111(30), 9001.

110. Muradov, N.; Smith, F.; T-Raissi, A., *Catal. Today*, **2005**, 102-103, 225.

111. (a) Nakajima, T.; Nakane, K.; Kawaguchi, M.; Watanabe, N., *Carbon*, **1987**, 25, 685. (b) Nakajima, T; Matsui, T.; Motoyama, M.; Mizutani, Y., *Carbon*, **1988**, 26, 831. (c) Nakajima, T.; Molinier, M., *Synth. Metals*, **1989**, 34, 103 (d) Nakajima, T.; Nagai, Y.; Motoyama, M., *Eur. J. Solid State Inorg. Chem*., **1992**, 29, 919. (e) Nakajima, T.; Watanabe, N., *Graphite Fluorides and Carbon-Fluorine Compounds*, CRC Press, Boca Raton, Fla., **1990**. (f) Nakajima, T.; Tressaud, A., *Fluorine-Carbon and Fluoride-Carbon Materials—Chemistry, Physics and Applications*, Marcel Dekker, NewYork, **1995**. (g) Nakajima, T.; Matsuo, Y.; Zemwa, B.; Jesih, A., *Carbon*, **1996**, 34, 1595. (h) Nakajima, T.; Gupta, V.; Ohzawa, Y.; Groult, H.; Mazej, Z.; Zemwa, B., *J. Power Sources*, **2004**, 137, 80.

112. (a) Nalimova, V.A.; Chepurko, S.N.; Avdeev, V.V.; Semenenko, K. N., *Synth. Metals*, **1991**, 40, 267. (b) Nalimova, V.A.; Guérard, D.; Lelaurain, M.; Fateev, O.V., *Carbon*, **1995**, 33, 177.

113. Nicholas, R.J.; Mainwood, A.; Eaves, L., *Phil. Trans. R. Soc. A*, **2008**, 366, 189.

114. Niyogi, S.; Bekyarova, E.; Itkis, M.E.; McWilliams, J.L.,; Hamon, M.A.; Haddon R.C., *J. Am. Chem. Soc*., **2006**, 128, 7720.

115. (a) Nixon, D.E.; Parry, G.S.; Ubbelohde, A.R., *Proc. Roy. Soc*. London, **1964**, A291, 324. (b) Nixon, D.E.; Parry, G.S.; Ubbelohde, A.R., *Proc. Roy. Soc.* London, **1966**, 291A, 32.

116. Niyori, Y.; Katsukawa, H.; Yoshida, H.; Takeuchi, M.; Okamura, M., U.S. Pat. 6487086, **2002**.

117. Nikonorov, Y.I., *Kinet. Kutal.*, **1979**, 20, 1598.

118. Norley, J. Graphite-based heat sink. U.S. Pat. 6503626, January 7, **2003**.

119. Novoselov, K.S.; Geim, A.K.; Morozov, S.V.; Jiang, D.; Zhang, Y.; Dubonos, S.V.; Grigorieva, I.V.; Firsov, A.A., *Science*, **2004**, 306, 666.

120. Oesten, R.; Heider, U.; Schmidt, M., *Solid State Ionics*, **2002**, 148, 391.

121. Ohhashi, K., *In Graphite Intercalation Compounds*; Watanabe, N., Ed., Kindai-Henshu Sha, Tokyo, **1986**, p165.

122. Okuyama, N.; Takahashi, T.; Kanayama, S.; Yasunaga, H., *Physica*, **1981**, 105B, 298.

123. O'Mahony, A.M.; Silvester, D.S.; Aldous, L.; Hardacre, C.; Compton, R.G., *J. Chem. Eng. Data*, **2008**, 53(12), 2884.

124. Oriakhi, C.O.; Lerner, M.M., *Nanocomposites and Intercalation compounds*, *Encylopedia of Physical Science and Technology*, 3rd Ed., Academic Press, **2002**, volume 10.

125. (a) Özmen-Monkul, B.; Lerner, M.M.; Pawelke, G.; Willner, H., *Carbon*, **2009**, 47, 1592. (b) Özmen-Monkul, B.; Lerner, M.M.; Hagiwara, R., *J. Fluorine Chem*., **2009**, 130, 581. (c) Özmen-Monkul, B.; Lerner, M.M., *Carbon*, accepted.

126. Paasonen, V.M., Nazarov, A.S., *Zhurnal Neorganicheskoi Khimii*, **1998**, 43(8), 1280.

127. Paci, J.T.; Belytschko, T.; Schatz, G.C., *J. Chem. Phys.* **2007**, 111(49), 18099.

128. Parry, G.S.; Nixon, D.E.; Lester, K.M.; Levene, B.C., *J. Phys. C.* **1969**, *2*, 2156.

129. Pawelke, G.; Willner, H., *Z. Anorg. Allg. Chem*., **2005**, 631, 759.

130. Pentenrieder, R.; Boehm, H.P., *Rev. Chim. Minér*., **1982**, 19, 371.

131. Petit, C.; Seredych, M.; Bandosz, T.J., *J. Mater. Chem*., **2009**, 19, 9176.

132. Pierson, H.O., *Handbook of Carbon, Graphite, Diamond and Fullerenes*, Noyes, Park Ridge, NJ **1993**, PV 93-24, p.1

133. Podall, H; Foster, W.E.; Giraitis, A.P., *J. Org. Chem*., **1958**, 23, 82.

134. Pollock, M.; Wetula, J.; Ford, B., U.S. Pat. 5443894, August 22, **1995**.

135. Pruvost, S.; Hérold, C., Hérold, A.; Lagrange, P., *Carbon*, **2004**, 42, 1825.

136. Ramanathan, T.; Abdala A.A.; Stankovich, S.; Dikin, D.A.; Herrera-Alonso, M.; Piner, R.D.; Adamson, D.H.; Schniepp, H.C.; Chen, X.; Ruoff, R.S.; Nguyen, S.T.; Aksay, I.A.; Prud'Homme, R.K.; Brinson, L.C., *Nat. Nanotechnol.*, **2008**, 3, 327.

137. Rashkov, I., *Mat. Sci. For*. **1992**, 91/3, 829.

138. Ravaine, D.; Boyce, J.; Hamwi, A.; Touzain, P., *Synth. Metals*, **1980**, 2, 249.

139. Rosenthal, G.L.; Mallouk, T.E.; Bartlett, N., *Synth. Met*., **1984**, 9, 433

140. (a) Ruisinger, B.; Boehm, H.P., *Angew. Chem. Int. Ed. Engl*., **1987**, 26, 253. (b) Ruisinger, B.; Boehm, H.P., *Carbon*, **1993**, 31, 1131.

141. Ruoff, R., *Nature Nanotechnol.*, **2008**, 3, 10.

142. Rudorff, U., *Adv. Inorg. Chem. Radiochem*., **1959**, 1, 223.

143. (a) Rüdorff, W.; Siecke, W.-F., *Chem. Ber*., **1958**, 91, 1348. (b) Rüdorff, W.; Hoffmann, U., *Z. Anorg. Allg. Chem*., **1938**, 238(1), 1. (c) Rudorff, W., *Z. Phys. Chem*., **1939**, B45, 42.

144. Sangster, J., *J. Phase Equilib. and Diffusion*, **2007**, 28(6), 571.

145. (a) Sato, Y.; Itoh, K.; Hagiwara, R.; Fukunaga, T.; Ito, Y., *Carbon*, **2004**, 42, 3243. (b) Sato, Y.; Shiraishib, S.; Mazejc, Z.; Hagiwara, R.; Ito, Y., *Carbon*, **2003**, 41, 1971.

146. Schaffäutl, P., *J. Praft. Chem*., **1841**, 21, 155.

147. Scharff, P., *Z. Naturforsch., Teil B*, **1989**, 44, 772.

148. (a) Schlögl, R.; Boehm, H.P., *Synth. Met*., **1988**, 23, 407. (b) Schlögl, R. in *Progress in Intercalation Research;* Müller-Warmuth, W.; Schöllhorn, R., Eds., Kluwer Academic: Dordrecht, the Netherlands, **1994**.

149. Schniepp H.C.; Li, J.-L.; McAllister, M.J.; Sai, H.; Herrera-Alonso, M.; Adamson, D.H.; Prud'homme, R.K.; Car, R.; Saville, D.A.; Aksay, I. A., *J. Phys. Chem. B*, **2006**, 110, 8535.

150. Schöllhorn, R., *Intercalation Compounds.* In *Inclusion Compounds;* Atwood, J.L.; Davies, J.E.D.; MacNicol, D.D., Eds., Academic Press, London, **1984**, Vol. 1, Chapter 7.

151. (a) Selig, H.; Sunder, W.A.; Vasile, M.J.; Stevie, F.A.; Gallagher, P.K.; Ebert, L.B., *J. Fluorine Chem*., **1978**, 12, 397. (b) Selig, H., *Graphite intercalation compounds with binary fluorides, in Inorganic Solid Fluorides*, P. Hagenmuller, ed., Academic Press, New York, **1985**, p354.

152. (a) Shioya, J.; Matsubara, H.; Murakami, S., *Synth. Metals*, **1986**, 14, 113. (b) Shioya, J.; Mizoguchi, A.; Yamaguchi, Y.; Yasuda, N., *Synth. Metals*, **1989**, 34, 151.

153. (a) Shioyama, H.; Crespin, M.; Setton, R; Bonnin, D.; Beguin, F., *Carbon*, **1993**, 31, 223. (b) Shioyama, H., *Tanso*, **1998**, 184, 202. (c) Shioyama, H., *Mol. Cryst. and Liq. Cryst*., **2000**, 340, 101.

154. Shornikova, O.N.; Dunaev, A.V.; Maksimova, N.V.; Avdeev V.V., *J. Phys. and Chem. of Solids*, **2006**, 67, 1193.

155. Shriver, D.; Atkins P., *Inorganic Chemisty*, W.H. Freeman and Company, USA, **2003**.

156. Si, Y.; Samulski, E.T., *Nano Lett.*, **2008**, 8(6), 1679.

157. Soneda, Y.; Toyoda, M.; Tani, Y.; Yamashita, J.; Kodama, M.; Hatori, H.; Inagaki, M. *J. Phys. Chem. Sol.* **2004**, 65, 219.

158. (a) Sorokina, N.E.; Maksimova, N.V.; Nikitin, A.V.; Shornikova O.N.; Avdeev, V.V., *Inorg. Mater*., **2001**, 37(6), 584. (b) Sorokina, N.E.; Maksimova, N.V.; Avdeev, V.V., *Inorg. Mater*., **2002**, 38(6), 564. (c) Sorokina, N.E.; Leshin, V.S.; Avdeev, V.V., *J. Phys. Chem. Solids*, **2004**, 65, 185. (d) Sorokina, N.E.; Nikol´skaya, I.V.; Ionov, S.G.; Avdeev, V.V., *Russ. Chem. Bull., Int. Ed.*, **2005**, 54(8), 1749.

159. (a) Stankovich, S. ; Dikin, D.A.; Dommett, G.H.B.; Kohlhaas, K.M.; Zimney, E.J.; Stach, E.A.; Piner, R.D.; SonBinh, T.N.; Ruoff, R.S., *Nature*. **2006**, 442(7100), 282. (b) Stankovich, S.; Piner, R.D.; Chen, X.; Wu, N.; Nguyen, S.T.; Ruoff, R.S., *J. Mater. Chem.*, **2006,** 16, 155. (c) Stankovich S.; Dikin, D.A.; Piner, R.D., Kohlhaas, K.A., Kleinhammes, A.; Jia, Y.; Wu, Y., *Carbon*, **2007**, 45(7), 1558.

160. Staudenmaier, L., *Ber Dtsch Chem Ges*, **1898**, 31, 1481.

161. Stoller, M. D.; Park, S.; Zhu, Y.; An, J.; Ruoff, R.S., *Nano Lett.*, **2008**, 8(10), 3498.

162. (a) Stumpp, E.; Nietfeld, G., *Z. Anorg. Allg. Chem*., **1969**, 456, 261. (b) Stumpp, E.; Wloka, K., *Synth. Metals*, **1981**, 3, 209.

163. Sun, R-Q.; Sun, L-B.; Chun, Y.; Xu, Q-H., *Carbon*, **2008**, 46, 1757.

164. Swatloski, R.P.; Holbrey, J.D.; Rogers, R.D., *Green Chem*., **2003**, 5(4), 361.

165. (a) Szabo, T; Tombacz, E; Illes, E.; Dekany, I., *Carbon*, **2006**, 44, 537. (b) Szabo, T; Berkesi, O.; Forgo, P.; Josepovits, K.; Sanakis, Y.; Petridisand, D.; Dekany, I, *Chem. Mater*., **2006**, 18, 2740.

166. Takahashi, Y; Oi, K; Terai, T; Otosaka, T; Akuzawa, N, *Materials Science Forum*, **1992**, 91-93, 133.

167. Takamoto, T.; Suematsu, H.; Murakami, Y., *Synth. Met*., **1990**, 34(1-3), 53.

168. Takenaka, H.; Kawaguchi, M.; Lerner, M. M.; Bartlett, N., *J. Chem. Soc., Chem. Commun.* **1987**, 19, 1431.

169. Teweldebrhan, D.; Balandin, A.A., *Appl. Phys. Lett*., **2009**, 94, 013101.

170. Thomas, J.M.; Millward, G.R.; Schlogl, R.; Boehm, H.P., *Mater. Res. Bull*., **1980**, 15, 671.

171. Thompson T.E.; McCarron E.M.; Bartlett N., *Synth. Metals*, **1981**, 3, 255.

172. Tirado, J.L., *Mater Sci & Eng, R: Reports*, **2003**, R40(3), 103.

173. Touhara, H.; Kadono, K.; Imoto, H.; Watanabe, N.; Tressaud, A.; Grannec, J., *Synth. Metals*, **1987**, 18, 549.

174. (a) Touzain, P.; Buscarlet, E.; Bonnetain, L, *Rev. Chim. Minér*., **1977**, 14, 482. (b) Touzain, P., *Carbon*, **1978**, 16, 403.

175. (a) Toyoda, M;. Katoh, H.; Inagaki, M., *Carbon*, **2001**, 39, 2231. (b) Toyoda, M; Shimizu, A.; Inagaki, M., *Carbon*, **2001**, 39, 1697. (c) Toyoda, M; Sedlacik, J.; Inagaki, M., *Synth. Met.*,**2002**, 130, 39.

176. Tressaud, A.; Hagenmuller, P., *J. Fluorine Chem*., **2001**,111, 221.

177. Tsuchiya, S.; Fukui, A.; Hara, M.; Imamura, H., *Proc. Int. Congr. Catal*. **1985**, 4, 635.

178. Ue, M.; Ida, K.; Mori, S., *J. Electrochem. Soc*., **1994**, 141, 2989.

179. Underhill C.; Krapchev, T.; Dresselhaus, M. S., *Synth. Met.* **1980**, *2*, 47.

180. Valerga Jiménez, P.; Arufe Martinez, M.I.; Martı´n Rodrıéz, A., *Carbon*, **1985**, 23, 473.

181. Vasse, R.; Furdin, G.; Melin J.; Herold, A., *Carbon*, **1981**, 19, 249.

182. Vogel, F.L.; Foley, G.M.T.; Zeller, C.; Falardeau, E.R.; Gan J., *Mater. Sci. Eng*., **1977**, 31, 261.

183. Wagman, D.D.; Evans, W.H.; Parker, V.B.; Schumm, R.H.; Bailey, S.M.; Hallow, I.; Churney, K.L.; Nuttall, R.L., *in Handbook of Chemistry and Physics*, 270(3)-270(8), Vol. 70, CRC Press, Boca Raton, FL, **1989-1990**.

184. Walter, J.; Heiermann, J.; Dyker, G.; Hara, S.; Shioyama, H., *Journal of Catalysis*, **2000**, 189, 449.

185. Wang, X.; Zhi, L.; Mullen, K., *Nano Lett*., **2008**, 8(1), 323.

186. Wang, Z.M.; Hoshinoo, K.; Xue, M.; Kanoh, H.; Ooi, K., *Chem Commun*, **2002**, 1696.

187. (a) Watanabe, N.; Touhara, H.; Nakajima, T.; Bartlett, N.; Mallouk, T.; Selig, H., *Fluorine intercalation compounds of graphite, in Inorganic Solid Fluorides* (P. Hagenmuller, ed.), Academic Press, New York, **1985**, p.331. (b) Watanabe, N.; Nakajima, T.; Touhara, H., *Graphite Fluorides*, Elsevier, Amsterdam, **1988.**

188. Watcharotone, S.; Dikin, D.A.; Stankovich, S.; Piner, R.; Jung, I.; Dommett, G.H.B.; Evmenenko, G.; Wu, S.-E.; Chen, S.-F.; Liu, C.-P.; Nguyen, S.T.; Ruoff, R.S, *Nano Lett.*, **2007**, 7(7), 1888.

189. Whittingham, M.S.; Jacobson, A.J., *Intercalation Chemistry*; Academic Press: New York, **1982**.

190. Winter, M.; Besenhard, J.O.; Spahr, M.E., Novak, P., *Adv. Mater*.,**1998**, 10(10), 725.

191. Worsley, K.A.; Ramesh, P.; Mandal, S.K.; Niyogi, S.; Itkis, M.E.; Haddon, R.C., *Chem. Phys. Lett*., **2007**, 445, 51.

192. Yakovlev, A.V.; Finaenov, A.I.; Zabud'kov, S.L.; Yakovleva, E.V., *Russian Journal of Applied Chemistry*, **2006**, 79(11), 1741.

193. (a) Yan, W.; Lerner, M.M., *J. Electrochem. Soc*., **2001**, 148(6), D83. (b) Yan, W.; Lerner, M.M., *J. Electrochem. Soc.*, **2003**, 150(9), D169. (c) Yan, W.; Lerner, M.M., *J. Electrochem. Soc*., **2004**, 151(2), J15. (d) Yan, W.; Kabalnova, L.; Sukpirom, N.; Zhang, S.; Lerner, M., *J. Fluorine Chem*., **2004**, 125(11), 1703. (e) Yan, W.; Lerner, M.M., *Carbon*, **2004**, 42, 2981.

194. Yan, W., Synthesis, characterization, and structural modeling of graphite intercalation compounds with fluoroanions, PhD thesis, Oregon State University, 2004.

195. Yazami, R.; Hany, P.; Masset, P.; Hamwi, A., *Mol. Cryst. Liq. Cryst*., **1998**, 310, 397.

196. Yin, W.; Jin, W.; Quan, X.; Li, Y.; Cui, X., *Feijinshukuang*, **2006**, 29(1), 35.

197. York, B.R.; Solin, S.A., *Phys. Rev. B*., **1985,** 31, 8206.

198. Zabel, H.; Solin, S.A., *Graphite Intercalation Compounds. Springer-Verlag, Berlin*, **1990**, 1.

199. Zein El Abedin, S.; Borissenko, N.; Endres, F., *Electrochem. Commun*., **2004**, 6(4), 422.

200. Zeng, Q.H.; Yu, A.B.; Lu, G.Q.; Paul, D.R., *J. Nanoscience and Nanotechnology*, **2005**, 5, 1574.

201. Zhang, D.; Wu, Z.; Zhang, X., *Huaxue Gongchengshi*, **2007**, 21(2), 8.

202. Zhang, H.Y.; Shen, W.C.; Wang, Z.D.; Zhang, F., *Carbon*, **1997**, 35(2), 285.

203. Zhang, X.; Lerner, M.M., *Chem. Mater*., **1999**, 11(4), 1100. (b) Zhang, X.; Sukpirom, N.; Lerner, M.M., *Mater. Res. Bull*., **1999**, 34, 363. (c) Zhang X.; Sukpirom, N.; Lerner, M.M., *Mol. Cryst. Liq. Cryst.*, **2000**, 340, 37.

204. (a) Zhang, Z.; Lerner, M.M., *J. Electrochem. Soc*., **1993**, 140(3), 742. (b) Zhang, Z., Lerner, M.M., *Chem. Mater*., **1996**, 8(1), 257.

205. Zhou, Z-B.; Matsumoto, H.; Tatsumi, K., *Chem. Eur. J*., **2006**, 12, 2196.